AN INTEGRAL EQUATION METHOD FOR CONFORMAL MAPPING OF DOUBLY AND MULTIPLY CONNECTED REGION VIA THE KERZMAN-STEIN AND NEUMANN KERNELS

KAEDAH PERSAMAAN KAMIRAN UNTUK PEMETAAN KONFORMAL BAGI RANTAU BERKAIT GANDA DUA DAN BERKAIT BERGANDA MELALUI INTI KERZMAN-STEIN DAN NEUMANN

ALI HASSAN MOHAMED MURID
HU LAEY NEE
MOHD NOR MOHAMAD
NURUL AKMAL MAHAMED
NOR IZZATI JAINI

Department of Mathematics
Faculty of Science
Universiti Teknologi Malaysia

2009

Acknowledgement

This work was supported in part by the Ministry of Science, Technology and Innovations (MOSTI), through IRPA funding —- (vote 78089). This support is gratefully acknowledged.

ABSTRACT

AN INTEGRAL EQUATION METHOD FOR CONFORMAL MAPPING
OF DOUBLY AND MULTIPLY CONNECTED REGION
VIA THE KERZMAN-STEIN AND NEUMANN KERNELS

(Keywords: Conformal mapping, Integral equations, Doubly connected region, Multiply connected regions, Kerzman-Stein kernel, Neumann kernel, Lavenberg-Marquardt algorithm, Cauchy's integral formula.)

This research develops some integral equations involving the Kerzman-Stein and the Neumann kernels for conformal mapping of multiply connected regions onto an annulus with circular slits and onto a disk with circular slits. The integral equations are constructed from a boundary relationship satisfied by a function analytic on a multiply connected region. The boundary integral equations involve the unknown parameter radii. For numerical experiments, discretizing each of the integral equations leads to a system of non-linear equations. Together with some normalizing conditions, a unique solution to the system is then computed by means of an optimization method. Once the boundary values of the mapping function are calculated, we can use the Cauchy's integral formula to determine the mapping function in the interior of the region. Typical examples for some test regions show that numerical results of high accuracy can be obtained for the conformal mapping problem when the boundaries are sufficiently smooth.

Researchers:

Assoc. Prof. Dr. Ali Hassan Mahamed Murid

Ms. Hu Laey Nee

Prof. Mohd Nor Mohamad

Ms. Nurul Akmal Mahamed

Ms. Nor Izzati Jaini

E-mail: ahmm@mel.fs.utm.my

Tel. No.: 07-5534245

ABSTRAK

KAEDAH PERSAMAAN KAMIRAN UNTUK PEMETAAN KONFORMAL BAGI RANTAU BERKAIT GANDA DUA DAN BERKAIT BERGANDA MELALUI INTI KERZMAN-STEIN DAN NEUMANN

(Katakunci: Pemetaan konformal, Persamaan kamiran, Rantau berkait ganda dua, Rantau berkait berganda, Inti Kerzman-Stein, Inti Neumann, Algoritma Lavenberg-Marquardt, Formula kamiran Cauchy.)

Penyelidikan ini membina beberapa persamaan kamiran melibatkan inti Kerzman-Stein dan Neumann untuk pemetaan konformal bagi rantau berkait berganda ke atas anulus dengan belahan membulat dan ke atas cakera dengan belahan membulat. Persamaan kamiran dibangunkan dari hubungan sempadan yang ditepati oleh fungsi yang analisis dalam rantau berkait berganda. Persaman kamiran sempadan ini melibatkan parameter jejari yang tidak diketahui. Untuk kajian berangka, setiap persamaan kamiran berkenaan telah didiskretkan menghasilkan suatu sistem persamaan tak linear. Bersama dengan beberapa syarat kenormalan, satu penyelesaian unik kepada sistem berkenaan dikira dengan kaedah pengoptimuman. Sesudah nilai sempadan bagi fungsi pemetaan dikira, kita boleh menggunakan formula kamiran Cauchy untuk menentukan fungsi pemetaan terhadap rantau pedalaman. Contoh tipikal untuk beberapa rantau ujikaji telah menunjukkan keputusan berangka berketepatan tinggi boleh diperoleh untuk masalah pemetaan konformal dengan sempadan licin.

Penyelidik:

Prof. Madya Dr. Ali Hassan Mahamed Murid

Pn. Hu Laey Nee

Prof. Mohd Nor Mohamad

Cik Nurul Akmal Mahamed

Cik Nor Izzati Jaini

E-mail: ahmm@mel.fs.utm.my

Tel. No.: 07-5534245

TABLE OF CONTENTS

LIST OF TABLES

LIST OF FIGURES

LIST OF APPENDICES

CHAPTER 1

INTRODUCTION

1.1 Introduction and Rationale

A conformal mapping, also called a conformal map, a conformal transformation, angle-preserving transformation, or biholomorphic map is a transformation $w = f(z)$ that preserves local angle. An analytic function is conformal at any point where it has nonzero derivatives. Conversely, any conformal mapping of a complex variable which has continuous partial derivatives is analytic.

Conformal mappings have been an important tool of science and engineering since the development of complex analysis. A conformal mapping uses functions of complex variables to transform a complicated boundary to a simpler, more manageable configuration. In various applied problems, by means of conformal maps, problems for certain *physical regions* are transplanted into problems on some standardized *model regions* where they can be solved easily. By transplanting back we obtain the solutions of the original problems in the physical regions. This process is used, for example, for solving problems about fluid flow, electrostatics, heat conduction, mechanics, aerodynamics and image

processing. For these and other physical problems that use conformal mapping techniques, see, for example, the books by Henrici (1974), Churchill and Brown (1984), Schinzinger and Laura (1991) and Kythe (1998). For theoretical aspects of conformal mappings, see, e.g., Andersen *et al.* (1962), Hille (1962), Ahlfors (1979), Goluzin (1969), Nehari (1975), Henrici (1974), and Wen (1992).

A special class of conformal mappings that map any simply connected region onto a unit disk is called Riemann map. The Riemann mapping function is closely connected to the Szegö or the Bergman kernels. These kernels can be computed as a solution of second kind integral equations. Hence to solve the conformal mapping problem it is sufficient to compute the boundary values of either the Szegö or the Bergman kernel.

An integral equation of the second kind that expressed the Szegö kernel as the solution is first introduced by Kerzman and Trummer (1986) using operator-theoretic approach. Henrici (1986) gave a markedly different derivation of the Kerzman-Stein-Trummer integral equation based on a function-theoretic approach. The discovery of the Kerzman-Stein-Trummer integral equation, briefly KST integral equation, for computing the Szegö kernel later leads to the formulation of an integral equation for the Bergman kernel as given in Murid (1997) and Razali *et al.* (1997). Both integral equations can be used effectively for numerical conformal mapping of simply connected regions.

The practical limitation of conformal mapping has always been that only for certain special regions are exact conformal maps known and others have to be computed numerically.

Henrici (1986), Kythe (1998), Murid (1997), Schinzinger and Laura (1991), Trefethen (1986), Wegmann (2005) and Wen (1992) have surveyed some methods for numerical approximation of conformal mapping function such as expansion methods, iterative methods, osculation methods, integral equation method,

Cauchy-Riemann equation methods and charge simulation methods. The integral equation methods mostly deal with computing the boundary correspondence function for solving numerical conformal mapping. This correspondence refer to a particular parametric representation of the boundary (Razali *et al.*, 1997; Henrici, 1986; Kerzman and Trummer, 1986).

Conformal mapping of multiply connected regions suffer form severe limitations compared to the simply connected region. There is no exact multiply equivalent of the Riemann mapping theorem that holds in multiply connected case. This implies that there is no guarantee that any two multiply connected regions of the same connectivity are conformally equivalent to each other.

Nehari (1975, p. 335), Bergman (1970) and Cohn (1967) described the five types of slit region as important canonical regions for conformal mapping of multiply connected regions, namely

(i) the disk with concentric circular slits (Figure 1.1a),
(ii) an annulus with concentric circular slits (Figure 1.1b),
(iii) the circular slit region (Figure 1.1c),
(iv) the radial slit region (Figure 1.1d), and
(v) the parallel slit region (Figure 1.1e).

The former two are bounded slit regions and the latter three are unbounded slit regions. It is known that any multiply connected region can be mapped conformally onto these canonical regions. In general the radii of the circular slits are unknown and have to be determined in the course of the numerical evaluation. However, exact mapping functions are not known except for some special regions.

By using a boundary relationship satisfied by a function analytic in a doubly connected region, Murid and Razali (1999) extended the construction to a doubly connected region and obtained a boundary integral equation for conformal mapping of doubly connected regions. Special realizations of this boundary integral equation are the integral equations for conformal mapping of doubly

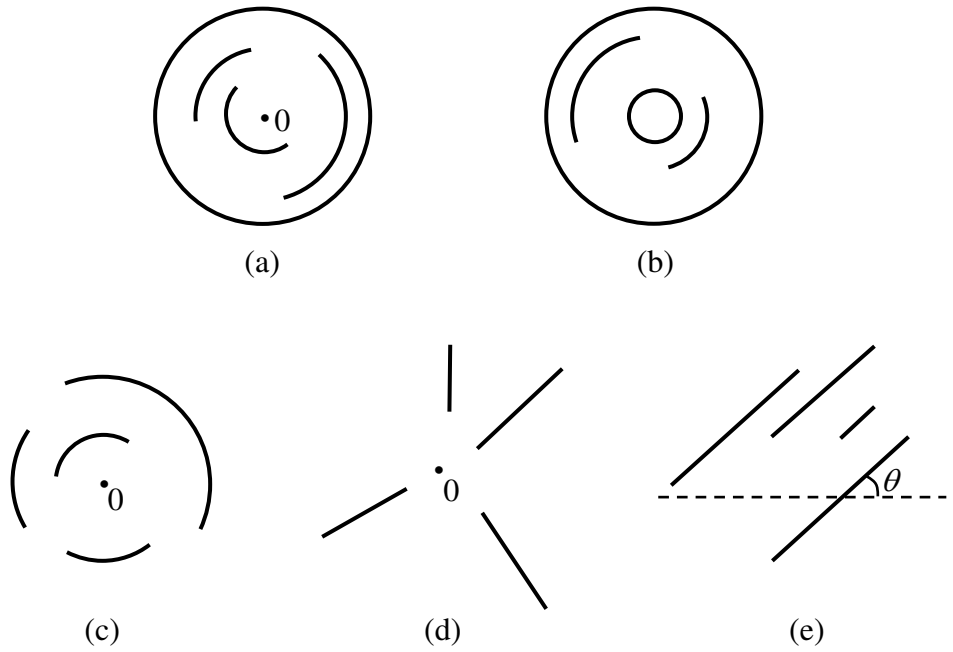

Figure 1.1: Canonical regions.

connected regions via the Kerzman-Stein and the Neumann kernels. However, the integral equations are not in the form of Fredholm integral equations and no numerical experiments are reported in Murid and Razali (1999).

1.2 Scope and Objectives

This research focuses on the integral equation method for the numerical computation of the conformal mapping of multiply connected regions. The theoretical development of the integral equation is based on the approach give by Murid and Razali (1999) for doubly connected regions.

In this project, some new boundary integral equations will be derived for conformal mapping of multiply connected regions via the Kerzman-Stein and the Neumann kernels. These integral equations will be applied to multiply connected regions onto an annulus with concentric circular slits and the disk with

concentric circular slits. For numerical experiments, these integral equations will be discretized that might leads to a system of equations. Some normalizing conditions might be needed to help achive unique solutions.

The research will also describe a numerical procedure based on Cauchy integral formula for computing the mapping of interior points. The research will present numerical examples to highlight the advantages of using the proposed method.

The objectives of this research are:

1. To improve and extend the construction of integral equation related to a boundary relationship satisfied by a function analytic in a doubly connected region by Murid and Razali (1999) to multiply connected regions.

2. To derive new boundary integral equation for conformal mapping of multiply connected regions onto a disk with concentric circular slits via the Neumann kernel.

3. To derive new boundary integral equations for conformal mapping of multiply connected regions onto an annulus with circular slits via the Neumann kernel and the Kerzman-Stein kernel.

4. To use the integral equations to solve numerically the boundary values of the conformal mapping of multiply connected regions onto an annulus with concentric circular slits and the disk with concentric circular slits.

5. To use the Cauchy's integral formula to determine the interior values of mapping functions.

6. To make numerical comparison of the proposed method with exact solution or with some existing methods.

1.3 Project Outline

This project consists of seven chapters. The introductory Chapter 1 details some discussion on the introduction, background of the problem, problem statement, objectives of research, scope of the study and chapter organization.

Chapter 2 gives an overview of methods for conformal mapping in particular of multiply connected regions as well as the conformal mapping of multiply connected regions. We discuss some theories of the Riemann mapping function. We also present some exact conformal mapping of doubly connected regions for certain special regions like annulus, frame of limacon, elliptic frame, frame of Cassini's oval and circular frame. Some numerical methods that have been proposed in the literature for conformal mapping of multiply connected regions are also presented in the Section 2.6 of Chapter 2. The boundary integral equation for conformal mapping of doubly regions derived by Murid and Razali (1999) is also presented.

In Chapter 3, we show how the integral equation for conformal mapping of doubly connected regions via the Kerzman-Stein kernel derived by Murid and Razali (1999) can be modified to a numerically tractable integral equation which involves the unknown inner radius, μ. This integral equation is avoid any prior knowledge on the zeroes and singularities of a mapping function. Numerical experiments on some tests are also presented.

In Chapter 4, we construct new boundary integral equation related to a boundary relationship satisfied by an analytic function on multiply connected

regions. The theoretical development is based on the boundary integral equation for conformal mapping of doubly connected region derived by Murid and Razali (1999) who have constructed an integral equation for the mapping of doubly connected regions onto an annulus involving the Neumann kernel. By using the boundary relationship satisfied by the mapping function, a related system of integral equation is constructed, including the unknown parameter radii. We apply the new boundary integral equation for conformal mapping of multiply connected regions onto a disk with circular slits and onto an annulus with circular slits via the Neumann and the Kerzman-Stein kernels. Special cases of this result is the integral equation involving the Kerzman-Stein kernel related to conformal mapping of doubly connected regions onto an annulus obtained in Chapter 3.

In Chapter 5, we apply the result of Chapter 4 to derive a new boundary integral equation related to conformal mapping $f(z)$ of multiply connected region onto an annulus with circular slits. We discretized the integral equation and imposed some normalizing conditions for the case doubly connected region via the Kerzman-Stein and the Neumann kernels. We also extend the construction of the boundary integral equation in Chapter 4 to a triply connected regions. The boundary values of $f(z)$ is completely determined from the boundary values of $f'(z)$ through a boundary relationship. Discretization of the integral equation leads to a system of non-linear equations. Together with some normalizing conditions, we show how a unique solution to the system can be computed by means of an optimization method. We report our numerical results and give comparisons with existing method for some test regions.

In Chapter 6, we apply the result of Chapter 4 to derive a new boundary integral equation related to conformal mapping $f(z)$ of multiply connected region onto a disk with circular slits. Discretization of the integral equation leads to a system of non-linear equations. Together with some normalizing conditions, we show how a unique solution to the system can be computed by means of an optimization method. Once the boundary values of the mapping function f are

known, we use the Cauchy's integral formula to determine the interior values of the mapping function. Numerical experiments on some test regions are also reported.

Finally the concluding chapter, Chapter 7, contains a summary of all the main results and several recommendations.

CHAPTER 2

OVERVIEW OF MAPPING OF MULTIPLY CONNECTED REGIONS

2.1 Introduction

In this chapter, some fundamental ideas of conformal mapping, the Riemann conformal mapping and the conformal mapping of multiply connected regions are presented in Section 2.2, 2.3, and 2.4 respectively. In Section 2.5, we present some exact conformal mappings of doubly connected regions for five selected regions i.e. annulus, circular frame, elliptic frame, frame of limacon and frame of Cassini's oval. These regions are used as test regions in our numerical experiments in Chapters 3, 5 and 6. Section 2.6 describes some several well-known numerical methods for conformal mapping of multiply connected regions.

2.2 Ideas of Conformal Mapping

Conformal mapping is a valuable tool in many areas of physics and engineering. The basic idea of such application is that an analytic mapping

can be used to map a given region to a simpler region on which the problem can be solved by inspection. By transforming back to the original region, the desired answer is obtained.

The graph of a real-valued function of a real variable can often be displayed on a two-dimensional coordinate diagram. However, for $w = f(z)$, where z and w are complex variables, a graphical representation of the function f would require displaying a collection of four real numbers in a four-dimensional coordinate diagram. A commonly used graphical representation of a complex-valued function of a complex variable, consists in drawing the domain of definition (z-plane) and the domain of values (w-plane) in separate complex planes. The function $w = f(z)$ is then regarded as a mapping of points in the z-plane onto points in the w-plane. The point w is called the image of the point z. More information is usually exhibited by sketching the images of specific families of curves in the z-plane.

The angle of inclination of $T(z_0)$ with respect to the positive x-axis is $\beta = \operatorname{Arg} z'(0)$. The image of C under the mapping $w = f(z)$ is the curve C'. $\gamma = \operatorname{Arg} f'(z_0) + \operatorname{Arg} z'(0) = \alpha + \beta$ is the angle of inclination of $T^*(w_0)$ with respect to the positive u-axis. The effect of the transformation $w = f(z)$ is the rotation of the angle of inclination of the tangent vector $T(z_0)$ at point z_0 through the angle $\alpha = \operatorname{Arg} f'(z_0)$ to obtain the angle of inclination of the tangent vector T^* at $w_0 = f(z_0)$. This situation is illustrated in Figure 2.1.

A mapping $w = f(z)$ is said to be angle preserving or conformal at z_0, if it preserves angles between oriented curve in magnitude as well as orientation. The following theorem exhibits a close relationship between analytic function and conformal mapping (Marsden, 1973, p. 266). Figure 2.2 shows a mapping by an analytic function that is conformal.

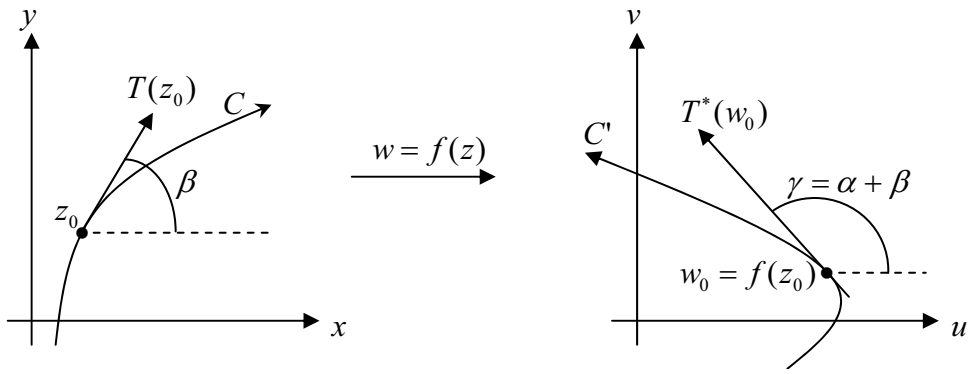

Figure 2.1: The tangents at the point z_0 and w_0, where $f(z)$ is an analytic function and $f'(z_0) \neq 0$.

Theorem 2.1

Let $f(z)$ be an analytic function in the domain Ω, and let z_0 be a point in Ω. If $f'(z_0) \neq 0$, then $f(z)$ is conformal at z_0.

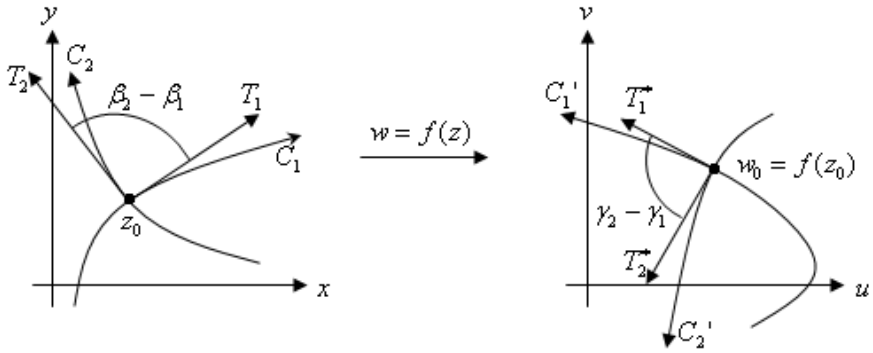

Figure 2.2: The analytic mapping $w = f(z)$ is conformal at point z_0 and w_0, where $f'(z_0) \neq 0$ and $\gamma_2 - \gamma_1 = \beta_2 - \beta_1$.

2.3 The Riemann Conformal Mapping

In various applied problem, problems for certain physical regions are transplanted into problems on some standardized model regions where they can be solved easily. In the application of conformal maps, the questions of existence and uniqueness of conformal maps are important. These equations have long

been settled by Bernhard Riemann (1826-1866), to whom the theory of conformal mapping owes its modern development. The fact that any two simply connected regions in the complex plane are conformally equivalent is known as the Riemann mapping theorem. A region Ω_1 is said to be conformal equivalent to Ω_2 if there is analytic function R such that R is one-to-one and $R(\Omega_1) = \Omega_2$. If both Ω_1 and Ω_2 can be mapped conformally onto the unit disk U, then Ω_1 can be mapped onto Ω_2 by first mapping Ω_1 onto unit disk U and then mapping the unit disk onto Ω_2.

The following is the famous theorem of Riemann that guarantees the existence and uniqueness of a conformal map of any simply connected region in the complex plane onto the unit disk (Henrici, 1986, p. 324).

Theorem 2.2

Let Ω be a simply connected region which is not the whole plane and let a in Ω. Then there exists a unique one-to-one analytic function $R : \Omega \to U = \{w : |w| < 1\}$ satisfying the conditions

$$R(a) = 0, \qquad R'(a) > 0 \tag{2.1}$$

and assuming every value in the unit disk U exactly once.

The function R of the Riemann mapping theorem is called Riemann mapping function. Suppose the Jordan curve Γ admits the counterclockwise parametrization $z(t)$, $0 \leq t \leq \beta$. Thus as $z(t)$ traverses along Γ, the image point $R(z(t))$ describes the unit circle such that

$$R(z(t)) = e^{\mathrm{i}\theta(t)}. \tag{2.2}$$

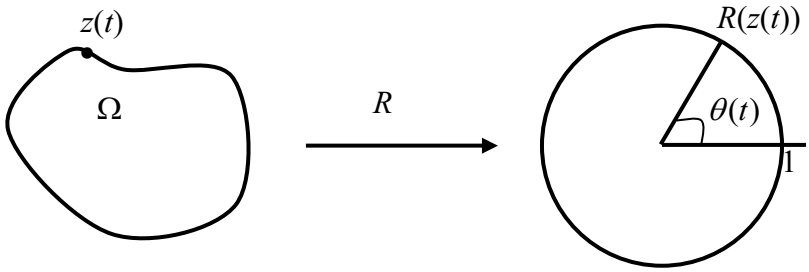

Figure 2.3: Boundary correspondence function $\theta(t)$.

The argument of $R(z(t))$ which is $\theta(t)$ is known as the boundary correspondence function for the map R (See Figure 2.3).

2.4 Conformal Mapping of Multiply Connected Regions

A connected region which is not simply connected is called multiply connected. Such region has holes in it. A region with one hole is called doubly connected. A region with two holes is called triply connected and so on.

By the Riemann mapping theorem, all the simply connected regions with more than one boundary point are conformally equivalent to each other. If we try to introduce the concept of the standard region or canonical domain into the theory of conformal mapping of multiply connected regions, we meet two initial obstacles. The first and less serious is the fact that conformal mapping is continuous and thus preserves the order of connectivity of a region. For example, a conformal map of a doubly connected region is again a doubly connected region. Therefore it becomes necessary to introduce distinct canonical regions for each order of connectivity. The second difficulty is caused by the fact that no exact equivalent of the Riemann mapping theorem holds in the multiply connected case. It is not true that any two regions of the some order of connectivity are conformally equivalent to each other. Not all regions of the same order of connectivity are of the same conformal type.

Let Ω denote a multiply connected region of connectivity $M+1$, $M = 0, 1, 2, ...$ such that a Jordan contour Γ_0 contains M Jordan contours Γ_j, $j = 1, 2, 3, ..., M$, in its interior and the origin is an interior point of Γ_1 (see Figure 2.4). The connectivity is taken as $M+1$ simply because the value of M tells the number of holes inside Γ_0. The boundary of the multiply connected regions shall be denoted by $\Gamma = \Gamma_0 \cup \Gamma_1 \cup \cdots \cup \Gamma_M$.

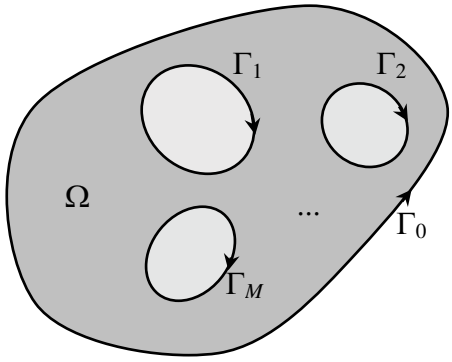

Figure 2.4: An $(M+1)$ connected region.

The theorems related to the mapping of multiply connected region are generally stated in the following form (Kythe, 1998, p. 360; Henrici, 1986, p. 451):

Theorem 2.3

Let Ω be a multiply connected region of connectivity $(M+1)$ inside the annulus $r < |z| < 1$ where $\Gamma_0 = |z| = 1$ and $\Gamma_1 = |z| = r$ are the two boundary components of Ω. Then there exists a unique univalent analytic function $w = f(z)$ in Ω such that (i) it maps Ω conformally onto a region G in the w-plane formed by removing n concentric circular arcs centered at $w = 0$ from the annulus $\rho < |w| < 1$, where $0 < \rho < 1$, and (ii) it maps the unit circle Γ_0 conformally onto the unit circle $|w| = 1$, and the circle $|w| < \rho$, with $f(1) = 1$.

Theorem 2.4

Under the hypotheses there exist M real numbers μ_j, $j = 1, 2, 3, ..., M$, such that $0 < \mu_M < \mu_j < 1$, $j = 1, 2, ..., M-1$, such that there is an analytic function f that

maps Ω *conformally onto the annulus* $\mu_M < |w| < 1$*, cut along* $M-1$ *mutually disjoint slits* Λ_j *located on the circles* $|w| = \mu_j$*,* $j = 1, 2, ..., M-1$*. The mapping function* f *can be extended analytically to the curves* Γ_j *bounding* Ω*. The images of* Γ_0 *and of* Γ_M *are the circles* $\Lambda_0 : |w| = 1$ *and* $\Lambda_M : |w| = \Gamma_j$ *respectively. The image of the curves* Γ_j *are the slits* Λ_j*,* $j = 1, 2, ..., M-1$*, traversed twice. The function* f *is determined up to a factor of modulus* 1*.*

The notations used and the assertions of Theorems 2.3 and 2.4 are illustrated in Figure 2.5 for the case $M = 3$.

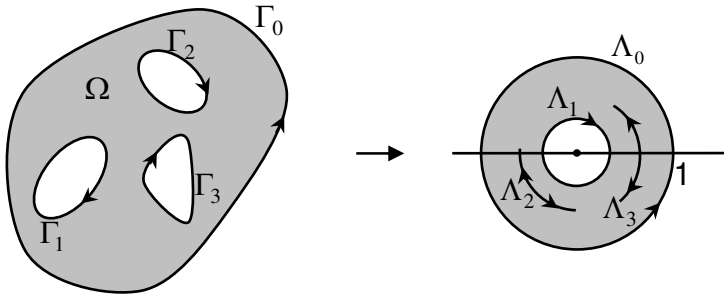

Figure 2.5: Mapping of a region of connectivity 4 onto an annulus with circular slits.

Theorem 2.5

Let Ω *be a multiply connected region of connectivity* $(M+1)$ *inside the unit disk* $|z| < 1$ *where* $\Gamma = |z| = 1$ *is boundary component of* Ω *and* $0 \in \Omega$*. There exists a unique, univalent analytic function* $w = f(z)$ *in* Ω *such that (i) it maps* Ω *conformally onto a region* G *inside the unit disk* $|w| < 1$ *which has* M *circular cuts centered at* $w = 0$ *and (ii) it maps the unit circle* $|z| = 1$ *conformally onto unit circle* $|w| = 1$ *with* $f(0) = 0$ *and* $f(1) = 1$*.*

The assertions of Theorem 2.5 is illustrated in Figure 2.6 for the case $M = 3$.

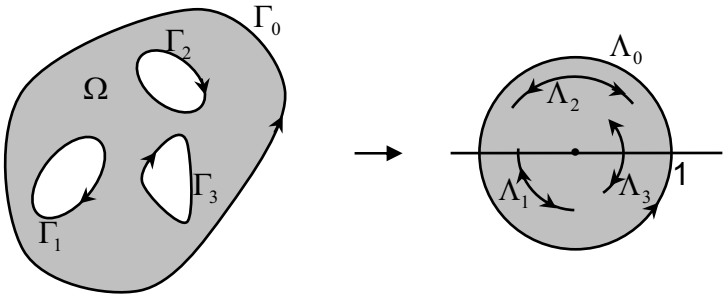

Figure 2.6: Mapping of a region of connectivity 4 onto a disk with circular slits.

The boundary correspondence function, $\theta(t)$ set up for the simply connected case can also be extended to the doubly connected regions. Let the outer and inner boundary curves of a doubly connected region Ω be given in parametric representation as follows (Henrici, 1986, p. 461) :

$$\Gamma_0 : z = z_0(t), \quad 0 \leq t \leq \beta_0,$$

$$\Gamma_1 : z = z_1(t), \quad 0 \leq t \leq \beta_1.$$

If f is a function which maps the region Ω bounded by Γ_0 and Γ_1 onto the annulus $A : \mu < |w| < 1$ so that the inner and the outer boundaries correspond to each other, the boundary correspondence function θ_0 (outer boundary) and θ_1 (inner boundary) are continuous function satisfying

$$f(z_0(t)) = e^{\mathrm{i}\theta_0(t)}, \quad 0 \leq t \leq \beta_0, \tag{2.3}$$

$$f(z_1(t)) = \mu e^{\mathrm{i}\theta_1(t)}, \quad 0 \leq t \leq \beta_1, \tag{2.4}$$

where the expressions on the left are to be understood as the continuous extensions of the mapping function to the boundary.

2.5 Exact Mapping Function of Doubly Connected Regions for Some Selected Regions

In this section, we present some of the exact conformal mapping $f(z)$ of doubly connected regions onto an annulus $A = \{z : \tilde{r} < |w_1| < 1\}$, where $0 < \tilde{r} < 1$. Later, the exact conformal mapping of annulus onto a unit disk with a circular slit, denoted by $h(z)$ is given. The composite $g = h \circ f$ then directly maps the doubly connected regions onto a disk with a circular slit (see Figure 2.7). The special regions considered are annulus, frame of limacon, circular frame, elliptic frame and frame of Cassini's oval.

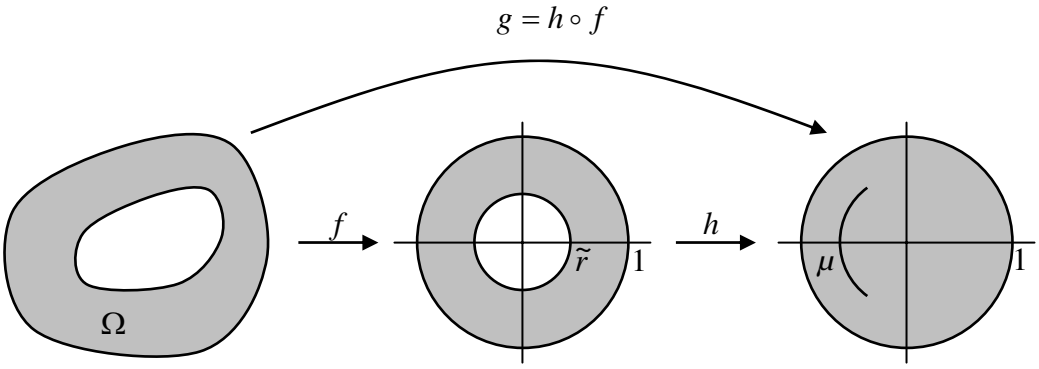

Figure 2.7: The composite $g = h \circ f$.

2.5.1 Annulus Onto A Disk With A Circular Slit

The exact conformal mapping of doubly connected regions onto a unit disk with a slit is adapted from von Koppenfels and Stallmann, (1959, p 362). Consider a frame of circular annulus $A = \{z : \tilde{r} < |z| < 1\}$, $\tilde{r} > 0$,

$$\begin{aligned} \Gamma_0 : z(t) &= \cos t + \mathrm{i} \sin t, \\ \Gamma_1 : z(t) &= \tilde{r}(\cos t + \mathrm{i} \sin t), \qquad 0 \leq t \leq 2\pi. \end{aligned}$$

Under the mapping $p(z) = \dfrac{1}{2\pi} \log z$, the annulus A is mapped onto the rectangle

$$R = \left\{ w_1 = x + \mathrm{i}\, y : 0 < x < \pi,\, 0 < y < \frac{\pi\tau}{2} \right\}. \tag{2.5}$$

Suppose $q = e^{-\pi\tau}$ and $\theta_4(z;q)$ be the Jacobi Theta-functions with the nome q (Abramowitz and Stegun, 1970; Whittaker and Watson, 1927). Then

$$d(z) = -e^{2\sigma}\frac{\theta_4\left(z + \dfrac{\mathrm{i}\pi\tau}{2} - \mathrm{i}\sigma;\, q\right)}{\theta_4\left(z + \dfrac{\mathrm{i}\pi\tau}{2} + \mathrm{i}\sigma;\, q\right)} \tag{2.6}$$

maps R conformally onto the unit disk with a circular slit at radius $\mu = e^{-2\sigma}$. The composite function $h = d \circ p$ maps the annulus A to the unit disk with a circular slit (see Figure 2.8).

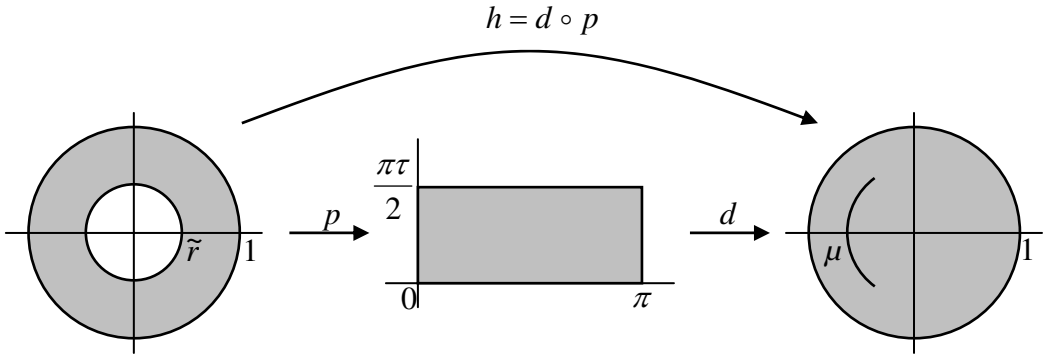

Figure 2.8: The composite function $g = h \circ p$.

By choosing real numbers $\tau > 0$, $\sigma > 0$, $\sigma < \pi\tau/2$, the function

$$\begin{aligned} h(z) &= (d \circ p)(z) \\ &= d\left[\frac{1}{2\mathrm{i}}\log z\right] \\ &= -e^{2\sigma}\frac{\theta_4\left(\dfrac{1}{2\mathrm{i}}\log z + \dfrac{\mathrm{i}\pi\tau}{2} - \mathrm{i}\sigma;\, q\right)}{\theta_4\left(\dfrac{1}{2\mathrm{i}}\log z + \dfrac{\mathrm{i}\pi\tau}{2} + \mathrm{i}\sigma;\, q\right)} \end{aligned} \tag{2.7}$$

with $\tilde{r} = q = e^{-\pi\tau}$ maps Γ_0 onto the unit circle, and maps Γ_1 onto a concentric circular slit of radius $\mu = e^{-2\sigma}$.

2.5.2 Circular Frame

Consider a pair of circles (see Saff and Snider, 2003, A-21)

$$\begin{aligned} \Gamma_0 : z(t) &= e^{\mathrm{i}t}, \\ \Gamma_1 : z(t) &= c + \rho e^{\mathrm{i}t}, \qquad 0 \le t \le 2\pi \end{aligned}$$

such that the domain bounded by Γ_0 and Γ_1 is the domain between a unit circle and a circle center at c with radius ρ.

The mapping function given by

$$f(z) = \frac{z - \lambda}{\lambda z - 1} \tag{2.8}$$

with

$$\lambda = \frac{2c}{1 + (c^2 - \rho^2) + \sqrt{(1 - (c - \rho)^2)(1 - (c + \rho)^2)}},$$

maps Γ_0 onto the unit circle and Γ_1 onto a circle of radius

$$\tilde{r} = \frac{2\rho}{1 - (c^2 - \rho^2) + \sqrt{(1 - (c - \rho)^2)(1 - (c + \rho)^2)}}.$$

From Section 2.5.1, we set $\tilde{r} = q = e^{-\pi\tau}$. This implies $\tau = \dfrac{\ln(\tilde{r})}{-\pi}$. We choose a real number σ such that $0 < \sigma < \pi\tau/2$. Then the mapping function given by

$$g(z) = e^{2\sigma} \frac{\theta_4\left(\dfrac{1}{2\mathrm{i}} \log f(z) + \dfrac{\mathrm{i}\pi\tau}{2} - \mathrm{i}\sigma;\, q\right)}{\theta_4\left(\dfrac{1}{2\mathrm{i}} \log f(z) + \dfrac{\mathrm{i}\pi\tau}{2} + \mathrm{i}\sigma;\, q\right)}, \qquad 0 < \sigma < \frac{\pi\tau}{2}, \tag{2.9}$$

maps Γ_0 onto the unit circle and Γ_1 onto a concentric circular slit of radius $\mu = e^{-2\sigma}$.

2.5.3 Frame of Limacon

Consider a pair of Limacon (see Kythe, 1998, p. 307)

$$\Gamma_0 : z(t) = a_0 \cos t + b_0 \cos 2t + \mathrm{i}(a_0 \sin t + b_0 \sin 2t), \quad a_0 > 0,\ b_0 > 0,$$
$$\Gamma_1 : z(t) = a_1 \cos t + b_1 \cos 2t + \mathrm{i}(a_1 \sin t + b_1 \sin 2t), \quad a_1 > 0,\ b_1 > 0,$$

where $t : 0 \leq t \leq 2\pi$. When $b_1/b_0 = (a_1/a_0)^2$, the mapping function given by

$$f(z) = \frac{\sqrt{a_0^2 + 4b_0 z} - a_0}{2b_0}, \tag{2.10}$$

maps Γ_0 onto the unit circle and Γ_1 onto a circle of radius $\tilde{r} = \dfrac{a_1}{a_0}$.

We set $\tilde{r} = q = e^{-\pi\tau}$, this implies $\tau = \dfrac{\ln(\tilde{r})}{-\pi}$. We choose a real number σ satisfying $0 < \sigma < \pi\tau/2$. The mapping function given by

$$g(z) = -e^{2\sigma} \frac{\theta_4\left(\dfrac{1}{2\mathrm{i}} \log f(z) + \dfrac{\mathrm{i}\pi\tau}{2} - \mathrm{i}\sigma;\ q\right)}{\theta_4\left(\dfrac{1}{2\mathrm{i}} \log f(z) + \dfrac{\mathrm{i}\pi\tau}{2} + \mathrm{i}\sigma;\ q\right)}, \qquad 0 < \sigma < \frac{\pi\tau}{2}, \tag{2.11}$$

then maps Γ_0 onto the unit circle and Γ_1 onto a concentric circular slit of radius $\mu = e^{-2\sigma}$.

2.5.4 Elliptic Frame

Elliptic frame is the domain bounded by two Jordan curves, Γ_0 and Γ_1 such that

$$\Omega : \frac{x^2}{a_0^2} + \frac{y^2}{b_0^2} < 1, \qquad \frac{x^2}{a_1^2} + \frac{y^2}{b_1^2} > 1,$$

with the complex parametric of its boundary is given by (see Amano, 1994)

$$\begin{aligned} \Gamma_0 : z(t) &= a_0 \cos t + \mathrm{i} b_0 \sin t, \quad a_0 > 0,\ b_0 > 0, \\ \Gamma_1 : z(t) &= a_1 \cos t + \mathrm{i} b_1 \sin t, \quad a_1 > 0,\ b_1 > 0, \quad 0 \leq t \leq 2\pi. \end{aligned}$$

When the two ellipses Γ_0 and Γ_1 are confocal such that $a_0^2 - b_0^2 = a_1^2 - b_1^2$, the mapping given by

$$f(z) = \frac{z + \sqrt{z^2 - (a_0^2 - b_0^2)}}{a_0 + b_0}, \qquad \tilde{r} = \frac{a_1 + b_1}{a_0 + b_0}, \tag{2.12}$$

maps Γ_0 onto the unit circle and Γ_1 onto a circle of radius $\tilde{r}$.

We set $\tilde{r} = q = e^{-\pi\tau}$, this implies $\tau = \dfrac{\ln(\tilde{r})}{-\pi}$. We choose a real number σ satisfying $0 < \sigma < \pi\tau/2$. Then the mapping function given by equation (2.11), maps Γ_0 onto the unit circle and Γ_1 onto a concentric circular slit of radius $\mu = e^{-2\sigma}$.

2.5.5 Frame of Cassini's Oval

If Ω is the region bounded by two Cassini's oval, then the complex parametric equation of its boundary is given by (see Amano, 1994)

$$\Gamma_0 : z(t) = \sqrt{b_0^2 \cos 2t + \sqrt{a_0^4 - b_0^4 \sin^2 2t}}\, e^{it}, \quad a_0 > 0,\ b_0 > 0,$$

$$\Gamma_1 : z(t) = \sqrt{b_1^2 \cos 2t + \sqrt{a_1^4 - b_1^4 \sin^2 2t}}\, e^{it}, \quad a_1 > 0,\ b_1 > 0, \quad 0 \le t \le 2\pi,$$

such that

$$\Omega : |z^2 - b_0^2| < a_0^2, \qquad |z^2 - b_1^2| > a_1^2.$$

The boundaries Γ_0 and Γ_1 are chosen such that $(a_0^4 - b_0^4)/b_0^2 = (a_1^4 - b_1^4)/b_1^2$. The mapping given by

$$f(z) = \frac{a_0 z}{\sqrt{b_0^2 z^2 + a_0^4 - b_0^4}}, \qquad \tilde{r} = \frac{a_0 b_1}{a_1 b_0}, \tag{2.13}$$

then maps Γ_0 onto the unit circle and Γ_1 onto a circle of radius $\tilde{r}$.

We set $\tilde{r} = q = e^{-\pi\tau}$, this implies $\tau = -\ln(\tilde{r})/\pi$. We choose a real number σ satisfying $0 < \sigma < \pi\tau/2$. Then the mapping function given by equation (2.11), maps Γ_0 onto the unit circle and Γ_1 onto a concentric circular slit of radius $\mu = e^{-2\sigma}$.

2.6 Some Numerical Methods for Conformal Mapping of Multiply Connected Regions

While conformal maps are indispensable tools in many problems of modern technology, the practical use of conformal maps has always been limited by the fact that exact conformal maps are only known for certain special regions. Since conformal maps cannot be obtained in closed form, in general, we have to resort to numerical approximations of such maps. With the aid of digital computers which are getting faster and less costly nowadays, much research has been done to discuss algorithms for the constructions of conformal maps.

Several methods have been proposed in the literature for the numerical evaluation for conformal mapping of multiply connected regions. For some perspectives, see Amano (1994), Crowdy and Marshall (2006), Ellacott (1979), Henrici (1974), Hough and Papmichael (1983), Kokkinos *et al.* (1990), Mayo (1986), Murid and Razali (1999), Nasser (2009), Papamicheal and Warby (1984), Papamicheal and Kokkinos (1984), Okano *et al.* (2003), Reichel (1986), and Symm (1969). Generally, these methods fall into three types, namely expansion method, iterative method, and integral equation method. It is hard to find methods that are at once fast, accurate, and reliable for conformal mapping of the multiply connected case because it also involved the unknown conformal modulus, μ^{-1} that has to be determined in the course of numerical solution. The integral equation and iterative methods are more preferable and effective for numerical conformal mapping.

The classical integral equation method of Symm (1969) is well-known for computing the conformal maps of doubly connected regions by means of the singular Fredholm integral equations of the first kind. Some Fredholm integral equations of the second kind for conformal mapping of doubly connected regions are of Warschawski and Gerschgorin as discussed in e.g., Henrici (1986). All these integral equations are extensions of those maps for simply connected regions.

However, there are two recently derived integral equations for conformal mapping of simply connected regions which have no analogue for the doubly connected case. These are the KST integral equation and the integral equation for the Bergman kernel as derived in Kerzman and Trummer (1986), Henrici (1986) and Razali *et al.* (1997). An effort for such extension has been given by Murid and Razali (1999). These integral equations are based on a boundary relationship satisfied by a function which is analytic in a doubly connected region. Next, we present some well-known numerical methods that have been proposed in the literature and regarded with great favor for solving numerical conformal mapping of doubly and multiply connected regions.

2.6.1 Wegmann's Iterative Method

An iterative method by Wegmann (2005) consider the conformal mapping from an annulus, $A = \{w : \mu < |w| < 1\}$ onto a given doubly connected region. The method is based on a certain Riemann-Hilbert problem. In view of its quadratic convergence and its $\mathrm{O}(n \log n)$ operations count per iteration step, Wegmann's method is almost certainly the fastest yet devised for this problem (see, e.g., Trefethen (1986)).

The conformal mapping $\Phi : A_\mu \rightarrow \emptyset$, the inverse of the mapping f, is uniquely determined up to a rotation of A_μ. To fix this ambiguity one can impose the condition

$$\Phi(1) = \eta_1(0).$$

Conjugation on the annulus A_μ is effected by a (real) linear operator $\mathbf{K}_\mu(\phi_1, \phi_2)$ which is most easily defined in terms of the complex or real Fourier series

$$\phi_j(t) = \sum_{n=-\infty}^{\infty} A_{n,j}\, e^{\mathrm{i}nt} = a_{0,j} + \sum_{n=1}^{\infty} (a_{n,j} \cos nt + b_{n,j} \sin nt)$$

of the function $\phi_j, \quad j = 1, 2$. Then

$$\mathbf{K}_\mu(\phi_1, \phi_2)(t) = \sum_{n=-\infty}^{\infty} B_n \, e^{\mathrm{i}nt} = \sum_{n=1}^{\infty} (\alpha_{n,j} \cos nt + \beta_{n,j} \, \sin nt)$$

with the coefficients

$$B_0 = 0, \qquad B_n := \frac{2\mathrm{i}A_{n,2} - (\mu^{-n} - \mu^n)\mathrm{i}A_{n,1}}{\mu^{-n} - \mu^n} \quad \text{for } n \neq 0$$

and

$$\alpha_n := \frac{2b_{n,2} - (\mu^{-n} - \mu^n)b_{n,1}}{\mu^{-n} - \mu^n}, \qquad \beta_n := \frac{2a_{n,2} - (\mu^{-n} - \mu^n)a_{n,1}}{\mu^{-n} - \mu^n}$$

for $l = 1, 2, ...$ The analytic solution Φ can be constructed in terms of the conjugation operator

$$\Phi(e^{\mathrm{i}t}) = \phi_1(t) + \mathrm{i}\mathbf{K}_\mu(\phi_1, \phi_2)(t) + \mathrm{i}\gamma,$$
$$\Phi(\mu e^{\mathrm{i}t}) = \phi_2(t) - \mathrm{i}\mathbf{K}_\mu(\phi_2, \phi_1)(t) + \mathrm{i}\gamma,$$

where γ is an arbitrary real constant.

2.6.2 Symm's Integral Equations

Symm's integral equation is one of the well-known integral equation underlying numerical method for conformal mapping which lies on the potential theoretic formulation.

The pair of integral equations of first kind which still contain the unknown parameter μ

$$\begin{aligned} \int_\Gamma \log|z - \zeta|\sigma(\zeta)|d\zeta| &= -\log|z|, \quad z \in \Gamma_0, \\ \int_\Gamma \log|z - \zeta|\sigma(\zeta)|d\zeta| - \log\mu &= -\log|z|, \quad z \in \Gamma_1, \end{aligned}$$

and the condition equation

$$\int_{\Gamma_1} \sigma(\zeta)|d\zeta| = 0$$

are coupled integral equations for densities $\sigma(\zeta)$ and μ and known as Symm's integral equations for conformal mapping of doubly connected regions (Symm, 1969).

2.6.3 Charge Simulation Method

For doubly connected region onto an annulus, a pair of conjugate harmonic functions are approximated by a linear combination of complex logarithmic potentials without integration. The charges Q_i, $i = 1, ..., N$, are determined to satisfy the Dirichlet boundary conditions at N_1 and N_2 collocation points arranged on the boundary components Γ_0 and Γ_1 respectively. That is to say, they are solutions of a system of N simultaneously linear equations

$$\sum_{i=1}^{N} Q_i \log |z_j - \zeta_i| = \begin{cases} 0, & z_j \in \Gamma_0, j = 1, \ldots, N_1, \\ 1, & z_j \in \Gamma_1, j = N_1 + 1, \ldots, N. \end{cases}$$

(See, e.g., Amano (1994)).

For cases involving mapping of bounded multiply connected regions mapped onto a disk with concentric circular slits and an annulus with concentric circular slits , together with some normalizing conditions, they obtain the charge Q_{11}, ..., Q_{nN_n}, the approximation of the constants $\log \mu_1, ..., \log \mu_n$, and the the mapping functions

$$F(z) = \frac{z - u}{v - u} \exp \sum_{l=1}^{n} \sum_{j=1}^{N_l} Q_{lj} \log \frac{z - \zeta_{lj}}{v - \zeta_{lj}}.$$

(See, e.g., Okano *et al.* (2003)).

2.6.4 Mikhlin's Integral Equation

Mayo (1986) solves the multiply connected mapping problems by means of an integral equation of the second kind attributed to Mikhlin. Mikhlin assumes that the solution of the modified Dirichlet problem can be rewritten as the integral of a double layer density function, ν given as follows:

$$u(x, y) = \frac{1}{2\pi \mathrm{i}} \int_{\Gamma} \nu(s) \frac{\partial \log r(x, y, \tilde{x}(s), \tilde{y}(s))}{\partial n_s} ds,$$

where

$$r^2 = (x - \tilde{x}(s))^2 + (y - \tilde{y}(s))^2.$$

Mikhlin showed that the solution $\nu(t)$ can be determined from the integral equation

$$\nu(t) + \frac{1}{\pi} \int_\Gamma \nu(s) \left[\frac{\partial \log r(s,t)}{\partial n_s} - a(s,t) \right] ds = -2 \log |t - \alpha|,$$

where

$$a(s,t) = \begin{cases} 1, & \text{if } s,t \text{ lie on the same curve,} \\ 0, & \text{otherwise.} \end{cases}$$

2.6.5 Fredholm Integral Equation

Reichel (1986) describes a fast iterative method for solving Fredholm integral equations of the first kind whose kernels have a logarithmic principal part for multiply connected regions. The method is a Fourier-Galerkin method, and due to the singularity of the kernel, the linear system of simultaneous equations is block diagonally dominant and can be solved rapidly by an iterative method.

The numerical method involves solving the the system of integral equations

$$q_k + \sum_{j=1}^{n} \int_{\Gamma_j} \ln \frac{1}{|z - \zeta|} \sigma_j(\zeta) |d\zeta| = f_k(z), \quad z \in \Gamma_k, \quad 1 \le k \le n,$$

$$\int_{\Gamma_k} \sigma_k(\zeta) |d\zeta| = 0, \quad 1 \le k \le n.$$

for $q_j \in \mathbb{R}$, $\sigma_j^* \in L^2(\Gamma_j)$. The mapping function $\phi(z)$ is defined by

$$\phi(z) := z \exp \left(\sum_{j=1}^{n} \int_{\Gamma_j} \ln \frac{1}{(z - \zeta)} \sigma_j^*(\zeta) |d\zeta| \right).$$

2.6.6 Warschawski's and Gershgorin's Integral Equations

Henrici (1986) discussed two classical integral equations underlying numerical conformal mapping for doubly connected regions which are Warschawski's and Gershgorin's integral equations. These well-known integral equations are stated in Theorem 2.6 and 2.7 (see, Henrici, 1986, p. 466-468).

Theorem 2.6 (Warschawski's Integral Equations for Doubly Connected Regions) *If the boundary curves are such that z_i'' is continuous and the boundary correspondence functions θ_i' have continuous derivatives, then the function θ_0' and θ_1' satisfy the system of integral equations*

$$\theta_0'(\sigma) + \int_0^{\beta_0} v_{0,0}(\tau,\sigma)\theta_0'(\tau)\,d\tau - \int_0^{\beta_1} v_{0,1}(\tau,\sigma)\theta_1'(\tau)\,d\tau = 0,$$
$$\theta_1'(\sigma) + \int_0^{\beta_0} v_{1,0}(\tau,\sigma)\theta_0'(\tau)\,d\tau - \int_0^{\beta_1} v_{1,1}(\tau,\sigma)\theta_1'(\tau)\,d\tau = 0,$$

where the kernels $v_{i,j}$ are the Neumann kernels defined as

$$v_{0,0}(\tau,\sigma) = \frac{1}{\pi}\,\mathrm{Im}\,\frac{z_0'(\sigma)}{z_0(\sigma) - z_0(\tau)},$$
$$v_{0,1}(\tau,\sigma) = \frac{1}{\pi}\,\mathrm{Im}\,\frac{z_0'(\sigma)}{z_0(\sigma) - z_1(\tau)},$$
$$v_{1,0}(\tau,\sigma) = \frac{1}{\pi}\,\mathrm{Im}\,\frac{z_1'(\sigma)}{z_1(\sigma) - z_0(\tau)},$$
$$v_{1,1}(\tau,\sigma) = \frac{1}{\pi}\,\mathrm{Im}\,\frac{z_1'(\sigma)}{z_1(\sigma) - z_1(\tau)}.$$

Theorem 2.7 (Gershgorin's Integral Equations for Doubly Connected Regions) *Under the hypothesis of Theorem 2.6, the functions θ_0' and θ_1' satisfy the system of integral equations*

$$\theta_0(\sigma) - \int_0^{\beta_0} v_{0,0}(\sigma,\tau)\theta_0(\tau)\,d\tau + \int_0^{\beta_1} v_{1,0}(\sigma,\tau)\theta_1(\tau)\,d\tau = 2\arg\frac{z_0(\sigma) - z_1(0)}{z_0(\sigma) - z_0(0)},$$
$$\theta_1(\sigma) - \int_0^{\beta_0} v_{0,1}(\sigma,\tau)\theta_0(\tau)\,d\tau + \int_0^{\beta_1} v_{1,1}(\sigma,\tau)\theta_1(\tau)\,d\tau = 2\arg\frac{z_1(\sigma) - z_1(0)}{z_1(\sigma) - z_0(0)}.$$

Both, the Warschawski's and Gershgorin's integral equations do not involve the modulus μ^{-1} of the given doubly connected regions. If the functions

θ_0, θ_1 and/or their derivatives are known, the modulus may be determined from the following formula:

$$\begin{aligned}\mathrm{Log}\frac{1}{\mu} = \log\left|\frac{z_0(0)-z}{z_1(0)-z}\right| - \frac{1}{2\pi}\int_0^{\beta_0} \mathrm{Re}\frac{z_0'(\tau)}{z_0(\tau)-z}\theta_0(\tau)\,d\tau \\ + \frac{1}{2\pi}\int_0^{\beta_1} \mathrm{Re}\frac{z_1'(\tau)}{z_1(\tau)-z}\theta_1(\tau)\,d\tau, \end{aligned} \tag{2.14}$$

which holds for arbitrary z interior to Γ_1.

2.6.7 The Boundary Integral Equation via the Kerzman-Stein and the Neumann Kernels

Based on a certain boundary relationship satisfied by a function which is analytic in a region interior to a closed Jordan curve, Murid *et al.* (1999) construct a boundary integral equation related to the analytic function. Special realizations of this integral equation are the integral equations related to the Szegö kernel, the Bergman kernel, and the Riemann map. The kernels arise in the integral equations are the Kerzman-Stein kernel and the Neumann kernel.

Murid and Razali (1999) extend the similar construction to a doubly connected region using a boundary relationship

$$D(z) = c(z)\left[\frac{T(z)Q(z)D(z)}{P(z)}\right]^{-}, \quad z \in \Gamma, \tag{2.15}$$

where $D(z)$ is analytic and single-valued with respect to $z \in \Omega$ and is continuous on $\Omega \cup \Gamma$, while c, P, and Q are complex-valued functions defined on Γ with the following properties:

(P1) $c(z) = \begin{cases} c_0, & z \in \Gamma_0, \\ c_1, & z \in \Gamma_1, \end{cases}$

(P2) $P(z)$ is analytic and single-valued with respect to $z \in \Omega$,

(P3) $P(z)$ is continuous on $\Omega \cup \Gamma$,

(P4) $P(z)$ has a finite number of zeroes at $a_1, a_2, \ldots, a_n$,

(P5) $P(z) \neq 0, Q(z) \neq 0, z \in \Gamma$.

The integral equation for D that is related to the boundary relationship (2.15) is as shown below (Murid and Razali, 1999).

Theorem 2.8

Let u and v be any complex-valued functions that are defined on Γ. Then

$$\begin{aligned}
&\frac{1}{2}\left[v(z) + \frac{u(z)}{\overline{T(z)Q(z)}}\right] D(z) \\
&\quad + PV\frac{1}{2\pi \mathrm{i}} \int_\Gamma \left[\frac{u(z)}{(\overline{w}-\overline{z})\overline{Q(w)}} - \frac{v(z)T(w)}{w-z}\right] D(w)\,|dw| \\
&\qquad = -c(z)u(z)\left[\sum_{a_j inside \Gamma} \operatorname*{Res}_{w=a_j} \frac{D(w)}{(w-z)P(w)}\right]^- \\
&\qquad\quad - u(z)(c_0 - c_1)\left[\frac{1}{2\pi \mathrm{i}} \int_{\Gamma_2} \frac{D(w)}{(w-z)P(w)}\,dw\right]^-, \quad z \in \Gamma, \quad (2.16)
\end{aligned}$$

where the minus sign in the superscript denotes complex conjugation and where

$$\Gamma_2 = \begin{cases} -\Gamma_1, & \text{if } z \in \Gamma_0, \\ \Gamma_0, & \text{if } z \in \Gamma_1. \end{cases}$$

Special realization of this integral equation with the assignment

$$c(z) = \mathrm{i}|f(z)|,\ P(z) = f(z),\ D(z) = \sqrt{f'(z)},\ Q(z) = 1, \qquad (2.17)$$

and the choice of $u(z) = \overline{T(z)Q(z)}$ and $v(z) = 1$ is the integral equation with the Kerzman-Stein kernel, i.e.,

$$\begin{aligned}
\sqrt{f'(z)} \;+\; &\int_\Gamma A(z,w)\sqrt{f'(w)}|dw| \\
= \; &-\mathrm{i}(1-\mu)\overline{T(z)}\left[\frac{1}{2\pi \mathrm{i}} \int_{\Gamma_2} \frac{\sqrt{f'(w)}}{(w-z)f(w)} dw\right]^-, \quad z \in \Gamma, \quad (2.18)
\end{aligned}$$

where

$$A(z,w) = \begin{cases} \overline{H(w,z)} - H(z,w), & \text{if } w,z \in \Gamma, w \neq z, \\ 0, & \text{if } w = z \in \Gamma, \end{cases}$$

and

$$H(w,z) = \frac{1}{2\pi \mathrm{i}} \frac{T(z)}{(z-w)}, \quad w \in \Omega \cup \Gamma, z \in \Gamma, w \neq z.$$

The kernel A is known as the Kerzman-Stein kernel (Kerzman and Trummer, 1986) and is smooth and skew-Hermitian. The kernel H is usually referred to as the Cauchy kernel.

Another realization of the boundary integral equation with the assignment

$$c(z) = -|f(z)|^2,\ P(z) = f(z)^2,\ D(z) = f'(z),\ Q(z) = T(z), \tag{2.19}$$

and the choice of $u(z) = \overline{T(z)Q(z)}$ and $v(z) = 1$ is given as

$$f'(z) + \int_\Gamma M(z,w) f'(w) |dw| = (1-\mu^2)\overline{T(z)}^2 \left[\frac{1}{2\pi \mathrm{i}} \int_{\Gamma_2} \frac{f'(w)}{(w-z)f(w)} dw \right]^-, \quad z \in \Gamma, \tag{2.20}$$

where

$$M(z,w) = \begin{cases} \dfrac{T(w)}{2\pi \mathrm{i}} \left[\dfrac{\overline{T(z)}^2}{\overline{w} - \overline{z}} - \dfrac{1}{w-z} \right], & \text{if } w,z \in \Gamma, w \neq z, \\ \dfrac{1}{2\pi} \dfrac{\mathrm{Im}[z''(t)\overline{z'(t)}]}{|z'(t)|^3}, & \text{if } w = z \in \Gamma. \end{cases}$$

Multiplying both sides of (2.20) by $T(z)$ and using the fact that $T(z)\overline{T(z)} = |T(z)|^2 = 1$ gives

$$\begin{aligned} T(z)f'(z) \ &+ \ \int_\Gamma N(z,w) T(w) f'(w) |dw| \\ &= \ (1-\mu^2)\overline{T(z)} \left[\frac{1}{2\pi \mathrm{i}} \int_{\Gamma_2} \frac{f'(w)}{(w-z)f(w)^2} dw \right]^-, \quad z \in \Gamma, \end{aligned} \tag{2.21}$$

where N is the Neumann kernel (see, e.g., Henrici, 1986, p. 282) defined by

$$N(z,w) = \begin{cases} \dfrac{1}{\pi} \mathrm{Im} \left[\dfrac{T(z)}{z-w} \right], & \text{if } w,z \in \Gamma, w \neq z, \\ \dfrac{1}{2\pi} \dfrac{\mathrm{Im}[z''(t)\overline{z'(t)}]}{|z'(t)|^3}, & \text{if } w = z \in \Gamma. \end{cases} \tag{2.22}$$

However, the integral equations (2.18) and (2.21) are not in the form of Fredholm integral equations and no numerical experiments have been reported in Murid and Razali (1999). In Chapter 3, we shows the integral equations (2.18) can be modified to a numerically tractable integral equation which involves the unknown inner radius, μ.

In this project, we also derive some boundary integral equation satisfied by a function analytic on a multiply connected regions subject to certain conditions. This derivation improves the boundary integral equation (2.16) derived by Murid and Razali (1999) which was limited to doubly connected regions. Furthermore it leads to a much simpler derivation of a system of an integral equations developed in Chapter 3. Another two special cases of this result are the integral equation involving the Neumann kernel related to conformal mapping of multiply connected regions onto an annulus with circular slits and onto a disk with circular slits. All these are described in Chapter 4 and the numerical conformal mappings are discussed in Chapters 5 and 6.

CHAPTER 3

AN INTEGRAL EQUATION METHOD FOR CONFORMAL MAPPING OF DOUBLY CONNECTED REGIONS VIA THE KERZMAN-STEIN KERNEL

3.1 Introduction

Let the outer and inner boundary curves be given in parametric representation as follows:

$$\Gamma_0 : z = z_0(t), \quad 0 \leq t \leq \beta_0,$$

$$\Gamma_1 : z = z_1(t), \quad 0 \leq t \leq \beta_1.$$

If f is a function which maps the region Ω bounded by Γ_0 and Γ_1 onto the annulus $A = \{w : \mu < |w| < 1\}$ so that the inner and the outer boundaries correspond to each other, the boundary correspondence function θ_0 (outer boundary) and θ_1 (inner boundary) are continuous functions satisfying

$$f(z_0(t)) = e^{\mathrm{i}\theta_0(t)}, \quad 0 \leq t \leq \beta_0, \tag{3.1}$$

$$f(z_1(t)) = \mu e^{\mathrm{i}\theta_1(t)}, \quad 0 \leq t \leq \beta_1. \tag{3.2}$$

If the unit tangent to Γ at $z(t)$ is denoted by $T(z(t)) = z'(t)/|z'(t)|$, then it can be shown that

$$f(z_0(t)) = \frac{1}{\mathrm{i}} T(z_0(t)) \frac{f'(z_0(t))}{|f'(z_0(t))|}, \tag{3.3}$$

$$f(z_1(t)) = \frac{\mu}{\mathrm{i}} T(z_1(t)) \frac{f'(z_1(t))}{|f'(z_1(t))|}. \tag{3.4}$$

The boundary relationships (3.3) and (3.4) can be combined as

$$f(z) = \frac{|f(z)|}{\mathrm{i}} T(z) \frac{f'(z)}{|f'(z)|}, \qquad z \in \Gamma, \tag{3.5}$$

where $\Gamma = \Gamma_0 \cup \Gamma_1$.

3.2 The Integral Equation for conformal Mapping of Doubly Connected Regions via the Kerzman-Stein kernel

Consider again the boundary integral equation for conformal mapping of doubly connected regions via Kerzman-Stein kernel as in (2.18), i.e.,

$$\begin{aligned} \sqrt{f'(z)} \;+\; & \int_\Gamma A(z,w) \sqrt{f'(w)}\, |dw| \\ = \; & -\mathrm{i}(1-\mu)\overline{T(z)} \left[\frac{1}{2\pi\mathrm{i}} \int_{\Gamma_2} \frac{\sqrt{f'(w)}}{(w-z) f(w)} dw \right]^{-}, \qquad z \in \Gamma, \end{aligned} \tag{3.6}$$

where the minus sign in the superscript denotes complex conjugation, and

$$A(z,w) = \begin{cases} \overline{H(w,z)} - H(z,w), & w, z \in \Gamma, w \neq z, \\ 0, & w = z \in \Gamma, \end{cases} \tag{3.7}$$

$$H(w,z) = \frac{1}{2\pi\mathrm{i}} \frac{T(z)}{(z-w)}, \qquad w \in \Omega \cup \Gamma, z \in \Gamma, w \neq z, \tag{3.8}$$

and

$$\Gamma_2 = \begin{cases} -\Gamma_1, & \text{if } z \in \Gamma_0, \\ \Gamma_0, & \text{if } z \in \Gamma_1. \end{cases}$$

The single integral equation in (3.6) can be separated into a system of two integral equations given by

$$\begin{aligned}\sqrt{f'(z_0)} \;&+\; \int_\Gamma A(z_0,w)\sqrt{f'(w)}\,|dw| \\ &=\; -\;\mathrm{i}(1-\mu)\overline{T(z_0)}\left[\frac{1}{2\pi\mathrm{i}}\int_{-\Gamma_1}\frac{\sqrt{f'(w)}}{(w-z_0)f(w)}dw\right]^-, \quad z=z_0\in\Gamma_0,\end{aligned} \tag{3.9}$$

$$\begin{aligned}\sqrt{f'(z_1)} \;&+\; \int_\Gamma A(z_1,w)\sqrt{f'(w)}\,|dw| \\ &=\; -\;\mathrm{i}(1-\mu)\overline{T(z_1)}\left[\frac{1}{2\pi\mathrm{i}}\int_{\Gamma_0}\frac{\sqrt{f'(w)}}{(w-z_1)f(w)}dw\right]^-, \quad z=z_1\in\Gamma_1,\end{aligned} \tag{3.10}$$

Taking the boundary relationship (3.5) into account, (3.9) and (3.10) become

$$\begin{aligned}&\sqrt{f'(z_0)}+\int_\Gamma A(z_0,w)\sqrt{f'(w)}\,|dw| \\ &\quad=-\mathrm{i}(1-\mu)\overline{T(z_0)}\left[\frac{1}{2\pi\mathrm{i}}\int_{-\Gamma_1}\frac{\sqrt{f'(w)}}{(w-z_0)\left[\frac{\mu}{\mathrm{i}}T(w)\frac{f'(w)}{|f'(w)|}\right]}dw\right]^-, \quad z=z_0\in\Gamma_0,\end{aligned} \tag{3.11}$$

$$\begin{aligned}&\sqrt{f'(z_1)}+\int_\Gamma A(z_1,w)\sqrt{f'(w)}\,|dw| \\ &\quad=-\mathrm{i}(1-\mu)\overline{T(z_1)}\left[\frac{1}{2\pi\mathrm{i}}\int_{\Gamma_0}\frac{\sqrt{f'(w)}}{(w-z_1)\left[\frac{1}{\mathrm{i}}T(w)\frac{f'(w)}{|f'(w)|}\right]}dw\right]^-, \qquad z=z_1\in\Gamma_1.\end{aligned} \tag{3.12}$$

Using $|f'(w)| = \sqrt{f'(w)}\overline{\sqrt{f'(w)}}$ and $T(w)\,|dw| = dw$, after some mathematical manipulations, integral equations (3.11) and (3.12) become

$$\begin{aligned}\sqrt{f'(z_0)} \;&+\; \int_\Gamma A(z_0,w)\sqrt{f'(w)}\,|dw| \\ &=\; \frac{1}{2\pi\mathrm{i}\mu}(1-\mu)\overline{T(z_0)}\int_{-\Gamma_1}\frac{\sqrt{f'(w)}}{(\overline{w}-\overline{z_0})}\,|dw|, \qquad z=z_0\in\Gamma_0,\end{aligned} \tag{3.13}$$

$$\begin{aligned}\sqrt{f'(z_1)} \;&+\; \int_\Gamma A(z_1,w)\sqrt{f'(w)}\,|dw| \\ &=\; \frac{1}{2\pi\mathrm{i}}(1-\mu)\overline{T(z_1)}\int_{\Gamma_0}\frac{\sqrt{f'(w)}}{(\overline{w}-\overline{z_1})}\,|dw|, \qquad z=z_1\in\Gamma_1.\end{aligned} \tag{3.14}$$

Since $\Gamma = \Gamma_0 \cup \Gamma_1$, (3.13) and (3.14) may be written as

$$\sqrt{f'(z_0)}+\int_{\Gamma_0} A(z_0,w)\sqrt{f'(w)}\,|dw|-\int_{-\Gamma_1} A(z_0,w)\sqrt{f'(w)}\,|dw|$$

$$=\frac{1}{2\pi\mathrm{i}\mu}\int_{-\Gamma_1}\frac{\overline{T(z_0)}}{(\overline{w}-\overline{z_0})}\sqrt{f'(w)}\,|dw|-\frac{1}{2\pi\mathrm{i}}\int_{-\Gamma_1}\frac{\overline{T(z_0)}}{(\overline{w}-\overline{z_0})}\sqrt{f'(w)}\,|dw|,\ z=z_0\in\Gamma_0,$$

$$\sqrt{f'(z_1)}+\int_{\Gamma_0} A(z_1,w)\sqrt{f'(w)}\,|dw|-\int_{-\Gamma_1} A(z_1,w)\sqrt{f'(w)}\,|dw|$$

$$=\frac{1}{2\pi\mathrm{i}}\int_{\Gamma_0}\frac{\overline{T(z_1)}}{(\overline{w}-\overline{z_1})}\sqrt{f'(w)}\,|dw|-\frac{\mu}{2\pi\mathrm{i}}\int_{\Gamma_0}\frac{\overline{T(z_1)}}{(\overline{w}-\overline{z_1})}\sqrt{f'(w)}\,|dw|,\ z=z_1\in\Gamma_1.$$

Applying definition (3.7) to $A(z_0,w)$ in $\int_{-\Gamma_1}$ of the first equation, and to $A(z_1,w)$ in $\int_{\Gamma_0}$ of the second equation, we obtain

$$\sqrt{f'(z_0)}+\int_{\Gamma_0} A(z_0,w)\sqrt{f'(w)}\,|dw|-\int_{-\Gamma_1}\frac{1}{2\pi\mathrm{i}}\left[\frac{\overline{T(z_0)}}{(\overline{w}-\overline{z_0})}-\frac{T(w)}{(w-z_0)}\right]\sqrt{f'(w)}\,|dw|$$

$$=\frac{1}{2\pi\mathrm{i}\mu}\int_{-\Gamma_1}\frac{\overline{T(z_0)}}{(\overline{w}-\overline{z_0})}\sqrt{f'(w)}\,|dw|-\frac{1}{2\pi\mathrm{i}}\int_{-\Gamma_1}\frac{\overline{T(z_0)}}{(\overline{w}-\overline{z_0})}\sqrt{f'(w)}\,|dw|,\quad z=z_0\in\Gamma_0,$$

$$\sqrt{f'(z_1)}+\int_{\Gamma_0}\frac{1}{2\pi\mathrm{i}}\left[\frac{\overline{T(z_1)}}{(\overline{w}-\overline{z_1})}-\frac{T(w)}{(w-z_1)}\right]\sqrt{f'(w)}\,|dw|-\int_{-\Gamma_1} A(z_1,w)\sqrt{f'(w)}\,|dw|$$

$$=\frac{1}{2\pi\mathrm{i}}\int_{\Gamma_0}\frac{\overline{T(z_1)}}{(\overline{w}-\overline{z_1})}\sqrt{f'(w)}\,|dw|-\frac{\mu}{2\pi\mathrm{i}}\int_{\Gamma_0}\frac{\overline{T(z_1)}}{(\overline{w}-\overline{z_1})}\sqrt{f'(w)}\,|dw|,\quad z=z_1\in\Gamma_1.$$

After some cancellations, we get

$$\begin{aligned}\sqrt{f'(z_0)} \;+\; &\int_{\Gamma_0} A(z_0,w)\sqrt{f'(w)}\,|dw|+\frac{1}{2\pi\mathrm{i}}\int_{-\Gamma_1}\frac{T(w)}{(w-z_0)}\sqrt{f'(w)}\,|dw| \\ &= \frac{1}{2\pi\mathrm{i}\mu}\int_{-\Gamma_1}\frac{\overline{T(z_0)}}{(\overline{w}-\overline{z_0})}\sqrt{f'(w)}\,|dw|,\qquad z=z_0\in\Gamma_0, \end{aligned}\tag{3.15}$$

$$\begin{aligned}\sqrt{f'(z_1)} \;-\; &\frac{1}{2\pi\mathrm{i}}\int_{\Gamma_0}\frac{T(w)}{(w-z_1)}\sqrt{f'(w)}\,|dw|-\int_{-\Gamma_1} A(z_1,w)\sqrt{f'(w)}\,|dw| \\ &= -\frac{\mu}{2\pi\mathrm{i}}\int_{\Gamma_0}\frac{\overline{T(z_1)}}{(\overline{w}-\overline{z_1})}\sqrt{f'(w)}\,|dw|,\qquad z=z_1\in\Gamma_1. \end{aligned}\tag{3.16}$$

Rearranging, (3.15) and (3.16) yield

$$\sqrt{f'(z_0)}+\int_{\Gamma_0} A(z_0,w)\sqrt{f'(w)}\,|dw|$$

$$-\int_{-\Gamma_1}\frac{1}{2\pi\mathrm{i}}\left[\frac{\overline{T(z_0)}}{\mu(\overline{w}-\overline{z_0})}-\frac{T(w)}{(w-z_0)}\right]\sqrt{f'(w)}\,|dw|=0,\qquad z=z_0\in\Gamma_0,\tag{3.17}$$

$$\sqrt{f'(z_1)}+\int_{\Gamma_0}\frac{1}{2\pi \mathrm{i}}\left[\frac{\mu\overline{T(z_1)}}{(\overline{w}-\overline{z_1})}-\frac{T(w)}{(w-z_1)}\right]\sqrt{f'(w)}\,|dw|$$
$$-\int_{-\Gamma_1}A(z_1,w)\sqrt{f'(w)}\,|dw|=0, \qquad z=z_1\in\Gamma_1. \tag{3.18}$$

Note that there are three unknown quantities in the integral equations (3.17) and (3.18), namely, $\sqrt{f'(z_0)}$, $\sqrt{f'(z_1)}$ and μ. For numerical purposes, a third equation involving μ is needed so that the system of integral equations above can be solved simultaneously.

Consider equations (3.1) and (3.2) which on differentiation give

$$\begin{aligned} f'(z_0(t))z_0'(t) &= e^{\mathrm{i}\theta_0(t)}\mathrm{i}\theta_0'(t), \\ f'(z_1(p))z_1'(p) &= \mu e^{\mathrm{i}\theta_1(p)}\mathrm{i}\theta_1'(p). \end{aligned}$$

Taking the modulus on both sides of the equations, we obtain

$$|f'(z_0(t))z_0'(t)| = \quad |e^{\mathrm{i}\theta_0(t)}\mathrm{i}\theta_0'(t)| \quad = |e^{\mathrm{i}\theta_0(t)}|\mathrm{i}|\theta_0'(t)|, \tag{3.19}$$
$$|f'(z_1(t))z_1'(p)| = |\mu e^{\mathrm{i}\theta_1(p)}\mathrm{i}\theta_1'(p)| = |\mu||e^{\mathrm{i}\theta_1(p)}|\mathrm{i}|\theta_1'(p)|. \tag{3.20}$$

The absolute values of $e^{\mathrm{i}\theta_0(t)}$ and $e^{\mathrm{i}\theta_1(p)}$ are both equal to 1. The boundary correspondence functions $\theta_0(t)$ and $\theta_1(p)$ are increasing monotone functions and thus the derivative of them are never negative which imply $|\theta_0'(t)| = \theta_0'(t)$ and $|\theta_1'(p)| = \theta_1'(p)$. The quantity μ is the inner radius of the annulus $A = \{w : \mu < |w| < 1\}$ where $0 < \mu < 1$. Thus (3.19) and (3.20) can now be written as

$$|f'(z_0(t))z_0'(t)| = \theta_0'(t), \tag{3.21}$$
$$|f'(z_1(t))z_1'(p)| = \mu\theta_1'(p). \tag{3.22}$$

Upon integrating (3.21) and (3.22) with respect to t and p respectively from 0 to 2π gives

$$\int_0^{2\pi}|f'(z_0(t))z_0'(t)|\,dt = \int_0^{2\pi}\theta_0'(t)\,dt = \theta_0'(t)|_0^{2\pi} = 2\pi, \tag{3.23}$$
$$\int_0^{2\pi}|f'(z_1(p))z_1'(p)|\,dp = \mu\int_0^{2\pi}\theta_1'(p)\,dp = \mu\theta_1'(p)|_0^{2\pi} = \mu 2\pi. \tag{3.24}$$

Subtracting (3.23) from (3.24) multiplied by μ, we obtain

$$\mu \int_0^{2\pi} |f'(z_0(t))z_0'(t)|\, dt - \int_0^{2\pi} |f'(z_1(p))z_1'(p)|\, dp = 0. \tag{3.25}$$

Observe that no knowledge of zeroes or singularities of $f(z)$ is required in constructing equations (3.17) and (3.18). Note also that the system of integral equations in (3.17), (3.18) and (3.25) is homogeneous and does not have a unique solution; if $\{\mu, \sqrt{f'(z)}\}$ is the solution set, then so is $\{\mu, \kappa\sqrt{f'(z)}\}$ for arbitrary complex number κ. A technique for determining a unique solution will be described in the next section.

Defining

$$\begin{aligned} g(z) &= \sqrt{f'(z)}, \\ B(z,w) &= \frac{1}{2\pi \mathrm{i}} \left[\frac{\overline{T(z)}}{\mu(\overline{w} - \overline{z})} - \frac{T(w)}{(w-z)} \right], \\ D(z,w) &= \frac{1}{2\pi \mathrm{i}} \left[\frac{\mu\overline{T(z)}}{(\overline{w} - \overline{z})} - \frac{T(w)}{(w-z)} \right], \end{aligned}$$

(3.17), (3.18) and (3.25) can be written briefly as

$$g(z_0) + \int_{\Gamma_0} A(z_0,w)g(w)\,|dw| - \int_{-\Gamma_1} B(z_0,w)g(w)\,|dw| = 0, \quad z = z_0 \in \Gamma_0, \tag{3.26}$$

$$g(z_1) + \int_{\Gamma_0} D(z_1,w)g(w)\,|dw| - \int_{-\Gamma_1} A(z_1,w)g(w)\,|dw| = 0, \quad z = z_1 \in \Gamma_1, \tag{3.27}$$

$$\mu \int_0^{2\pi} |g(z_0(t))^2 z_0'(t)|\, dt - \int_0^{2\pi} |g(z_1(p))^2 z_1'(p)|\, dp = 0. \tag{3.28}$$

3.3 Numerical Implementation

Using parametric representation $z_0(t)$ of Γ_0 for $t : 0 \le t \le \beta_0$ and $z_1(p)$ of Γ_1 for $p : 0 \le p \le \beta_1$, (3.26) and (3.27) become

$$\begin{aligned} g(z_0(t)) &+ \int_0^{\beta_0} A(z_0(t), z_0(s)) g(z_0(s)) |z_0'(s)|\, ds \\ &- \int_0^{\beta_1} B(z_0(t), z_1(q)) g(z_1(q)) |z_1'(q)|\, dq = 0, \quad z_0(t) \in \Gamma_0, \quad (3.29) \\ g(z_1(p)) &+ \int_0^{\beta_0} D(z_1(p), z_0(s)) g(z_0(s)) |z_0'(s)|\, ds \\ &- \int_0^{\beta_1} A(z_1(p), z_1(q)) g(z_1(q)) |z_1'(q)|\, dq = 0, \quad z_1(p) \in \Gamma_1. \quad (3.30) \end{aligned}$$

Multiply (3.29) and (3.30) respectively by $|z_0'(t)|^{1/2}$ and $|z_1'(p)|^{1/2}$ gives

$$|z_0'(t)|^{1/2} g(z_0(t)) + \int_0^{\beta_0} |z_0'(t)|^{1/2} |z_0'(s)|^{1/2} A(z_0(t), z_0(s)) g(z_0(s)) |z_0'(s)|^{1/2}\, ds$$

$$- \int_0^{\beta_1} |z_0'(t)|^{1/2} |z_1'(q)|^{1/2} B(z_0(t), z_1(q)) g(z_1(q)) |z_1'(q)|^{1/2}\, dq = 0, \qquad z_0(t) \in \Gamma_0, \tag{3.31}$$

$$|z_1'(p)|^{1/2} g(z_1(p)) + \int_0^{\beta_0} |z_1'(p)|^{1/2} |z_0'(s)|^{1/2} D(z_1(p), z_0(s)) g(z_0(s)) |z_0'(s)|^{1/2}\, ds$$

$$- \int_0^{\beta_1} |z_1'(p)|^{1/2} |z_1'(q)|^{1/2} A(z_1(p), z_1(q)) g(z_1(q)) |z_1'(q)|^{1/2}\, dq = 0, \qquad z_1(p) \in \Gamma_1. \tag{3.32}$$

Defining

$$\begin{aligned} \phi_0(t) &= |z_0'(t)|^{1/2} g(z_0(t)), \\ \phi_1(p) &= |z_1'(p)|^{1/2} g(z_1(p)), \\ K_{00}(t,s) &= |z_0'(t)|^{1/2} |z_0'(s)|^{1/2} A(z_0(t), z_0(s)), \\ K_{01}(t,q) &= |z_0'(t)|^{1/2} |z_1'(q)|^{1/2} B(z_0((t), z_1(q)), \\ K_{10}(p,s) &= |z_1'(p)|^{1/2} |z_0'(s)|^{1/2} D(z_1(p), z_0(s)), \\ K_{11}(p,q) &= |z_1'(p)|^{1/2} |z_1'(q)|^{1/2} A(z_1(p), z_1(q)), \end{aligned}$$

and so (3.31) and (3.32) become

$$\phi_0(t) + \int_0^{\beta_0} K_{00}(t,s)\ \phi_0(s)\ ds - \int_0^{\beta_1} K_{01}(t,q)\ \phi_1(q)\ dq = 0, \quad z_0(t) \in \Gamma_0, \quad (3.33)$$

$$\phi_1(p)+\int_0^{\beta_0} K_{10}(p,s)\ \phi_0(s)\ ds-\int_0^{\beta_1} K_{11}(p,q)\ \phi_1(q)\ dq=0, \quad z_1(p)\in\Gamma_1. \tag{3.34}$$

Note that the kernel $K_{00}(t,s)$ and $K_{11}(p,q)$ preserve the skew-Hermitian properties. Applying the same procedure to the third equation (3.28), we get

$$\mu\int_0^{2\pi} |\phi_0(t)|^{\ 2}\ dt-\int_0^{2\pi} |\phi_1(p)|^{\ 2}\ dp=0. \tag{3.35}$$

which is the third equation involving μ that can be solved simultaneously with integral equations (3.33) and (3.34).

Choosing n equidistant collocation points $t_i=(i-1)\beta_0/n,\ \ 1\le i\ \le n$ and m equidistant collocation points $p_\imath=(\imath\ -1)\beta_1/m\ ,\ \ 1\le\imath\le m$ and applying the trapezoidal rule for Nyström's method to discretize (3.33), (3.34) and (3.35), we obtain

$$\phi_0(t_i) \quad + \quad \frac{\beta_0}{n}\sum_{j=1}^{n} K_{00}(t_i,t_j)\ \phi_0(t_j)-\frac{\beta_1}{m}\sum_{\jmath=1}^{m} K_{01}(t_i,p_\jmath)\ \phi_1(p_\jmath)=0, \tag{3.36}$$

$$\phi_1(p_\imath) \quad + \quad \frac{\beta_0}{n}\sum_{j=1}^{n} K_{10}(p_\imath,t_j)\ \phi_0(t_j)\ -\frac{\beta_1}{m}\sum_{\jmath=1}^{m} K_{11}(p_\imath,p_\jmath)\phi_1(p_\jmath)=0, \tag{3.37}$$

$$\mu \quad \frac{\beta_0}{n}\sum_{i=1}^{n}\ |\phi_0(t_i)|^2-\frac{\beta_1}{m}\sum_{\imath=1}^{m}|\phi_1(p_\imath)|^2=0. \tag{3.38}$$

Note that in the third equation (3.38),

$$|\phi_0|=\sqrt{(\mathrm{Re}\ \phi_0)^2+(\mathrm{Im}\ \phi_0)^2},$$
$$|\phi_1|=\sqrt{(\mathrm{Re}\ \phi_1)^2+(\mathrm{Im}\ \phi_1)^2}.$$

Equations (3.36), (3.37) and (3.38) lead to a system of $(n+m+1)$ non-linear complex equations in n unknowns $\phi_0(t_i)$, m unknowns $\phi_1(p_\imath)$ and μ. By defining the matrices

$$\begin{aligned} B_{ij} &= \frac{\beta_0}{n}K_{00}(t_i,t_j),\\ C_{i\imath} &= \frac{\beta_1}{m}K_{01}(t_i,p_\jmath),\\ E_{\imath j} &= \frac{\beta_0}{n}K_{10}(p_\imath,t_j),\\ D_{\imath\imath} &= \frac{\beta_1}{m}K_{11}(p_\imath,p_\jmath), \end{aligned}$$

$$\begin{aligned} x_{0i} &= \phi_0(t_i), \\ x_{1\imath} &= \phi_1(p_\imath), \end{aligned}$$

the system of equations in (3.36) and (3.37) can be written as $n+m$ by $n+m$ system

$$[I_{nn} + B_{nn}]\, \mathbf{x}_{0n} - C_{nm}\mathbf{x}_{1m} = \mathbf{0}_{0n}, \tag{3.39}$$

$$E_{mn}\mathbf{x}_{0n} + [\, I_{mm} - D_{mm}]\, \mathbf{x}_{1m} = \mathbf{0}_{1m}. \tag{3.40}$$

In addition, equation (3.38) becomes

$$\mu\frac{\beta_0}{n}\sum_{i=1}^{n}\, ((\mathrm{Re}\; x_{_{0i}})^2 + (\mathrm{Im}\; x_{_{0i}})^2) - \frac{\beta_1}{m}\sum_{\imath=1}^{m}((\mathrm{Re}\; x_{1\imath})^2 + (\mathrm{Im}\; x_{1\imath})^2) = 0. \tag{3.41}$$

The result in matrix form for system of equations (3.39) and (3.40) is

$$\begin{pmatrix} I_{nn} + B_{nn} & \vdots & -C_{nm} \\ \cdots & \cdots & \cdots \\ E_{mn} & \vdots & I_{mm} - D_{mm} \end{pmatrix} \begin{pmatrix} \mathbf{x}_{0n} \\ \cdots \\ \mathbf{x}_{1m} \end{pmatrix} = \begin{pmatrix} \mathbf{0}_{0n} \\ \cdots \\ \mathbf{0}_{1m} \end{pmatrix}.$$

Defining

$$A = \begin{pmatrix} I_{nn} + B_{nn} & \vdots & -C_{nm} \\ \cdots & \cdots & \cdots \\ E_{mn} & \vdots & I_{mm} - D_{mm} \end{pmatrix} \quad \text{and} \quad \mathbf{x} = \begin{pmatrix} \mathbf{x}_{0n} \\ \cdots \\ \mathbf{x}_{1m} \end{pmatrix},$$

the previous $(n+m)\times(n+m)$ complex system can be written briefly as $A\mathbf{x} = \mathbf{0}$. Separating A and $\mathbf{x}$ in terms of the real and imaginary parts, the system can be written as

$$\mathrm{Re}\; A\; \mathrm{Re}\; \mathbf{x} - \mathrm{Im}\; A\; \mathrm{Im}\; \mathbf{x} + \mathrm{i}\; (\mathrm{Re}\; A\; \mathrm{Im}\; \mathbf{x} + \mathrm{Im}\; A\; \mathrm{Re}\; \mathbf{x}) = \mathbf{0} + \mathbf{0}\mathrm{i}.$$

Thus, the single $(n+m)\times(n+m)$ complex linear system above is equivalent to the $2(n+m)\times 2(n+m)$ real system involving the Re and Im of the unknown functions, i.e.,

$$\begin{pmatrix} \mathrm{Re}A & \vdots & -\mathrm{Im}A \\ \cdots & \cdots & \cdots \\ \mathrm{Im}A & \vdots & \mathrm{Re}A \end{pmatrix} \begin{pmatrix} \mathrm{Re}\mathbf{x} \\ \cdots \\ \mathrm{Im}\mathbf{x} \end{pmatrix} = \begin{pmatrix} \mathbf{0} \\ \cdots \\ \mathbf{0} \end{pmatrix}. \tag{3.42}$$

Therefore, the linear system above can be solved simultaneously with the non-linear equation (3.41) which also involves the Re and Im parts of the unknown functions. Since the system of integral equations (3.17), (3.18) and (3.25) has no unique solution, the system of equations (3.42) and (3.41) also in general has no unique solution. For uniqueness, we turn to the conditions $f'(a) > 0$ or $f'(z^*) = 1$.

Since we are dealing with boundary values, the condition $f'(z^*) = 1$ looks more appropriate for our numerical purpose. However, it leads to a difficulty as discussed next. We first assume that $z_0(t_1) = z_0(0)$ is to be mapped onto 1 under the mapping function f. For the test regions that we have chosen in Section 2.5, the unit tangent vector $T(z_0(t_1))$ is equal to i. For $z = z_0(t_1)$, the boundary relationship (3.5) yields

$$1 = \frac{f'(z_0(t_1))}{|f'(z_0(t_1))|},$$

or

$$f'(z_0(t_1)) = |f'(z_0(t_1))|. \tag{3.43}$$

Making use of $|f'(z_0(t))z_0'(t)| = \theta_0'(t)$ and (3.43) give

$$\mathrm{Re}x_{01} + \mathrm{i}\mathrm{Im}x_{01} = \phi_0(t_1) = \sqrt{f'(z_0(t_1))|z_0'(t_1)|} = \sqrt{\theta_0'(t_1)}, \tag{3.44}$$

which yields immediately the conditions

$$\begin{cases} \mathrm{Re}x_{01} = \sqrt{\theta_0'(t_1)}, \\ \mathrm{Im}x_{01} = 0. \end{cases} \tag{3.45}$$

But $\theta_0'(t_1)$ is unknown in advance. By knowing only the imaginary part of x_{01} without its real part will not yield a unique solution of equations (3.42) and (3.41). A different strategy for getting the required uniqueness condition is described next.

As is well known that the mapping function, f exists up to a rotation of the annulus, that is up to a factor of modulus 1. For a given f, suppose f is made unique by prescribing $f(z_0(0)) = 1$, then, the function, F such that

$$F(z) = e^{\mathrm{i}\alpha} f(z), \tag{3.46}$$

for arbitrary $\alpha \in \Re$, also maps a doubly connected region onto an annulus.

Differentiating (3.46) gives

$$F'(z) = e^{\mathrm{i}\alpha} f'(z) \qquad \text{or} \qquad \sqrt{F'(z)} = \sqrt{e^{\mathrm{i}\alpha} f'(z)}. \tag{3.47}$$

Note that if $\{\mu, \sqrt{f'(z)}\}$ is a solution set of (3.17), and (3.18), then so is $\{\mu, \kappa\sqrt{F'(z)}\} = \{\mu, \kappa\sqrt{e^{\mathrm{i}\alpha} f'(z)}\}$ where κ is any complex number, C.

Suppose

$$F^*(z) = re^{\mathrm{i}\alpha} f(z), \qquad r, \alpha \in \Re. \tag{3.48}$$

is a mapping function that maps a doubly connected region onto an annulus $A^* = \{w : r\mu < |w| < r\}$. Thus $\mathrm{Arg}(F^*(z))$. Thus $\mathrm{Arg}(f(z))$ differ by α.

Differentiating (3.48), gives

$$F^{*\prime}(z) = re^{\mathrm{i}\alpha} f'(z) \qquad \text{or} \qquad \sqrt{F^{*\prime}(z)} = \sqrt{re^{\mathrm{i}\alpha} f'(z)}. \tag{3.49}$$

Since $\sqrt{r} \in \Re \subseteq C$, then $\{\mu, \sqrt{F^{*\prime}(z)}\}$ is also a solution set of our integral equations (3.17) and (3.18). Note that $F^{*\prime}$ also satisfies (3.25).

The boundary relationship (3.5) implies

$$e^{\mathrm{i}\alpha} f(z) = \frac{|e^{\mathrm{i}\alpha} f(z)|}{\mathrm{i}} T(z) \frac{re^{\mathrm{i}\alpha} f'(z)}{|re^{\mathrm{i}\alpha} f'(z)|}, \qquad z \in \Gamma. \tag{3.50}$$

Since $e^{\mathrm{i}\alpha} f(z) = F(z)$ and $re^{\mathrm{i}\alpha} f(z) = F^*(z)$, (3.50) can also be written as

$$F(z) = \frac{|F(z)|}{\mathrm{i}} T(z) \frac{F^{*\prime}(z)}{|F^{*\prime}(z)|}, \qquad z \in \Gamma, \tag{3.51}$$

where $|F(z)|$ is either 1 or μ. The idea now is to solve for the unique solution $\sqrt{F^{*\prime}(z)}$ from the system of integral equations (3.17), (3.18) and (3.25) with a prescribing value of $F^{*\prime}(z_0(0))$. If $F^{*\prime}(z_0(0)) = B^*$, then

$$\phi_0(t_1) = \mathrm{Re}\ x_{01} + \mathrm{iIm}\ x_{01} = \sqrt{F^{*\prime}(z_0(t_1))|z_0'(t_1)|} = \sqrt{B^*\,|z_0'(t_1)|}.$$

or

$$\begin{cases} \text{Re } x_{01} = \text{Re}\sqrt{B^* \, |z_0'(t_1)|}, \\ \text{Im } x_{01} = \text{Im}\sqrt{B^* \, |z_0'(t_1)|}. \end{cases} \tag{3.52}$$

The boundary values of $F(z)$ are then computed according to equation (3.51). By means of equation (3.46), we then have

$$f(z) = e^{-\mathrm{i}\alpha} F(z), \qquad z \in \Gamma.$$

It remains to determine α. Observe that

$$F^*(z_0(t)) = re^{\mathrm{i}\alpha} f(z_0(t)) = re^{\mathrm{i}\alpha} e^{\mathrm{i}\theta_0(t)}. \tag{3.53}$$

Differentiating (3.53), we obtain

$$F^{*\prime}(z_0(t)) z_0'(t) = re^{\mathrm{i}\alpha} \mathrm{i}\theta_0'(t) e^{\mathrm{i}\theta_0(t)}.$$

Substituting $t_1 = 0$, gives

$$F^{*\prime}(z_0(0)) z_0'(0) = re^{\mathrm{i}\alpha} \mathrm{i}\theta_0'(0).$$

Since $F^{*\prime}(z_0(0)) = B^*$, α is then calculated by the formula

$$\alpha = \text{Arg}[-iz_0'(0)B^*]. \tag{3.54}$$

The system of equations (3.42), (3.41) and (3.52) is an over-determined system of non-linear equations involving $2(n+m)+3$ equations in $2(n+m)+1$ unknowns. Method for solving system having unequal number of equations and unknowns are best dealt with as problems in optimization (Woodford, 1992, p. 146). The solution of this system of equations will coincide with the minimizer of a function which is produced by taking the sum of squares of the left-hand sides of the over-determined system of the non-linear equations (the right-hand sides of the equations being zero). We use Gauss-Newton algorithm to solve this non-linear least square problem which is a modification of Newton's method. Some discussion on this method can be found in, see e.g., Antia (1991, pp. 271-345), Murray (1972, pp. 29-55) and Wolfe (1978, pp. 218-247).

Our non-linear least squares problem consists in finding the vector $\mathbf{p}$ for which the function $S : R^{2(n+m)+3} \rightarrow R^1$ defined by the sum

$$S(\mathbf{p}) = \mathbf{f}^T\mathbf{f} = \sum_{i=1}^{2(n+m)+3} (f_i(\mathbf{p}))^2$$

is minimal. Here, $\mathbf{p}$ stands for the $(2n+2m+1)$-vector (Rex_{01}, Rex_{02}, ..., Rex_{0n}, Rex_{11}, Rex_{12}, ..., Rex_{1m}, Imx_{01}, Imx_{02}, ..., Imx_{0n}, Imx_{11}, Imx_{12}, ..., Imx_{1m}, μ), and $\mathbf{f} = (f_1, f_2, ..., f_{2n+2m+3})$.

The Gauss-Newton algorithm is an iterative procedure and we have to provide an initial guess for the vector $\mathbf{p}$, denoted as $\mathbf{p}^0$.This initial approximation, which, if at all possible, should be a well-informed guess and generate a sequence of approximations $\mathbf{p}^1, \mathbf{p}^2, \mathbf{p}^3, ...$ based on the formula

$$\mathbf{p}^{k+1} = \mathbf{p}^k - ((J_{\mathbf{f}}(\mathbf{p}^k))^{\mathrm{T}} J_{\mathbf{f}}(\mathbf{p}^k))^{-1}(J_{\mathbf{f}}(\mathbf{p}^k))^{\mathrm{T}}\mathbf{f}(\mathbf{p}^k), \tag{3.55}$$

where $J_{\mathbf{f}}(\mathbf{p})$ denotes the Jacobian of $\mathbf{f}$ at $\mathbf{p}$ (note that $J_{\mathbf{f}}(\mathbf{p})$ is not square but $(2n + 2m + 3) \times (2n + 2m + 1)$ matrix). It is reasonable to use the convergence criterion

$$||\mathbf{p}^{(k+1)} - \mathbf{p}^{(k)}|| \leq \varepsilon, \qquad \text{and} \qquad |S^{(k+1)} - S^{(k)}| \leq \varepsilon,$$

where ε is predefined tolerances expressing the desired level of accuracy which has been chosen as 1×10^{-13} and $||\ ||$ is the vector norm.

The numerical implementations on some test regions show that the Gauss-Newton method is successful for all test regions except for the frame of Cassini's oval. This problem occurs since our initial estimation is quite far off the final minimum. The strategy for getting the initial estimation is based on (3.1) and (3.2) where upon differentiating and squaring the two equations, we obtain

$$\begin{aligned} \phi_0(t) &= \sqrt{f'(z_0(t))z_0'(t)} = \sqrt{\mathrm{i}\theta_0'(t)e^{\mathrm{i}\theta_0(t)}}, \\ \phi_1(t) &= \sqrt{f'(z_1(p))z_1'(p)} = \sqrt{\mu\mathrm{i}\theta_1'(p)e^{\mathrm{i}\theta_1(p)}}. \end{aligned}$$

The boundary correspondence functions $\theta_0(t)$ and $\theta_1(p)$ are initially approximated by $\theta_0(t) \approx t$ and $\theta_1(p) \approx p$ respectively which implies $\theta_0'(t) \approx$

$\theta_1'(p) \approx 1$. The inner radius , μ is initially approximated by $\mu \approx 0.5$ for all regions, except for circular frame which is approximated by ρ. These initial guesses are applied for the lowest number of n and m of our experiments. In all our numerical experiments, we have chosen the number of collocation points on Γ_0 and Γ_1 being equal, i.e., $n = m$. The information from the solution of lower n is then exploited to calculate the starting vector $\mathbf{p^0}$ related to $2n$ number of collocation points.

It has been discussed in the literature (see, e.g., Wolfe (1978, pp. 218-247), Fletcher (1986)) that the Gauss-Newton method is too naive for the solution of the least squares problems. Most of the effective methods for solving the least squares problem which are currently in use are, however, modifications of the Gauss-Newton method. As a general rule, if one faces with a convergence problem with the Gauss-Newton algorithm, then it is recommended to use the one of the modification of the Gauss-Newton named Lavenberg-Marquardt with the Fletcher's algorithm (see, e.g., Wolfe (1978, pp. 233-246)). This method is more robust than the Gauss-Newton algorithm and is reasonably efficient and reliable. The Lavenberg-Marquardt algorithm combines the Gauss-Newton method and steepest descent method. Whereas Gauss-Newton method converges quadratically in a neighborhood of the root, the steepest descent method converges only linearly. However, the steepest descent method converges to one of the local minima starting from almost arbitrary starting values while the Gauss-Newton method requires a good initial approximation.

The key to the Lavenberg-Marquardt algorithm is to replace (3.55) by

$$\mathbf{p}^{k+1} = \mathbf{p}^k - H(\mathbf{p}^k)\mathbf{f}(\mathbf{p}^k), \qquad \lambda^k \geq 0, \tag{3.56}$$

where $H(\mathbf{p}^k) = ((J_{\mathbf{f}}(\mathbf{p}^k))^{\mathrm{T}} J_{\mathbf{f}}(\mathbf{p}^k) + \lambda^k)^{-1} (J_{\mathbf{f}}(\mathbf{p}^k))^{\mathrm{T}}$.

For $\lambda^k = 0$, it yields the Gauss-Newton method, whereas as λ^k increases, the direction specified by $H(\mathbf{p}^k)$ tends to that of the steepest descent method.

Thus, in this algorithm, we start with a large value of λ^k and go on reducing it as the solution is approached, so as to switch from the method of steepest descent to the Newton's method. This Lavenberg-Marquardt with Fletcher's algorithm is applied in our numerical implementation. The difference between the methods of original Lavenberg-Marquardt algorithm and with Fletcher's algorithm lies in the technique used to determined suitable values for the λ^k.

By means of (3.46), the boundary correspondence function $\theta(t)$ is computed by

$$\theta(t) = \mathrm{Arg}(e^{-\mathrm{i}\alpha}F(z(t))) = -\alpha + \mathrm{Arg}F(z(t)).$$

Applying (3.51), we have

$$\theta(t) = -\alpha + \mathrm{Arg}[-\mathrm{i}z'(t)F^{*\prime}(z(t))].$$

Having computed the values of $\phi_0(t_i) = \mathrm{Re}x_{0i} + \mathrm{iIm}x_{0i} = \sqrt{F^{*\prime}(z_0(t_i))|z_0{}'(t_i)|}$, and $\phi_1(p_\imath) = \mathrm{Re}x_{1\imath} + \mathrm{iIm}x_{1\imath} = \sqrt{F^{*\prime}(z_1(p_\imath))|z_1{}'(p_\imath)|}$, we can then compute the indicated boundary correspondence functions $\theta_0(t)$ and $\theta_1(p)$ by the formula

$$\begin{aligned}\theta_0(t) &= -\alpha + \mathrm{Arg}(-\mathrm{i}\ z_0'(t)\ \phi_0^2(t)),\\ \theta_1(p) &= -\alpha + \mathrm{Arg}(-\mathrm{i}\ z_1'(p)\phi_1^2(p)).\end{aligned}$$

The computed values of $\theta_0(t)$ and $\theta_1(p)$ are then compared with the exact boundary correspondence functions for four selected regions, namely frame of limacon, frame of Cassini's oval, elliptic frame and circular frame.

3.4 Examples and Numerical Results

In our numerical experiments, we have used four test regions whose exact boundary correspondence functions are known as discussed in Section 2.5. The results for the sub-norm error of the boundary correspondence functions $\theta_0(t)$

and $\theta_1(p)$ and the value μ are shown in Tables 3.1 to 3.4. All the computations are done using MATHEMATICA package (Wolfram, 1991) in single precision (16 digit machine precision).

The numerical computations for the elliptic frame and frame of Cassini's oval are compared with those obtained by Amano (1994), though his distribution is different from ours. The notations E_M and E_A that are used by Amano are defined as follows:

$$\begin{aligned} E_M &= \max\{\max_i ||f(z_0(t_i)| - 1|, \max_i ||f(z_1(t_i)| - \mu|\}, \\ E_A &= \max\{\|\tau_0(t) - \tau_{0n}(t)\|_\infty, \|\tau_1(p) - \tau_{1m}(p)\|_\infty\}. \end{aligned}$$

Example 3.1. *Frame of Limacon:*

Table 3.1: Error Norm (frame of limacon).

$n = m$	$\|\tau_0(t) - \tau_{0n}(t)\|_\infty$	$\|\tau_1(p) - \tau_{1m}(p)\|_\infty$	$\|\mu - \mu_m\|_\infty$
16	9.7(−06)	5.1(−06)	2.8(−05)
32	4.2(−10)	3.1(−10)	2.1(−10)
64	1.3(−15)	1.8(−15)	1.1(−16)

Example 3.2. *Frame of Cassini's Oval:*

Table 3.2 shows the results using the proposed approach. The results obtained using Amano's method (1994) are also shown in Table 3.3 for comparison.

Table 3.2: Error Norm (frame of Cassini's Oval) using the proposed method.

$n = m$	$\|\tau_0(t) - \tau_{0n}(t)\|_\infty$	$\|\tau_1(p) - \tau_{1m}(p)\|_\infty$	$\|\mu - \mu_m\|_\infty$
16	6.4(−03)	2.5(−03)	2.1(−03)
32	6.9(−05)	2.7(−05)	2.1(−05)
64	1.1(−08)	3.7(−09)	3.9(−09)

Table 3.3: Error Norm (frame of Cassini's oval) using Amano's method.

$n = m$	E_A	E_M
16	9.7(−03)	9.1(−03)
32	3.8(−04)	3.4(−04)
64	5.0(−07)	6.9(−07)

Example 3.3. *Circular Frame:*

Table 3.4: Error Norm (circular frame).

$n = m$	$\|\tau_0(t) - \tau_{0n}(t)\|_\infty$	$\|\tau_1(p) - \tau_{1m}(p)\|_\infty$	$\|\mu - \mu_m\|_\infty$
8	9.8(−11)	4.6(−09)	1.4(−06)
16	8.9(−16)	7.1(−15)	9.5(−11)

Example 3.4. *Elliptic Frame:*

Tables 3.5 and 3.6 shows our results and Amano's results (1994) respectively.

Table 3.5: Error Norm (elliptic frame) using the proposed method.

$n = m$	$\|\tau_0(t) - \tau_{0n}(t)\|_\infty$	$\|\tau_1(p) - \tau_{1m}(p)\|_\infty$	$\|\mu - \mu_m\|_\infty$
16	4.0(−04)	3.2(−04)	3.7(−05)
32	5.1(−06)	1.0(−05)	3.7(−06)
64	2.7(−09)	5.9(−09)	2.2(−09)
128	3.6(−15)	5.8(−15)	1.8(−15)

Table 3.6: Error Norm (elliptic frame) using Amano's method.

$n = m$	E_A	E_M
16	3.8(−03)	2.8(−02)
32	7.0(−04)	3.2(−03)
64	2.7(−05)	8.4(−05)

CHAPTER 4

AN INTEGRAL EQUATION RELATED TO A BOUNDARY RELATIONSHIP

4.1 Introduction

Murid *et al.* (1999) have derived boundary integral equations for conformal mapping of simply connected region via the Kerzman-Stein and the Neumann kernels. These integral equations have been used effectively for numerical conformal mapping. In Chapter 2, the boundary integral equations for conformal mapping of doubly connected regions via the Kerzman-Stein and the Neumann kernels have been discussed. These boundary integral equations are the extensions from those of simply connected region. In this chapter, we focus on improving and extending the boundary integral equation derived by Murid and Razali (1999) in Section 2.6.7 to the case of multiply connected regions.

4.2 The Boundary Integral Equation

Let $\Gamma_0, \Gamma_1, \ldots, \Gamma_M$ be $M+1$ smooth Jordan curves in the complex z-plane such that $\Gamma_1, \Gamma_2, \ldots, \Gamma_M$ lies in the interior of Γ_0. Denote by Ω the bounded

$(M+1)$-connected region bounded by Γ_0, Γ_1, ..., Γ_M. The positive direction of the contour $\Gamma = \Gamma_0 \cup \Gamma_1 \cup \cdots \cup \Gamma_M$ is usually that for which Ω is on the left as one traces the boundary (see Figure 2.4).

It is well known that if h is analytic and single-valued in Ω and continuous on $\Omega \cup \Gamma$, we have (Hille, 1973, p. 176)

$$\frac{1}{2\pi \mathrm{i}} \int_{\Gamma} \frac{h(w)}{w-z} dw = \frac{1}{2} h(z), \quad z \in \Gamma. \tag{4.1}$$

Suppose $D(z)$ is analytic and single-valued with respect to $z \in \Omega$ and is continuous on $\Omega \cup \Gamma$. Furthermore, suppose that D satisfies the boundary relationship

$$D(z) = c(z) \left[\frac{T(z)Q(z)D(z)}{P(z)} \right]^{-}, \quad z \in \Gamma, \tag{4.2}$$

where the minus sign in the superscript denotes complex conjugation, $T(z) = z'(t)/|z'(t)|$ is the complex unit tangent function at $z \in \Gamma$, while c, P, and Q are complex-valued functions defined on Γ with the following properties:

(P1) $D(z)$ and $P(z)$ are analytic and single-valued with respect to $z \in \Omega$,

(P1) $D(z)$ and $P(z)$ are continuous on $\Omega \cup \Gamma$,

(P1) $P(z)$ has a finite number of zeroes at $a_1, a_2, ..., a_M$ in Ω,

(P1) $c(z) \neq 0, P(z) \neq 0, Q(z) \neq 0, D(z) \neq 0, z \in \Gamma$.

Note that the boundary relationship (4.2) also has the following equivalent form:

$$P(z) = \overline{c(z)} \frac{T(z)Q(z)D(z)^2}{|D(z)|^2}, \quad z \in \Gamma. \tag{4.3}$$

By means of (4.1), an integral equation for D may be constructed that is related to the boundary relationship (4.2) as shown below:

Theorem 4.1

Let u and v be any complex-valued functions that are defined on Γ. Then

$$\frac{1}{2}\left[v(z)+\frac{u(z)}{\overline{T(z)Q(z)}}\right]D(z)+$$
$$\mathrm{PV}\frac{1}{2\pi\mathrm{i}}\int_\Gamma\left[\frac{c(z)u(z)}{c(w)(\overline{w}-\overline{z})\overline{Q(w)}}-\frac{v(z)T(w)}{w-z}\right]D(w)|dw|$$
$$=-c(z)u(z)\left[\sum_{a_j\ inside\,\Gamma}\operatorname*{Res}_{w=a_j}\frac{D(w)}{(w-z)P(w)}\right]^-,\quad z\in\Gamma,\tag{4.4}$$

where the minus sign in the superscript denotes complex conjugation.

Proof. Consider the integral

$$I_1(z)=\mathrm{PV}\frac{1}{2\pi\mathrm{i}}\int_\Gamma\frac{v(z)T(w)D(w)}{w-z}|dw|,\quad z\in\Gamma.\tag{4.5}$$

Using $T(w)|d(w)|=dw$ and (4.1), since D is analytic on Ω, we obtain

$$I_1(z)=\frac{1}{2}v(z)D(z),\qquad z\in\Gamma.\tag{4.6}$$

Next we consider the integral

$$I_2(z)=\mathrm{PV}\frac{1}{2\pi\mathrm{i}}\int_\Gamma\frac{c(z)u(z)D(w)}{c(w)(\overline{w}-\overline{z})\overline{Q(w)}}|dw|,\quad z\in\Gamma.\tag{4.7}$$

Using the boundary relationship (4.3), $|D(w)|^2=D(w)\overline{D(w)}$ and $\overline{T(w)}|dw|=\overline{dw}$, we get

$$I_2(z)=-c(z)u(z)\left[\frac{1}{2\pi\mathrm{i}}\int_\Gamma\frac{D(w)}{(w-z)P(w)}dw\right]^-.\tag{4.8}$$

Applying the residue theory and formula (4.1) to the integral in (4.8), $I_2(z)$ becomes

$$I_2(z)=-c(z)u(z)\left[\frac{1}{2}\frac{D(z)}{P(z)}+\sum_{a_j inside\Gamma}\operatorname*{Res}_{w=a_j}\frac{D(w)}{(w-z)P(w)}\right]^-.\tag{4.9}$$

Applying the boundary relationship (4.2) to the first term on the right-hand side yields

$$I_2(z)=-\frac{u(z)D(z)}{2\overline{T(z)Q(z)}}-c(z)u(z)\left[\sum_{a_j inside\Gamma}\operatorname*{Res}_{w=a_j}\frac{D(w)}{(w-z)P(w)}\right]^-.\tag{4.10}$$

Finally looking at $I_2(z) - I_1(z)$, yields

$$\begin{aligned}
&\mathrm{PV}\frac{1}{2\pi \mathrm{i}}\int_\Gamma \frac{c(z)u(z)D(w)}{c(w)(\overline{w}-\overline{z})\overline{Q(w)}}|dw| - \mathrm{PV}\frac{1}{2\pi \mathrm{i}}\int_\Gamma \frac{v(z)T(w)D(w)}{(w-z)}|dw| \\
&\quad = -\frac{u(z)D(z)}{2\overline{T(z)Q(z)}} - c(z)u(z)\left[\sum_{a_j inside \Gamma} \operatorname*{Res}_{w=a_j} \frac{D(w)}{(w-z)P(w)}\right]^- \\
&\qquad - \frac{1}{2}v(z)D(z), \quad z \in \Gamma. \qquad (4.11)
\end{aligned}$$

Rearrangement of (4.11), gives (4.4). This completes the proof. ■

Remark 1. If $P(z)$ does not have any zeroes in Ω, then the right-hand side of (4.4) becomes zero.

4.3 Application to Conformal Mapping of Doubly Connected Regions onto an Annulus via the Kerzman-Stein Kernel

Let $w = f(z)$ be the analytic function which maps the doubly connected region Ω bounded by the two smooth Jordan curves Γ_0 and Γ_1 onto the annulus $A = \{w : \mu < |w| < 1\}$ so that Γ_0 and Γ_1 correspond respectively to $|w| = 1$ and $|w| = \mu$ (see Figure 4.1). As is well known such a mapping function f exists up to a rotation of the annulus, and the function f could be made unique by prescribing that

$$f(a) = 0, \quad f'(a) > 0 \quad \text{or} \quad f(z^*) = 1, \qquad (4.12)$$

where $a \in \Omega$ and $z^* \in \Gamma_0$ are fixed points.

The boundary values of f can be represented in the form

$$f(z_0(t)) = e^{\mathrm{i}\theta_0(\mathrm{t})}, \quad \Gamma_0 : z = z_0(t), \quad 0 \le t \le \beta_0, \qquad (4.13)$$

$$f(z_1(t)) = \mu e^{\mathrm{i}\theta_1(t)}, \quad \Gamma_1 : z = z_1(t), \quad 0 \le t \le \beta_1, \qquad (4.14)$$

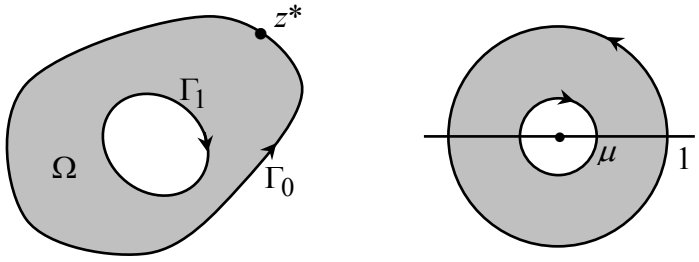

Figure 4.1: Mapping of a doubly connected region Ω onto an annulus.

where $\theta_0(t)$ and $\theta_1(t)$ are the boundaries correspondence functions of Γ_0 and Γ_1 respectively.

The unit tangent to Γ at $z(t)$ is denoted by $T(z(t)) = z'(t)/|z'(t)|$. Thus it can be shown that

$$f(z_0(t)) = \frac{1}{\mathrm{i}} T(z_0(t)) \frac{\theta_0'(t)}{|\theta_0'(t)|} \frac{f'(z_0(t))}{|f'(z_0(t))|} = \frac{1}{\mathrm{i}} T(z_0(t)) \frac{f'(z_0(t))}{|f'(z_0(t))|}, \quad z_0 \in \Gamma_0, \quad (4.15)$$

$$f(z_1(t)) = \frac{\mu}{\mathrm{i}} T(z_1(t)) \frac{\theta_1'(t)}{|\theta_1'(t)|} \frac{f'(z_1(t))}{|f'(z_1(t))|} = \frac{\mu}{\mathrm{i}} T(z_1(t)) \frac{f'(z_1(t))}{|f'(z_1(t))|}, \quad z_1 \in \Gamma_1. \quad (4.16)$$

The boundary relationships (4.15) and (4.16) can be unified as

$$f(z) = \frac{|f(z)|}{\mathrm{i}} T(z) \frac{f'(z)}{|f'(z)|}, \quad z \in \Gamma. \quad (4.17)$$

Note that the values of $|f(z)|$ is either 1 or μ for $z \in \Gamma = \Gamma_0 \cup \Gamma_1$. Also note that since $f'(z)$ is different from 0 and analytic in $\Omega \cup \Gamma$, thus an analytic square root, denoted by $\sqrt{f'(z)}$, may be defined on $\Omega \cup \Gamma$. Comparing (4.17) with (4.3) leads to a choice of $c(z) = \mathrm{i}|f(z)|$, $P(z) = f(z)$, $D(z) = \sqrt{f'(z)}$, $Q(z) = 1$, $u(z) = \overline{T(z)Q(z)}$ and $v(z) = 1$. With these assignments, Theorem 4.1 and Remark 1, imply

$$\sqrt{f'(z)} + \mathrm{PV} \frac{1}{2\pi\mathrm{i}} \int_\Gamma \left[\frac{|f(z)|\overline{T(z)}}{|f(w)|(\overline{w} - \overline{z})} - \frac{T(w)}{(w - z)} \right] \sqrt{f'(w)} |dw| = 0, \quad z \in \Gamma. \quad (4.18)$$

Note that (4.18) does not posses a unique solution. If $f(z)$ satisfies (4.18), then so is $re^{\mathrm{i}\alpha}f(z)$, i.e.

$$\sqrt{[re^{\mathrm{i}\alpha}f(z)]'} + \mathrm{PV}\frac{1}{2\pi\mathrm{i}}\int_\Gamma \left[\frac{|re^{\mathrm{i}\alpha}f(z)|\overline{T(z)}}{|re^{\mathrm{i}\alpha}f(w)|(\overline{w}-\overline{z})} - \frac{T(w)}{(w-z)}\right]\sqrt{[re^{\mathrm{i}\alpha}f(w)]'}|dw| = 0, \qquad z \in \Gamma, \tag{4.19}$$

for any real constant $r > 0$ and α.

To achieve uniquenee, several condition need to be imposed. Suppose

$$F(z) = re^{\mathrm{i}\alpha}f(z), \qquad r,\, \alpha \in \Re \tag{4.20}$$

is a mapping function that maps a doubly connected regions onto an annulus $\tilde{A} = w : r\mu < |w| < r$. The $\mathrm{Arg}(F(z))$ and $\mathrm{Arg}(f(z))$ differ by α.

As is well known such a mapping function $F(z)$ exists up to a rotation and the rotation could be fixed by prescribing $F(z^*) = r$, where $z^* \in \Gamma_0$ is fixed point.

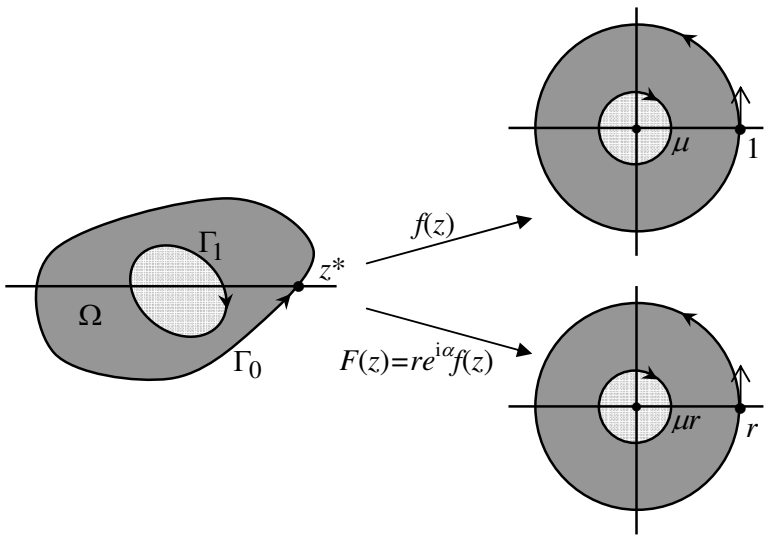

Figure 4.2: Mapping of doubly connected region onto an annulus

The equation (4.20) with $z = z^*$ implies

$$F(z^*) = re^{\mathrm{i}\alpha}f(z^*) = r,$$

and Figure 4.2 implies

$$\begin{cases} \operatorname{Re}[F'(z^*)] = 0, \\ \operatorname{Im}[F'(z^*)] > 0. \end{cases} \tag{4.21}$$

Note that

$$\begin{aligned} F'(z^*) &= re^{\mathrm{i}\alpha} f'(z^*) \\ &= re^{\mathrm{i}\alpha}(\operatorname{Re} f'(z^*) + \mathrm{i}\, \operatorname{Im} f'(z^*)) \\ &= -r\sin\alpha \operatorname{Im} f'(z^*) + \mathrm{i}\, r\cos\alpha \operatorname{Im} f'(z^*). \end{aligned} \tag{4.22}$$

Applying the condition in (4.21), we obtain

$$\sin\alpha \operatorname{Im} f'(z^*) = 0,$$

$$\cos\alpha \operatorname{Im} f'(z^*) > 0,$$

which admit the solution $\alpha = 0$ since $\operatorname{Im} f'(z^*) > 0$. Thus α is now fixed.

So the equation (4.20) becomes

$$F(z) = rf(z). \tag{4.23}$$

To fix r, we observe that

$$F(z_0(t)) = re^{\mathrm{i}\theta_0(t)}, \quad z_0(t) \in \Gamma_0. \tag{4.24}$$

Differentiating and taking modulus on both sides of equation (4.24), we obtain

$$|F'(z_0(t))z_0'(t)| = |r\mathrm{i}\theta_0'(t)e^{\mathrm{i}\theta_0(t)}| = |\theta_0'(t)|. \tag{4.25}$$

The boundary correspondence function $\theta_0(t)$ is an increasing monotone function and it's derivative is positive, we have $|\theta_0'(t)| = \theta_0'(t)$. Thus, integrating (4.25) with respect to t to 2π gives

$$\int_0^{2\pi} |F'(z_0(t))z_0'(t)|dt = |r| \int_0^{2\pi} \theta_0'(t)dt = 2\pi|r|,$$

Setting the condition

$$\int_0^{2\pi} |F'(z_0(t))z_0'(t)|dt = 2\pi,$$

implies $r = 1$. Hence $F(z) = f(z)$.

The integral equation (4.18) can also be written briefly as

$$\sqrt{f'(z)} + \int_\Gamma A^*(z,w)\sqrt{f'(w)}|dw| = 0, \qquad z \in \Gamma, \tag{4.26}$$

where

$$A^*(z,w) = \frac{1}{2\pi \mathrm{i}} \left[\frac{|f(z)|\overline{T(z)}}{|f(w)|(\overline{w} - \overline{z})} - \frac{T(w)}{(w-z)} \right].$$

This result has already been given in Chapter 3 but the derivation presented here is much simpler. The integral equation will be used in Section 5.2, Chapter 5 for the numerical conformal mapping of doubly connected region onto an annulus with some normalizing conditions different from Chapter 3.

4.4 Application to Conformal Mapping of Multiply Connected Regions onto an Annulus with Circular Slits via the Neumann Kernel

This section gives an application of Theorem 4.1 to conformal mapping of multiply connected region Ω of connectivity $M+1$. Let $w = f(z)$ be the analytic function which maps Ω conformally onto an annulus ($\mu_1 < |w| < 1$) with circular slits of radii $\mu_2 < 1$, ..., $\mu_M < 1$ (see Figure 4.3). The mapping function f is determined up to a rotation of the annulus. The function f could be made unique by prescribing (4.12).

The boundary values of f can be represented in form

$$f(z_0(t)) = e^{\mathrm{i}\theta_0(\mathrm{t})}, \quad \Gamma_0 : z = z_0(t), \quad 0 \le t \le \beta_0, \tag{4.27}$$

$$f(z_p(t)) = \mu_p e^{\mathrm{i}\theta_p(t)}, \Gamma_p : z = z_p(t), \quad 0 \le t \le \beta_p, \quad p = 1, 2, ..., M, \tag{4.28}$$

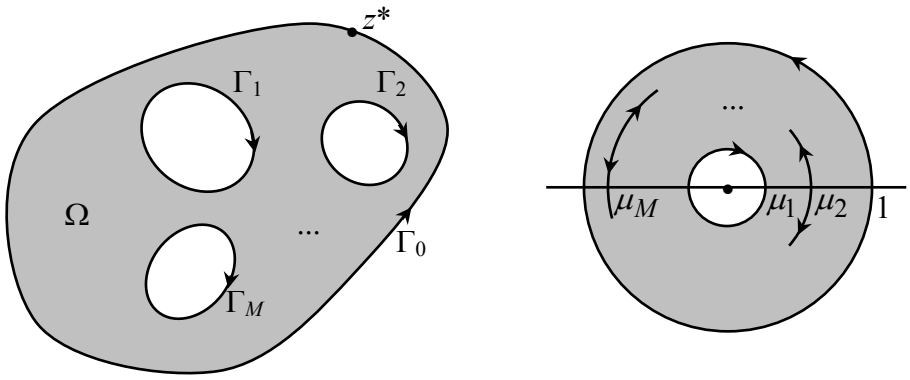

Figure 4.3: Mapping of a multiply connected region Ω of connectivity $M+1$ onto an annulus with circular slits.

where $\theta_0(t), \theta_1(t), ..., \theta_M(t)$ are the boundaries correspondence functions of Γ_0, Γ_1, ..., Γ_M respectively.

The unit tangent to Γ at $z(t)$ is denoted by $T(z(t)) = z'(t)/|z'(t)|$. Thus it can be shown that

$$f(z_0(t)) = \frac{1}{\mathrm{i}} T(z_0(t)) \frac{\theta_0'(t)}{|\theta_0'(t)|} \frac{f'(z_0(t))}{|f'(z_0(t))|} = \frac{1}{\mathrm{i}} T(z_0(t)) \frac{f'(z_0(t))}{|f'(z_0(t))|}, \quad z_0 \in \Gamma_0, \tag{4.29}$$

$$f(z_1(t)) = \frac{\mu_1}{\mathrm{i}} T(z_1(t)) \frac{\theta_1'(t)}{|\theta_1'(t)|} \frac{f'(z_1(t))}{|f'(z_1(t))|} = \frac{\mu_1}{\mathrm{i}} T(z_1(t)) \frac{f'(z_1(t))}{|f'(z_1(t))|}, \quad z_1 \in \Gamma_1, \tag{4.30}$$

$$f(z_p(t)) = \frac{\mu_p}{\mathrm{i}} T(z_p(t)) \frac{\theta_p'(t)}{|\theta_p'(t)|} \frac{f'(z_p(t))}{|f'(z_p(t))|} = \pm \frac{\mu_p}{\mathrm{i}} T(z_p(t)) \frac{f'(z_p(t))}{|f'(z_p(t))|}, \quad z_p \in \Gamma_p, \tag{4.31}$$

for $p = 2, ..., M$. If $M = 1$, then relationship (4.31) does not exist; i.e., only (4.29) and (4.30) hold. Note that $\theta_0'(t) > 0$ and $\theta_1'(t) > 0$ while $\theta_p'(t)$ may be positive or negative since each circular slit $f(\Gamma_p)$ is traversed twice (see Figure 4.3). Thus $\theta_p'(t)/|\theta_p'(t)| = \pm 1$.

The boundary relationships (4.29), (4.30) and (4.31) can be unified as

$$f(z) = \pm \frac{|f(z)|}{\mathrm{i}} T(z) \frac{f'(z)}{|f'(z)|}, \quad z \in \Gamma, \tag{4.32}$$

where $\Gamma = \Gamma_0 \cup \Gamma_1 \cup \cdots \cup \Gamma_M$. Note that the value of $|f(z)|$ is either 1, μ_1 or μ_p for $z \in \Gamma$. However we cannot compare (4.32) with (4.3) due to the presence of the $\pm$ sign. To overcome this problem, we square both sides of the boundary relationship (4.32) to get

$$f(z)^2 = -|f(z)|^2 T(z)^2 \frac{f'(z)^2}{|f'(z)|^2}, \quad z \in \Gamma. \tag{4.33}$$

Comparison of (4.3) and (4.33) leads to a choice of $c(z) = -|f(z)|^2$, $P(z) = f(z)^2$, $D(z) = f'(z)$, $Q(z) = T(z)$, $u(z) = \overline{T(z)Q(z)}$ and $v(z) = 1$. Substituting these assignments into (4.4) leads to an integral equation satisfied by $f'(z)$, i.e.,

$$\begin{aligned} f'(z) + \mathrm{PV}\frac{1}{2\pi \mathrm{i}} \int_\Gamma \left[\frac{|f(z)|^2 \overline{T(z)^2}}{|f(w)|^2 (\overline{w} - \overline{z}) \overline{T(w)}} - \frac{T(w)}{(w-z)} \right] f'(w)|dw| \\ = |f(z)|^2 \overline{T(z)^2} \left[\sum_{a_j inside \Gamma} \operatorname*{Res}_{w=a_j} \frac{f'(w)}{(w-z) f(w)^2} \right]^-, \qquad z \in \Gamma. \end{aligned} \tag{4.34}$$

For the case where Ω is a multiply connected regions being mapped onto an annulus with concentric circular slits, $f(z)$ does not have any zeroes in Ω. Thus the right-hand side of (4.34) vanishes and the integral equation (4.34) becomes

$$f'(z) + \mathrm{PV}\frac{1}{2\pi \mathrm{i}} \int_\Gamma \left[\frac{|f(z)|^2 \overline{T(z)^2}}{|f(w)|^2 (\overline{w} - \overline{z}) \overline{T(w)}} - \frac{T(w)}{(w-z)} \right] f'(w)|dw| = 0, \quad z \in \Gamma. \tag{4.35}$$

Multiply both sides by $T(z)$ and using the fact $T(z)\overline{T(z)} = |T(z)|^2 = 1$ gives

$$T(z) f'(z) + \mathrm{PV}\frac{1}{2\pi \mathrm{i}} \int_\Gamma \left[\frac{|f(z)|^2 \overline{T(z)}}{|f(w)|^2 (\overline{w} - \overline{z})} - \frac{T(z)}{(w-z)} \right] T(w) f'(w)|dw| = 0, \quad z \in \Gamma. \tag{4.36}$$

Note that (4.36) does not posses a unique solution. If $f(z)$ satisfies (4.36), then so is $re^{\mathrm{i}\alpha} f(z)$, i.e.

$$\begin{aligned} & T(z)[re^{\mathrm{i}\alpha} f(z)]' \\ & \quad + \mathrm{PV}\frac{1}{2\pi \mathrm{i}} \int_\Gamma \left[\frac{|re^{\mathrm{i}\alpha} f(z)|^2 \overline{T(z)}}{|re^{\mathrm{i}\alpha} f(w)|^2 (\overline{w} - \overline{z})} - \frac{T(z)}{(w-z)} \right] T(w)[re^{\mathrm{i}\alpha} f(w)]'|dw| = 0, \quad z \in \Gamma. \end{aligned} \tag{4.37}$$

for any real constants $r > 0$ and α.

Suppose

$$F(z) = re^{\mathrm{i}\alpha} f(z), \qquad r,\, \alpha \in \Re \tag{4.38}$$

is a mapping function that maps a multiply connected regions onto an annulus ($r\mu_1 < |w| < r$) with circular slits of radii $r\mu_2 < r$, ..., $r\mu_M < 1$ and the $\mathrm{Arg}(F(z))$ and $\mathrm{Arg}(f(z))$ differ by α. As is well known such a mapping function $F(z)$ exists up to a rotation and the rotation could be fixed by prescribing $F(z^*) = f$, where $z* \in \Gamma_0$ is fixed point. Using the same ideas presented in Section 4.3, imposing the conditions

$$\sin\alpha \,\mathrm{Im}\, f'(z^*) = 0,$$

$$\cos\alpha \,\mathrm{Im}\, f'(z^*) > 0,$$

$$\int_0^{2\pi} |F'(z_0(t)) z_0'(t)| dt = 2\pi,$$

lead to $\alpha = 0$ and $r = 1$. Hence $F(z) = f(z)$.

The integral equation (4.36) can also be written briefly as

$$g(z) + \int_\Gamma N^*(z,w) g(w) |dw| = 0, \qquad z \in \Gamma, \tag{4.39}$$

where

$$\begin{aligned} g(z) &= T(z) f'(z), \\ N^*(z,w) &= \frac{1}{2\pi \mathrm{i}} \left[\frac{T(z)}{(z-w)} - \frac{|f(z)|^2 \overline{T(z)}}{|f(w)|^2 (\overline{z} - \overline{w})} \right]. \end{aligned} \tag{4.40}$$

This integral equation will be used in Sections 5.3 and 5.4 for the numerical conformal mapping of doubly connected region onto an annulus and triply connected region onto an annulus with a slit.

Comparing (4.3) and (4.33) yields still another possible assignments, i.e.,

$$c(z) = -1,\ P(z) = 1,\ D(z) = f'(z)/f(z) \text{ and } Q(z) = T(z).$$

Application of Theorem 4.4 with Remark 1 to these assignments, along with the choice of $u(z) = \overline{T(z)Q(z)}$ and $v(z) = 1$, gives

$$\frac{f'(z)}{f(z)} + \mathrm{PV}\frac{1}{2\pi \mathrm{i}} \int_\Gamma \left[\frac{\overline{T(z)^2}}{(\overline{w} - \overline{z})\overline{T(w)}} - \frac{T(w)}{(w-z)} \right] \frac{f'(w)}{f(w)} |dw| = 0, \quad z \in \Gamma. \tag{4.41}$$

If we multiply both sides of (4.41) by $T(z)$, we obtain

$$T(z)\frac{f'(z)}{f(z)} + \mathrm{PV}\frac{1}{2\pi \mathrm{i}} \int_\Gamma \left[\frac{\overline{T(z)}}{(\overline{w} - \overline{z})} - \frac{T(z)}{(w-z)} \right] T(w)\frac{f'(w)}{f(w)} |dw| = 0, \quad z \in \Gamma. \tag{4.42}$$

The integral equation (4.42) can also be written briefly as

$$\Phi(z) + \int_\Gamma N(z,w)\Phi(w)|dw| = 0, \quad z \in \Gamma, \tag{4.43}$$

where $\Phi(z) = T(z)f'(z)/f(z)$ and N is again the Neumann kernel (2.22).

From (4.27) and (4.28), we see that

$$f'(z_0(t))z_0'(t) = \mathrm{i}\theta_0'(t)e^{\mathrm{i}\theta_0(t)} = \mathrm{i}f(z_0(t))\theta_0'(t), \quad 0 \le t \le \beta_0, \tag{4.44}$$

$$f'(z_p(t))z_p'(t) = \mathrm{i}\mu_p\theta_p'(t)e^{\mathrm{i}\theta_p(t)} = \mathrm{i}f(z_p(t))\theta_p'(t), \quad 0 \le t \le \beta_p. \tag{4.45}$$

In other words,

$$f'(z(\tau))z'(\tau) = \mathrm{i}f(z(\tau))\theta'(\tau), \quad z(\tau) \in \Gamma,\ 0 \le \tau \le \beta,$$

which implies

$$\frac{f'(z(\tau))}{f(z(\tau))}z'(\tau) = \mathrm{i}\theta'(\tau), \quad z(\tau) \in \Gamma,\ 0 \le \tau \le \beta.$$

Substituting this result into (4.43) and using the definition that $T(z(\tau)) = z'(\tau)/|z'(\tau)|$, we get

$$\theta'(\tau) + \int_0^\beta k(\tau,\sigma)\theta'(\sigma)d\sigma = 0, \quad 0 \le \tau \le \beta, \tag{4.46}$$

where

$$k(\tau,\sigma) = |z'(\tau)|N(z(\tau),z(\sigma)) = \begin{cases} \dfrac{1}{\pi}\mathrm{Im}\left[\dfrac{z'(\tau)}{z(\tau)-z(\sigma)}\right], & \text{if } \tau \neq \sigma, \\ \dfrac{1}{2\pi}\mathrm{Im}\left[\dfrac{z''(t)}{z'(\tau)}\right], & \text{if } \tau = \sigma. \end{cases}$$

For doubly connected regions, the integral equation (4.46) is also known as the Warschawski's equation (see Section 2.6.6).

4.5 Application to Conformal Mapping of Multiply Connected Regions onto a Disk with Circular Slits via the Neumann Kernel

This section gives an application of Theorem 4.1 to conformal mapping of multiply connected region Ω of connectivity $M+1$ onto a disk with circular slits. Let $w = f(z)$ be the analytic function which maps Ω conformally onto a disk $|w| < r$ with circular slits of radii $\mu_p r$, where $0 < \mu_p < 1$, $p = 1, 2, ..., M$ (see Figure 4.4). The function f could be made unique by prescribing (4.12).

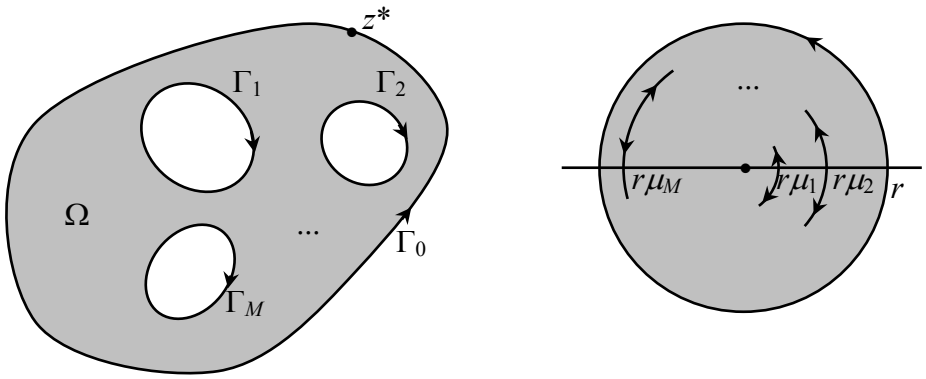

Figure 4.4: Mapping of a multiply connected region Ω of connectivity $M+1$ onto a disk with circular slits.

The boundary values of f can be represented in form

$$f(z_0(t)) = re^{\mathrm{i}\theta_0(\mathrm{t})}, \quad \Gamma_0 : z = z_0(t), \quad 0 \le t \le \beta_0, \tag{4.47}$$

$$f(z_p(t)) = \mu_p re^{\mathrm{i}\theta_p(t)}, \ \Gamma_p : z = z_p(t), \quad 0 \le t \le \beta_p, \quad p = 1, 2, ..., M, \tag{4.48}$$

where $\theta_0(t)$, $\theta_1(t)$, ..., $\theta_M(t)$ are the boundaries correspondence functions of Γ_0, Γ_1, ..., Γ_M respectively.

Thus it can be shown that

$$f(z_0(t)) = \frac{r}{\mathrm{i}} T(z_0(t)) \frac{\theta_0'(t)}{|\theta_0'(t)|} \frac{f'(z_0(t))}{|f'(z_0(t))|} = \frac{r}{\mathrm{i}} T(z_0(t)) \frac{f'(z_0(t))}{|f'(z_0(t))|}, \quad z_0 \in \Gamma_0, \tag{4.49}$$

$$f(z_p(t)) = \frac{\mu_p r}{\mathrm{i}} T(z_p(t)) \frac{\theta_p'(t)}{|\theta_p'(t)|} \frac{f'(z_p(t))}{|f'(z_p(t))|} = \pm \frac{\mu_p r}{\mathrm{i}} T(z_p(t)) \frac{f'(z_p(t))}{|f'(z_p(t))|}, \quad z_p \in \Gamma_p, \tag{4.50}$$

for $p = 1, 2, ..., M$. Note that $\theta_0'(t) > 0$ while $\theta_p'(t)$ may be positive or negative since the circular slit $f(\Gamma_p)$ is traversed twice. Thus $\theta_p'(t)/|\theta_p'(t)| = \pm 1$.

The boundary relationships (4.49) and (4.50) can be unified as

$$f(z) = \pm \frac{|f(z)|}{\mathrm{i}} T(z) \frac{f'(z)}{|f'(z)|}, \quad z \in \Gamma, \tag{4.51}$$

where $\Gamma = \Gamma_0 \cup \Gamma_1 \cup \cdots \cup \Gamma_M$. Note that the value of $|f(z)|$ is either r or $\mu_p r$ for $z \in \Gamma$. Squaring both sides of the boundary relationship (4.51) gives

$$f(z)^2 = -|f(z)|^2 T(z)^2 \frac{f'(z)^2}{|f'(z)|^2}, \quad z \in \Gamma. \tag{4.52}$$

Comparing (4.52) with (4.3), leads to a choice of $c(z) = -|f(z)|^2$, $P(z) = f(z)^2$, $D(z) = f'(z)$, $Q(z) = T(z)$, $u(z) = \overline{T(z)Q(z)}$ and $v(z) = 1$. Substituting these assignments into (4.4) leads to an integral equation satisfied by $f'(z)$, i.e.,

$$\begin{aligned} f'(z) + \mathrm{PV} \frac{1}{2\pi \mathrm{i}} \int_\Gamma \left[\frac{|f(z)|^2 \overline{T(z)^2}}{|f(w)|^2 (\overline{w} - \overline{z}) \overline{T(w)}} - \frac{T(w)}{(w - z)} \right] f'(w) |dw| \\ = |f(z)|^2 \overline{T(z)^2} \left[\sum_{a_j inside \Gamma} \operatorname*{Res}_{w = a_j} \frac{f'(w)}{(w - z) f(w)^2} \right]^-, \quad z \in \Gamma. \end{aligned} \tag{4.53}$$

To evaluate the residue in equation (4.53) we use the fact that if $f(w) = g(w)/h(w)$ where g and h are analytic at a, and $g(a) \neq 0$, $h(a) = h'(a) = 0$, $h''(a) \neq 0$, which means a is a double pole of $f(w)$, then (Gonzalez, 1992)

$$\operatorname*{Res}_{w=a} f(w) = 2\frac{g'(a)}{h''(a)} - \frac{2}{3}\frac{h'''(a)g(a)}{h''(a)^2}. \tag{4.54}$$

Applying (4.54) to the residue in (4.53) and after several algebraic manipulations, we obtain

$$\operatorname*{Res}_{w=a} \frac{f'(w)}{(w-z)f(w)^2} = -\frac{1}{(a-z)^2 f'(a)}. \tag{4.55}$$

Thus integral equation (4.53) becomes

$$\begin{aligned} f'(z) + \mathrm{PV}\frac{1}{2\pi \mathrm{i}} \int_\Gamma \left[\frac{|f(z)|^2 \overline{T(z)^2}}{|f(w)|^2(\overline{w}-\overline{z})\overline{T(w)}} - \frac{T(w)}{(w-z)} \right] f'(w)|dw| \\ = -|f(z)|^2 \frac{\overline{T(z)^2}}{(\overline{a}-\overline{z})^2 f'(a)}, \qquad z \in \Gamma. \end{aligned} \tag{4.56}$$

Multiply both sides of the equation by $f'(a)T(z)$ and use the fact that $T(z)\overline{T(z)} = |T(z)|^2 = 1$ gives

$$\begin{aligned} & f'(a)T(z)f'(z) \\ & + \mathrm{PV}\frac{1}{2\pi \mathrm{i}} \int_\Gamma \left[\frac{|f(z)|^2 \overline{T(z)}}{|f(w)|^2(\overline{w}-\overline{z})} - \frac{T(z)}{(w-z)} \right] f'(a)T(w)f'(w)|dw| \\ & = -|f(z)|^2 \frac{\overline{T(z)}}{(\overline{a}-\overline{z})^2}, \qquad z \in \Gamma. \end{aligned} \tag{4.57}$$

Equation (4.57) can also be written as

$$g(z,a) + \int_\Gamma N^*(z,w)g(w,a)|dw| = |f(z)|^2 h(a,z), \qquad z \in \Gamma. \tag{4.58}$$

where the kernel N^* is as given in (4.40) and

$$\begin{aligned} g(z,a) &= f'(a)T(z)f'(z), \\ h(a,z) &= -\frac{\overline{T(z)}}{(\overline{a}-\overline{z})^2}. \end{aligned}$$

This integral equation will be used in Chapter 6 for the numerical conformal mapping of multiply connected regions onto a disk with slits.

CHAPTER 5

NUMERICAL CONFORMAL MAPPING OF MULTIPLY CONNECTED REGIONS ONTO AN ANNULUS WITH CIRCULAR SLITS

5.1 Introduction

We have discussed in Chapter 4 the theoretical aspects of constructing some integral equations for conformal mapping of doubly connected region onto an annulus via the Kerzman-Stein kernel and conformal mapping of multiply connected regions onto an annulus with circular slits via the Neumann kernel. In this chapter, we shall discuss the numerical aspects of conformal mapping of multiply connected regions based on the integral equation developed in Chapter 4.

5.2 Conformal Mapping of Doubly Connected Regions onto an Annulus via the Kerzman-Stein Kernel

5.2.1 A System of Integral Equations

Suppose Ω is a doubly connected region bounded by Γ_0 and Γ_1 as shown in Figure 4.1. Since Ω is a doubly connected region, the single integral equation

in (4.26) can be separated into a system of equations

$$\eta(z_0) + \int_{\Gamma_0} A(z_0, w)\eta(w)|dw| - \int_{-\Gamma_1} P(z_0, w)\eta(w)|dw| = 0, \quad z_0 \in \Gamma_0, \tag{5.1}$$

$$\eta(z_1) + \int_{\Gamma_0} Q(z_1, w)\eta(w)|dw| - \int_{-\Gamma_1} A(z_1, w)\eta(w)|dw| = 0, \quad z_1 \in \Gamma_1, \tag{5.2}$$

where

$$\begin{aligned}
\eta(z) &= \sqrt{f'(z)}, \\
P(z,w) &= \frac{1}{2\pi \mathrm{i}} \left[\frac{\overline{T(z)}}{\mu(\overline{w} - \overline{z})} - \frac{T(w)}{(w-z)} \right], \\
Q(z,w) &= \frac{1}{2\pi \mathrm{i}} \left[\frac{\mu\overline{T(z)}}{(\overline{w} - \overline{z})} - \frac{T(w)}{(w-z)} \right], \\
A(z,w) &= \begin{cases} \overline{H(w,z)} - H(z,w), & w, z \in \Gamma, w \neq z, \\ 0, & w = z \in \Gamma, \end{cases} \\
H(w,z) &= \frac{1}{2\pi \mathrm{i}} \frac{T(z)}{(z-w)}, \quad w \in \Omega \cup \Gamma, z \in \Gamma, w \neq z.
\end{aligned}$$

The kernel A is known as the Kerzman-Stein kernel (Kerzman and Trummer, 1986) and is smooth and skew-Hermitian. The kernel H is usually referred to as the Cauchy kernel. The integral equations (5.1) and (5.2) involve the unknown parameter μ. To obtain a unique solution, we first consider applying the condition $f(z_0(0)) = 1$. For the test regions that we have chosen, the unit tangent vector $T(z_0(0))$ is equal to i. From equation (4.15), this implies $\eta(z_0(0))^2/|\eta(z_0(0))|^2 = 1$, which means

$$\mathrm{Re}\,[\eta(z_0(0))^2/|\eta(z_0(0)|^2] = 1, \tag{5.3}$$

$$\mathrm{Im}\,[\eta(z_0(0))^2] = 0. \tag{5.4}$$

Next we consider equation (4.13), which upon differentiation and taking modulus on both sides, gives

$$|f'(z_0(t))z_0'(t)| = |e^{\mathrm{i}\theta_0(t)}\mathrm{i}\theta_0'(t)| = |\theta_0'(t)|. \tag{5.5}$$

Since the boundary correspondence function $\theta_0(t)$ is an increasing monotone function and it's derivative is positive, we have $|\theta_0'(t)| = \theta_0'(t)$. Thus, upon integrating (5.5) with respect to t form 0 to 2π gives

$$\int_0^{2\pi} |f'(z_0(t))z_0'(t)|dt = \int_0^{2\pi} \theta_0'(t)dt = \theta_0(t)|_0^{2\pi} = 2\pi. \tag{5.6}$$

We note that, in Chapter 3 however did not use the conditions (5.3), (5.4) and (5.6) to achieve uniqueness, but instead

$$\mu \int_0^{2\pi} |\eta(z_0(t))z_0'(t)|dt - \int_0^{2\pi} |\eta(z_1(t))z_1'(t)|dt = 0$$

and

$$f'(z^*) = B^*$$

where B^* is predetermined.

Thus the system of integral equations comprising of (5.1), (5.2) with the conditions (5.3), (5.4) and (5.6) has a unique solution.

5.2.2 Numerical Implementation

In Chapter 3 have shown how to treat the equations (5.1) and (5.2) numerically and obtained the system (3.42) i.e.

$$\begin{pmatrix} \text{Re } \mathbf{A} & \cdots & \text{Im } \mathbf{A} \\ \vdots & \ddots & \vdots \\ \text{Im } \mathbf{A} & \cdots & \text{Re } \mathbf{A} \end{pmatrix} \begin{pmatrix} \text{Re } \mathbf{x} \\ \vdots \\ \text{Im } \mathbf{x} \end{pmatrix} = \begin{pmatrix} 0 \\ \vdots \\ 0 \end{pmatrix}. \tag{5.7}$$

The system of equations (5.6), (5.3) and (5.4) can be written briefly as

$$\int_0^{\beta_0} |\phi_0(s)|^2 ds = 2\pi, \tag{5.8}$$

$$\text{Re}\,[\phi_0(0)^2/|\phi_0(0)|^2] = 1, \tag{5.9}$$

$$\text{Im}\,[\phi_0(0)^2] = 0. \tag{5.10}$$

where

$$\begin{aligned}\phi_0(t) &= |z_0'(t)|^{1/2}\eta(z_0(t)),\\ \phi_1(t) &= |z_1'(t)|^{1/2}\eta(z_1(t)).\end{aligned}$$

Since $\phi = \mathrm{Re}\,\phi + \mathrm{i}\,\mathrm{Im}\,\phi$, equations (5.8), (5.9) and (5.10) become

$$\sum_{j=1}^{n}((\mathrm{Re}\,x_{0j})^2 + (\mathrm{Im}\,x_{0j})^2) = n, \tag{5.11}$$

$$\mathrm{Re}\,[x_{01}^2/((\mathrm{Re}\,x_{01})^2 + (\mathrm{Im}\,x_{01})^2)] = 1, \tag{5.12}$$

$$\mathrm{Im}\,x_{01}^2 = 0. \tag{5.13}$$

Therefore, the real nonlinear system in (5.7) can be solved simultaneously with the equations (5.11), (5.12) and (5.13) which also involves the Re and Im parts of the unknown functions. This system is an over-determined system of nonlinear equations involving $2(n+m)+3$ equations in $2(n+m)+1$ unknowns. As in Chapter 3, we also use Gauss-Newton method to solve this nonlinear least square problem.

5.2.3 Numerical Results

For our numerical experiments, we have used three test regions i.e. frame of Cassini's oval, ellipse/circle and elliptical domain with circular hole. The exact boundary correspondence function for Cassini's oval is discussed in Section 2.5.5. All the computations are done using MATHEMATICA package (Wolfram, 1991) in single precision (16 digit machine precision). We also show the comparisons of our numerical computations for the test regions with with those obtained by Amano (1994), Ellacott (1979), Papamicheal and Warby (1984) and Symm (1969).

Example 5.1. *Frame of Cassini's Oval:*

Let

$$\Gamma_0 : z(t) = \sqrt{b_0^2 \cos 2t + \sqrt{a_0^4 - b_0^4 \sin^2 2t}}\, e^{it}, \quad a_0 > 0,\ b_0 > 0,$$

$$\Gamma_1 : z(t) = \sqrt{b_1^2 \cos 2t + \sqrt{a_1^4 - b_1^4 \sin^2 2t}}\, e^{it}, \quad a_1 > 0,\ b_1 > 0, \quad 0 \le t \le 2\pi.$$

The exact mapping function is

$$f(z) = \frac{a_0 z}{\sqrt{b_0^2 z^2 + a_0^4 - b_0^4}}, \quad \mu = \frac{a_0 b_1}{a_1 b_0}.$$

Figure 5.1 shows the region and image based on our method. The results for the sub-norm error between the exact values of $\theta_0(t)$, $\theta_1(t)$, μ and their corresponding approximations $\theta_{0n}(t)$, $\theta_{1n}(t)$, μ_n are shown in Table 4.1. Table 4.2 shows the results obtained in Chapter 3 with different normalizing conditions from ours. Table 4.3 shows the results calculated by Amano (1994) and Symm (1969), though their distributions are different from ours. The notations E_M and E_A that are used by Amano or Symm are defined as follows:

$$E_M = \max\{\max_i ||f(z_0(t_i))| - 1|, \max_i ||f(z_1(t_i))| - \mu|\}, \tag{5.14}$$

$$E_A = \max\{\|\theta_0(t) - \theta_{0n}(t)\|_\infty, \|\theta_1(t) - \theta_{1n}(t)\|_\infty\}. \tag{5.15}$$

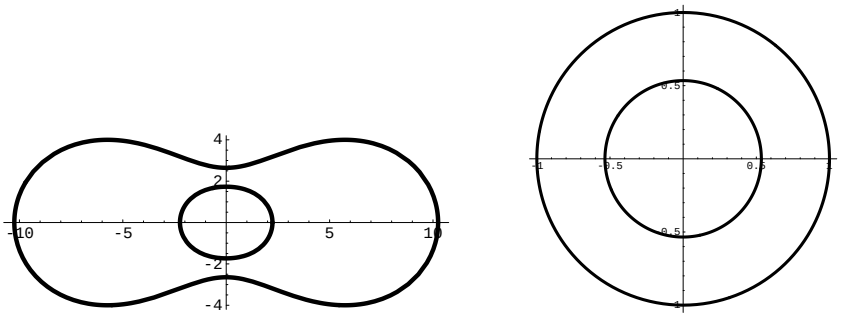

Figure 5.1: Frame of Cassini's Oval with $a_0 = 2\sqrt{14}, a_1 = 2, b_0 = 7$, and $b_1 = 1$.

Table 5.1: Error norm (frame of Cassini's oval) using our method

$n = m$	minimal $S(\mathbf{x})$	$\|\theta_0(t) - \theta_{0n}(t)\|_\infty$	$\|\theta_1(t) - \theta_{1n}(t)\|_\infty$	$\|\mu - \mu_n\|_\infty$
16	8.4(−31)	6.4(−03)	2.5(−03)	2.1(−03)
32	8.4(−30)	6.9(−05)	2.7(−05)	2.1(−05)
64	5.5(−30)	1.1(−08)	4.1(−09)	3.1(−09)
128	3.4(−28)	2.7(−15)	8.9(−16)	1.1(−16)

Table 5.2: Error norm (frame of Cassini's oval) in Chapter 3 with different conditions

$n = m$	$\|\theta_0(t) - \theta_{0n}(t)\|_\infty$	$\|\theta_1(t) - \theta_{1n}(t)\|_\infty$	$\|\mu - \mu_n\|_\infty$
16	6.4(−03)	2.5(−03)	2.1(−03)
32	6.9(−05)	2.7(−05)	2.1(−05)
64	1.1(−08)	3.7(−09)	3.9(−09)

Table 5.3: Error Norm (frame of Cassini's oval) using Amano's method and Symm's method

Amano's Method			Symm's Method	
$n = m$	E_M	E_A	$n = m$	E_M
16	9.1(−03)	9.7(−03)	64	1.94(−02)
32	3.4(−04)	3.8(−04)	128	3.00(−03)
64	6.9(−07)	5.0(−08)	256	7.00(−04)
128	7.7(−11)	7.7(−11)		

Example 5.2. *Ellipse/Circle:*

Let

$$\begin{aligned} \Gamma_0 : z(t) &= 2\cos t + \mathrm{i}\sin t, \\ \Gamma_1 : z(t) &= 0.5\,(\cos t + \mathrm{i}\sin t), \quad 0 \le t \le 2\pi. \end{aligned}$$

We have adopted this example problem from Ellacott (1979) with $\mu_E = 0.4141$ for comparison. See Table 4.4 for radius comparisons. Figure 5.2 shows the region and its image based on our method.

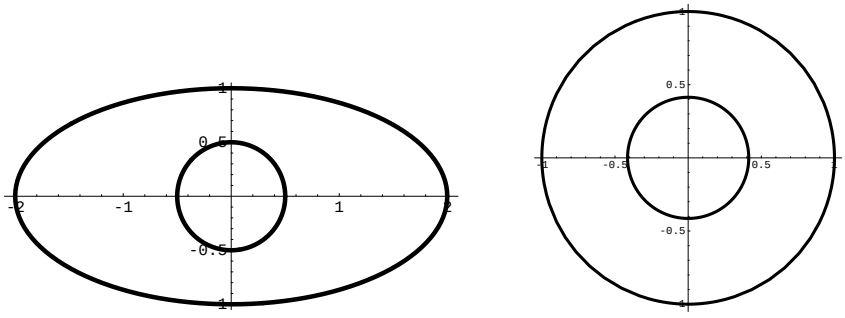

Figure 5.2: Conformal mapping ellipse/circle onto an annulus

Table 5.4: The radius comparison for ellipse/circle

$n = m$	minimal $S(\mathbf{x})$	Radius Comparison $\mu - \mu_E$	Value of μ
8	3.0(−31)	2.7(−02)	0.441484
16	4.9(−30)	3.8(−04)	0.4144811
32	4.2(−30)	2.0(−05)	0.4141199465
64	9.3(−28)	2.0(−05)	0.414119807860853

Example 5.3. *Elliptical Region with Circular Hole:*

Let

$$\Gamma_0 = \{(x, y) : (x + \frac{1}{2}a_0)^2/a_0^2 + y^2 = 1\},$$
$$\Gamma_1 = \{(x, y) : x^2 + y^2 = \frac{1}{9}a_0^2\}, \quad 1 < a_0 \leq 2.$$

We have adopted this example problem from Papamichael and Warby (1984) for comparison of μ. Since the conditions of the problem are somewhat different, $A = w : \mu < |w| < 1$ in ours and $a = w : 1 < |w| < M$ in Papamichael and Warby (1984), our radius μ should be multiplied by M for comparison (See

Table 4.5). In Table 4.6, we list the computed approximations of μ based on our method and the computed approximations to the modulus M based on Papamichael and Warby method. The notation E_N that is used by Papamichael and Warby is defined as

$$E_N = \max\{\max_i ||f(z_0(t_i))| - M||, \max_i ||f(z_1(t_i))| - 1||\}, \tag{5.16}$$

Figure 5.3 shows the region and its image based on our method.

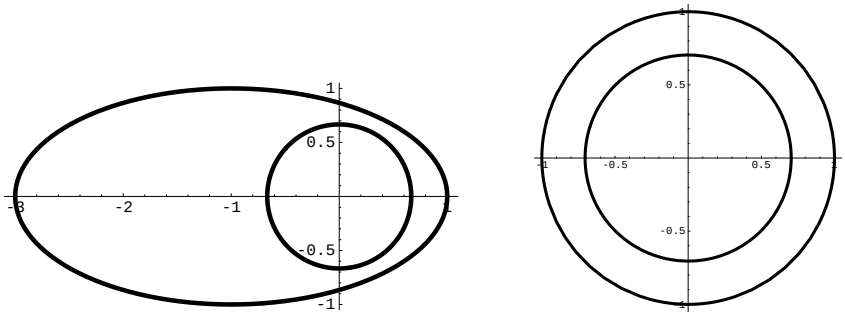

Figure 5.3: Conformal mapping elliptical region with circular hole onto an annulus with $a_0 = 0.20$.

Table 5.5: The computed approximations of μ and M for elliptical region with circular hole

	Our Method	Papamichael and Warby Method	
a_0	μ	M	$1/M$
1.04	0.4803797010421916	2.081686628	0.4803797010315426
1.08	0.4869154853494373	2.053744500	0.4869154853488348
1.20	0.5080480086200778	1.968317921	0.5080480085716803
1.40	0.5480734581257742	1.824572938	0.5480734582724585
1.60	0.5938360511745354	1.683966719	0.5938359640467455
1.80	0.6455396040618700	1.549091634	0.6455396040180280
2.00	0.7043817963286256	1.419684616	0.7043817963017217

Table 5.6: The radius comparison for elliptical region with circular hole

a_0	$n=m$	minimal $S(\mathbf{x})$	$\|\mu-1/M\|_\infty$	$n=m$	E_N
1.04	32	4.6(−29)	2.0(−06)	31	2.1(−05)
1.08	32	8.4(−31)	1.4(−06)	31	8.7(−06)
1.20	32	5.2(−30)	3.0(−07)	29	7.5(−08)
1.40	32	1.4(−29)	1.9(−08)	29	2.0(−06)
1.60	32	3.7(−29)	2.4(−06)	25	3.2(−05)
1.80	32	1.3(−29)	3.5(−05)	23	3.9(−04)
2.00	32	2.3(−29)	1.1(−04)	27	2.0(−03)

5.3 Conformal Mapping of Doubly Connected Regions onto an Annulus via the Neumann Kernel

5.3.1 A System of Integral Equations

Suppose Ω is a doubly connected region bounded by Γ_0 and Γ_1 (see Figure 4.3 with $M=1$). For the special case where Ω is a doubly connected region, the single integral equation in (4.39) can be separated into a system of equations

$$g(z_0)+\int_{\Gamma_0} N(z_0,w)g(w)|dw|-\int_{-\Gamma_1} P_0(z_0,w)g(w)|dw|=0, \quad z_0\in\Gamma_0, \tag{5.17}$$

$$g(z_1)+\int_{\Gamma_0} P_1(z_1,w)g(w)|dw|-\int_{-\Gamma_1} N(z_1,w)g(w)|dw|=0. \quad z_1\in\Gamma_1, \tag{5.18}$$

where

$$\begin{aligned}
g(z) &= T(z)f'(z),\\
P_0(z,w) &= \frac{1}{2\pi \mathrm{i}}\left[\frac{T(z)}{(z-w)}-\frac{\overline{T(z)}}{\mu_1^2(\overline{z}-\overline{w})}\right],\\
P_1(z,w) &= \frac{1}{2\pi \mathrm{i}}\left[\frac{T(z)}{(z-w)}-\frac{\mu_1^2\overline{T(z)}}{(\overline{z}-\overline{w})}\right],\\
N(z,w) &= \begin{cases} \dfrac{1}{\pi}\operatorname{Im}\left[\dfrac{T(z)}{z-w}\right], & \text{if } w,z\in\Gamma, w\neq z,\\ \dfrac{1}{2\pi}\dfrac{\operatorname{Im}[z''(t)\overline{z'(t)}]}{|z'(t)|^3}, & \text{if } w=z\in\Gamma. \end{cases}
\end{aligned}$$

The kernel N is also known as the Neumann kernel (Henrici, 1974). Note that the PV symbols are no longer required in (5.17) and (5.18) since the integrands are continuous along their respective paths of integrations. The integral equations (5.17) and (5.18) also involve the unknown parameter μ_1. Naturally it is also required that the unknown mapping function $f(z)$ be single-valued in the problem domain (Henrici, 1974, p. 217), i.e.,

$$\int_{-\Gamma_1} f'(w)dw = 0 \tag{5.19}$$

which implies

$$\int_{-\Gamma_1} g(w)|dw| = 0. \tag{5.20}$$

Note that the system of integral equations consisting of (5.17), (5.18) and (5.20) is homogeneous and does not have a unique solution. To obtain a unique solution, we need to impose some conditions on $g(z)$. First, we consider applying the condition $f(z_0(0)) = 1$. From (4.29), this implies $g(z_0(0))/|g(z_0(0))| = \mathrm{i}$, which means

$$\begin{aligned} \mathrm{Re}\,[g(z_0(0))] &= 0, & (5.21)\\ \mathrm{Im}\,[g(z_0(0))/|g(z_0(0)|] &= 1. & (5.22) \end{aligned}$$

Next we consider equations (4.27) and (4.28). Upon differentiation and taking modulus to both sides of equations (4.27) and (4.28), gives

$$\begin{aligned} |T(z_0(t))f'(z_0(t))z_0'(t)| &= |T(z_0(t))e^{\mathrm{i}\theta_0(\mathrm{t})}\mathrm{i}\theta_0'(\mathrm{t})| = |\theta_0'(\mathrm{t})|. & (5.23)\\ |T(z_1(t))f'(z_1(t))z_1'(t)| &= |T(z_1(t))\mu_1 e^{\mathrm{i}\theta_1(\mathrm{t})}\mathrm{i}\theta_1'(\mathrm{t})| = \mu_1|\theta_1'(\mathrm{t})|. & (5.24) \end{aligned}$$

Since the boundary correspondence functions $\theta_0(t)$ and $\theta_1(t)$ are increasing monotone functions, their derivatives are positive which implies $|\theta_0'(t)| = \theta_0'(t)$ and $|\theta_1'(t)| = \theta_1'(t)$. Upon integrating (5.23) and (5.24) with respect to t form 0 to 2π gives

$$\begin{aligned} \int_0^{2\pi} |g(z_0(t))z_0'(t)|dt &= \int_0^{2\pi} \theta_0'(t)dt = \theta_0(t)|_0^{2\pi} = 2\pi, & (5.25)\\ \int_0^{2\pi} |g(z_1(t))z_1'(t)|dt &= \mu_1 \int_0^{2\pi} \theta_1'(t)dt = \mu_1\theta_1(t)|_0^{2\pi} = \mu_1 2\pi. & (5.26) \end{aligned}$$

Thus the system of integral equations comprising of (5.17), (5.18), (5.20) with the conditions (5.21), (5.22), (5.25) and (5.26) has a unique solution.

5.3.2 Numerical Implementation

Suppose Γ_0 and Γ_1 be given in parametric representations as follows:

$$\begin{aligned}\Gamma_0 : &\qquad z = z_0(t), \quad 0 \le t \le \beta_0,\\ \Gamma_1 : &\qquad z = z_1(t), \quad 0 \le t \le \beta_1.\end{aligned}$$

Then the system of integral equations (5.17), (5.18), (5.20), (5.25) and (5.26) become

$$\begin{aligned} g(z_0(t)) + \int_0^{\beta_0} & N(z_0(t), z_0(s)) g(z_0(s)) |z_0'(s)| ds \\ & - \int_0^{\beta_1} P_0(z_0(t), z_1(s)) g(z_1(s)) |z_1'(s)| ds = 0, \quad z_0(t) \in \Gamma_0, \end{aligned} \tag{5.27}$$

$$\begin{aligned} g(z_1(t)) + \int_0^{\beta_0} & P_1(z_1(t), z_0(s)) g(z_0(s)) |z_0'(s)| ds \\ & - \int_0^{\beta_1} N(z_1(t), z_1(s)) g(z_1(s)) |z_1'(s)| ds = 0, \quad z_1(t) \in \Gamma_1, \end{aligned} \tag{5.28}$$

$$\int_0^{\beta_1} g(z_1(s)) |z_1'(s)| ds = 0, \tag{5.29}$$

$$\int_0^{\beta_0} |g(z_0(s)) z_0'(s)| ds = 2\pi, \tag{5.30}$$

$$\int_0^{\beta_1} |g(z_1(s)) z_1'(s)| ds = 2\pi\mu_1. \tag{5.31}$$

Multiply (5.27) and (5.28) respectively by $|z_0'(t)|$ and $|z_1'(t)|$ gives

$$\begin{aligned} |z_0'(t)| g(z_0(t)) + \int_0^{\beta_0} & |z_0'(t)| N(z_0(t), z_0(s)) g(z_0(s)) |z_0'(s)| ds \\ & - \int_0^{\beta_1} |z_0'(t)| P_0(z_0(t), z_1(s)) g(z_1(s)) |z_1'(s)| ds = 0, \quad z_0(t) \in \Gamma_0, \end{aligned} \tag{5.32}$$

$$\begin{aligned} |z_1'(t)| g(z_1(t)) + \int_0^{\beta_0} & |z_1'(t)| P_1(z_1(t), z_0(s)) g(z_0(s)) |z_0'(s)| ds \\ & - \int_0^{\beta_1} |z_1'(t)| N(z_1(t), z_1(s)) g(z_1(s)) |z_1'(s)| ds = 0, \quad z_1(t) \in \Gamma_1. \end{aligned} \tag{5.33}$$

Defining

$$\begin{aligned}
\phi_0(t) &= |z_0'(t)|g(z_0(t)),\\
\phi_1(t) &= |z_1'(t)|g(z_1(t)),\\
K_{00}(t_0,s_0) &= |z_0'(t)|N(z_0(t),z_0(s)),\\
K_{01}(t_0,s_1) &= |z_0'(t)|P_0(z_0(t),z_1(s)),\\
K_{10}(t_1,s_0) &= |z_1'(t)|P_1(z_1(t),z_0(s)),\\
K_{11}(t_1,s_1) &= |z_1'(t)|N(z_1(t),z_1(s)),
\end{aligned}$$

the system of equations (5.32), (5.33), (5.29), (5.30), (5.31), (5.21) and (5.22) can be briefly written as

$$\phi_0(t)+\int_0^{\beta_0}K_{00}(t_0,s_0)\phi_0(s)ds-\int_0^{\beta_1}K_{01}(t_0,s_1)\phi_1(s)ds = 0, \quad (5.34)$$

$$\phi_1(t)+\int_0^{\beta_0}K_{10}(t_1,s_0)\phi_0(s)ds-\int_0^{\beta_1}K_{11}(t_1,s_1)\phi_1(s)ds = 0, \quad (5.35)$$

$$\int_0^{\beta_1}\phi_1(s)ds = 0, \quad (5.36)$$

$$\int_0^{\beta_0}|\phi_0(s)|ds = 2\pi, \quad (5.37)$$

$$\int_0^{\beta_1}|\phi_1(s)|ds = 2\pi\mu_1, \quad (5.38)$$

$$\mathrm{Re}\,\phi_0(0) = 0, \quad (5.39)$$

$$\mathrm{Im}\,[\phi_0(0)/|\phi_0(0)|] = 1. \quad (5.40)$$

Since the functions ϕ and K in the above systems are β-periodic, a reliable procedure for solving (5.34) to (5.38) numerically is by using the Nyström's method. We choose $\beta_0 = \beta_1 = 2\pi$ and n equidistant collocation points $t_i = (i-1)\beta_0/n$, $1 \le i \le n$ on Γ_0 and m equidistant collocation points $t_{\tilde{i}} = (\tilde{i}-1)\beta_1/m$, $1 \le \tilde{i} \le m$, on Γ_1. Applying the Nyström's method with trapezoidal rule to discretize (5.34) to (5.38), we obtain

$$\phi_0(t_i)+\frac{\beta_0}{n}\sum_{j=1}^{n}K_{00}(t_i,t_j)\phi_0(t_j)-\frac{\beta_1}{m}\sum_{\tilde{j}=1}^{m}K_{01}(t_i,t_{\tilde{j}})\phi_1(t_{\tilde{j}}) = 0, \quad (5.41)$$

$$\phi_1(t_{\tilde{i}})+\frac{\beta_0}{n}\sum_{j=1}^{n}K_{10}(t_{\tilde{i}},t_j)\phi_0(t_j)-\frac{\beta_1}{m}\sum_{\tilde{j}=1}^{m}K_{11}(t_{\tilde{i}},t_{\tilde{j}})\phi_1(t_{\tilde{j}}) = 0, \quad (5.42)$$

$$\sum_{\tilde{j}=1}^{m} \phi_1(t_{\tilde{j}}) = 0, \tag{5.43}$$

$$\sum_{j=1}^{n} |\phi_0(t_j)| = n, \tag{5.44}$$

$$\sum_{\tilde{j}=1}^{m} |\phi_1(t_{\tilde{j}})| = m\mu_1. \tag{5.45}$$

Equations (5.41) to (5.45) lead to a system of $(n + m + 3)$ non-linear complex equations in n unknowns $\phi_0(t_i)$, m unknowns $\phi_1(t_{\tilde{i}})$ and μ_1. By defining the matrices

$$\begin{aligned} x_{0i} &= \phi_0(t_i), \\ x_{1\tilde{i}} &= \phi_1(t_{\tilde{i}}), \\ B_{ij} &= \frac{\beta_0}{n} K_{00}(t_i, t_j), \\ C_{i\tilde{j}} &= \frac{\beta_1}{m} K_{01}(t_i, t_{\tilde{j}}), \\ D_{\tilde{i}j} &= \frac{\beta_0}{n} K_{10}(t_{\tilde{i}}, t_j), \\ E_{\tilde{i}\tilde{j}} &= \frac{\beta_1}{m} K_{11}(t_{\tilde{i}}, t_{\tilde{j}}), \end{aligned}$$

the system of equations (5.41) and (5.42) can be written as $n + m$ by $n + m$ system of equations

$$[I_{nn} + B_{nn}]\mathbf{x}_{0n} - C_{nm}\mathbf{x}_{1m} = 0, \tag{5.46}$$

$$D_{mn}\mathbf{x}_{0n} + [I_{mm} - E_{mm}]\mathbf{x}_{1m} = 0. \tag{5.47}$$

The result in matrix form for the system of equations (5.46) and (5.47) is

$$\begin{pmatrix} I_{nn} + B_{nn} & \cdots & -C_{nm} \\ \vdots & \cdots & \vdots \\ D_{mn} & \cdots & I_{mm} - E_{mm} \end{pmatrix} \begin{pmatrix} \mathbf{x}_{0n} \\ \vdots \\ \mathbf{x}_{1m} \end{pmatrix} = \begin{pmatrix} 0_{0n} \\ \vdots \\ 0_{1m} \end{pmatrix}. \tag{5.48}$$

Defining

$$\mathbf{A} = \begin{pmatrix} I_{nn} + B_{nn} & \cdots & -C_{nm} \\ \vdots & \cdots & \vdots \\ D_{mn} & \cdots & I_{mm} - E_{mm} \end{pmatrix}, \mathbf{x} = \begin{pmatrix} \mathbf{x}_{0n} \\ \vdots \\ \mathbf{x}_{1m} \end{pmatrix} \text{ and } \mathbf{0} = \begin{pmatrix} 0_{0n} \\ \vdots \\ 0_{1m} \end{pmatrix},$$

the $(n+m)\times(n+m)$ system can be written briefly as $\mathbf{Ax}=\mathbf{0}$. Separating $\mathbf{A}$ and $\mathbf{x}$ in terms of the real and imaginary parts, the system can be written as

$$\mathrm{Re}\,\mathbf{A}\,\mathrm{Re}\,\mathbf{x}-\mathrm{Im}\,\mathbf{A}\,\mathrm{Im}\,\mathbf{x}+\mathrm{i}(\,\mathrm{Im}\mathbf{A}\,\mathrm{Re}\,\mathbf{x}+\mathrm{Re}\,\mathbf{A}\,\mathrm{Im}\,\mathbf{x})=\mathbf{0}+\mathbf{0}\mathrm{i}. \tag{5.49}$$

The single $(n+m)\times(n+m)$ complex system (5.49) above is equivalent to the $2(n+m)\times 2(n+m)$ system matrix involving the real (Re) and imaginary (Im) of the unknown functions, i.e.,

$$\begin{pmatrix} \mathrm{Re\ A} & \cdots & \mathrm{Im\ A} \\ \vdots & \cdots & \vdots \\ \mathrm{Im\ A} & \cdots & \mathrm{Re\ A} \end{pmatrix}\begin{pmatrix} \mathrm{Re}\,\mathbf{x} \\ \vdots \\ \mathrm{Im}\,\mathbf{x} \end{pmatrix}=\begin{pmatrix} 0 \\ \vdots \\ 0 \end{pmatrix}. \tag{5.50}$$

Note that the matrix in (5.50) contains the unknown parameter μ_1.

Since $\phi=\mathrm{Re}\,\phi+\mathrm{i}\,\mathrm{Im}\,\phi$, equations (5.43), (5.44), (5.45), (5.39) and (5.40) becomes

$$\sum_{\tilde{j}=1}^{m}(\mathrm{Re}\,x_{1\tilde{j}}+\mathrm{i}\,\mathrm{Im}\,x_{1\tilde{j}}) = 0, \tag{5.51}$$

$$\sum_{j=1}^{n}\sqrt{(\mathrm{Re}\,x_{0j})^2+(\mathrm{Im}\,x_{0j})^2} = n, \tag{5.52}$$

$$\sum_{\tilde{j}=1}^{m}\sqrt{(\mathrm{Re}\,x_{1\tilde{j}})^2+(\mathrm{Im}\,x_{1\tilde{j}})^2} = m\mu_1, \tag{5.53}$$

$$\mathrm{Re}\,x_{01} = 0, \tag{5.54}$$

$$\mathrm{Im}\,[x_{01}/\sqrt{(\mathrm{Re}\,x_{01})^2+(\mathrm{Im}\,x_{01})^2}] = 1. \tag{5.55}$$

We next proceed to solve simultaneously the real nonlinear system in (5.50) with the equations (5.51) to (5.55) which also involves the Re and Im parts of the unknown functions. This system is an over-determined system of nonlinear equations involving $2(n+m)+5$ equations in $2(n+m)+1$ unknowns.

We tried using the Gauss-Newton algorithm for solving this system. However, it turns out that this algorithm failed to converge. Following the

recommendation given in Wolfe (1978, p. 233-246), we then applied one of the modifications of the Gauss-Newton namely the Lavenberg-Marquardt with the Fletcher's algorithm on this problem. This Lavenberg-Marquardt algorithm is more robust than the Gauss-Newton algorithm and is reasonably efficient and reliable for all the least-squares problem. However, it tends to be a bit slower than the Gauss-Newton algorithm.

Our nonlinear least square problem consists in finding the vector $\mathbf{x}$ for which the function $S : R^{2(n+m)+5} \rightarrow R^1$ defined by the sum of squares

$$S(\mathbf{x}) = \mathbf{f}^{\mathrm{T}}\mathbf{f} = \sum_{i=1}^{2(n+m)+5} (f_i(\mathbf{x}))^2$$

is minimal. Here, $\mathbf{x}$ stands for the $2(n+m)+1$ vector ($\mathrm{Re}\, x_{01}$, $\mathrm{Re}\, x_{02}$, ..., $\mathrm{Re}\, x_{0n}$, $\mathrm{Re}\, x_{11}$, $\mathrm{Re}\, x_{12}$, ..., $\mathrm{Re}\, x_{1m}$, $\mathrm{Im}\, x_{01}$, $\mathrm{Im}\, x_{02}$, ..., $\mathrm{Im}\, x_{0n}$, $\mathrm{Im}\, x_{11}$, $\mathrm{Im}\, x_{12}$, ..., $\mathrm{Im}\, x_{1m}$, μ_1), and $\mathbf{f} = (f_1, f_2, ..., f_{2(n+m)+5})$.

The Lavenberg-Marquardt algorithm is an iterative procedure with starting value denoted as $\mathbf{x}_0$. This initial approximation, which, if at all possible, should be well-informed guess and generate a sequence of approximations $\mathbf{x}_1$, $\mathbf{x}_2$, $\mathbf{x}_3$, ... base on the formula

$$\mathbf{x}_{k+1} = \mathbf{x}_k - H(\mathbf{x}_k)\mathbf{f}(\mathbf{x}_k), \qquad \lambda_k \geq 0, \tag{5.56}$$

where $H(\mathbf{x}_k) = ((J_{\mathbf{f}}(\mathbf{x}_k))^{\mathrm{T}} J_{\mathbf{f}}(\mathbf{x}_k) + \lambda_k I)^{-1} (J_{\mathbf{f}}(\mathbf{x}_k))^{\mathrm{T}}$.

Our strategy for getting the initial estimation $\mathbf{x}_0$ is based on (4.27) and (4.28) which upon differentiating, we obtain

$$\begin{aligned} \phi_0(t) &= f'(z_0(t))z_0'(t) = \mathrm{i}\theta_0'(\mathrm{t})\mathrm{e}^{\mathrm{i}\theta_0(\mathrm{t})}, \\ \phi_1(t) &= f'(z_1(t))z_1'(t) = \mu_1 \mathrm{i}\theta_1'(\mathrm{t})\mathrm{e}^{\mathrm{i}\theta_1(\mathrm{t})}. \end{aligned}$$

For initial estimation, we assume $\theta_0(t) = \theta_1(t) = t$ which implies $\theta_0'(t) = \theta_1'(t) = 1$ and choose $\mu_1 = 0.5$ as our initial guess of the inner radius. In all our

experiments, we have chosen the number of collocation points on Γ_0 and Γ_1 being equal, i.e., $n = m$. Having solved the system of equations for the unknown functions $\phi_0(t) = |z_0'(t)|T(z_0(t))f'(z_0(t))$, $\phi_1(t) = |z_1'(t)|T(z_1(t))f'(z_1(t))$ and μ_1, the boundary correspondence functions $\theta_0(t)$ and $\theta_1(t)$ are then computed approximately by the formulas

$$\begin{aligned}\theta_0(t) &= \text{Arg } f(z_0(t)) \approx \text{Arg}\,(-\mathrm{i}\phi_0(t)),\\ \theta_1(t) &= \text{Arg } f(z_1(t)) \approx \text{Arg}\,(-\mathrm{i}\phi_1(t)).\end{aligned}$$

We note that the numerical implementation described here are basically the same as in Mohamed and Murid (2007b) but with set of conditions different from (5.36) to (5.40).

Once the boundary values of the mapping function f are known, the values of the mapping function can be calculated by quadrature at any interior points of its domain of definition through Cauchy's integral formula for doubly connected region which read as follows:

Theorem 5.1 (Cauchy's Integral Formula)
Let f be analytic on the boundaries $\Gamma = \Gamma_0 \cup \Gamma_1$ and the region Ω bounded by Γ_0 and Γ_1. If ζ is any point on Ω, then

$$\begin{aligned}f(\zeta) &= \frac{1}{2\pi\mathrm{i}}\int_{\Gamma}\frac{f(z)}{z-\zeta}dz\\ &= \frac{1}{2\pi\mathrm{i}}\int_{\Gamma_0}\frac{f(z)}{z-\zeta}dz - \frac{1}{2\pi\mathrm{i}}\int_{-\Gamma_1}\frac{f(z)}{z-\zeta}dz.\end{aligned} \tag{5.57}$$

The Cauchy's integral formula (5.57) can be also written in the parametrized form, i.e.

$$f(\zeta) = \frac{1}{2\pi\mathrm{i}}\int_0^{\beta_0}\frac{f(z_0(t))z_0'(t)}{z_0(t)-\zeta}dt - \frac{1}{2\pi\mathrm{i}}\int_0^{\beta_1}\frac{f(z_1(t))z_1'(t)}{z_1(t)-\zeta}dt. \tag{5.58}$$

By using of (4.27) and (4.28), the Cauchy's integral formula (5.57) can then be written in the form

$$f(\zeta) = \frac{1}{2\pi\mathrm{i}}\int_0^{\beta_0}\frac{e^{\mathrm{i}\theta_0(t)}z_0'(t)}{z_0(t)-\zeta}dt - \frac{1}{2\pi\mathrm{i}}\int_0^{\beta_1}\frac{\mu_1 e^{\mathrm{i}\theta_1(t)}z_1'(t)}{z_1(t)-\zeta}dt. \tag{5.59}$$

For the points which are not close to the boundary, the integrands are well behaved. However for the points near the boundary, the numerical integration is inaccurate due to the influence of the singularity. This difficulty is overcome through the introduction of an iterative technique as given in Swarztrauber (1972, p. 303). If we define $f_0(\zeta)$ to be $f(z)$ where z is a point on the boundary which is closest to ζ, then we can define

$$f_{k+1}(\zeta) = \frac{1}{2\pi \mathrm{i}} \int_{\Gamma} \frac{f(z) - f_k(\zeta)}{z - \zeta} dz + f_k(\zeta). \tag{5.60}$$

In practice the iteration converges rapidly. Using this technique, we are able to maintain the same accuracy throughout the region Ω.

5.3.3 Numerical Results

For numerical experiments, we have used seven common test regions based on the examples given in Amano (1994), Ellacott (1979), and Symm (1969). All the computations are done using MATHEMATICA package (Wolfram, 1991) in single precision (16 digit machine precision).

There are four test regions whose exact boundary correspondence functions are known i.e. circular frame, frame of Limacon, elliptic frame and frame of Cassini's oval as discussed in Section 2.5. N number of collocation points on each boundary has been chosen. The results for the sub-norm error between the exact values of $\theta_0(t)$, $\theta_1(t)$, μ_1, $f(\zeta)$ and their corresponding approximations $\theta_{0n}(t)$, $\theta_{1n}(t)$, μ_{1n}, $f_k(\zeta)$ are shown in Tables 5.7, 5.8, 5.10, 5.11, 5.13, 5.14, 5.16 and 5.17. We also compare our numerical results with those obtained by Amano (1994), Symm (1969) and Ellacott (1979), though their distribution are different from ours (see equations (5.14), (5.15) and (5.16)).

Some integral equations do not involve the modulus μ_1^{-1} of the given doubly connected region such as the Warschawski's and Gershgorin's integral

equations (See Section 2.6.6). In such cases, the functions $\theta_0(t)$, $\theta_1(t)$ are determined first. Then, the modulus is computed using formula (2.14)

$$\begin{aligned}\operatorname{Log}\frac{1}{\mu_1} &= \operatorname{Log}\left|\frac{z_0(0)-\omega}{z_1(0)-\omega}\right| - \frac{1}{2\pi}\int_0^{\beta_0} \operatorname{Re}\frac{z_0'(t)}{z_0(t)-\omega}\theta_0(t)dt \\ &\quad + \frac{1}{2\pi}\int_0^{\beta_1} \operatorname{Re}\frac{z_1'(t)}{z_1(t)-\omega}\theta_1(t)dt, \end{aligned} \tag{5.61}$$

for ω is a any arbitrary point z interior to Γ_1.

In this thesis we have used our computed solutions $\theta_{0n}(t)$ and $\theta_{1n}(t)$ to approximate μ_1, represented by μ_{1n}^*, based on the formula (5.61). Since $\theta_{0n}(t)$ and $\theta_{1n}(t)$ are computed based on Nyström's method with trapezoidal rule, the approximation μ_{1n}^* is calculated by means of

$$\begin{aligned}\operatorname{Log}\frac{1}{\mu_{1n}^*} &= \operatorname{Log}\left|\frac{z_0(0)-\omega}{z_1(0)-\omega}\right| - \frac{1}{n}\sum_{i=1}^{n} \operatorname{Re}\frac{z_0'(t_i)}{z_0(t_i)-\omega}\theta_0(t_i) \\ &\quad + \frac{1}{n}\sum_{i=1}^{n} \operatorname{Re}\frac{z_1'(t_i)}{z_1(t_i)-\omega}\theta_1(t_i). \end{aligned} \tag{5.62}$$

The error norm $\|\mu_1 - \mu_{1n}^*\|$ are also displayed in the tables.

Example 5.4. *Frame of Cassini's Oval:*

$$\begin{aligned}\Gamma_0 : z(t) &= \sqrt{b_0^2\cos 2t + \sqrt{a_0^4 - b_0^4\sin^2 2t}}\, e^{\mathrm{i}t}, \quad a_0 > 0,\ b_0 > 0, \\ \Gamma_1 : z(t) &= \sqrt{b_1^2\cos 2t + \sqrt{a_1^4 - b_1^4\sin^2 2t}}\, e^{\mathrm{i}t}, \quad a_1 > 0,\ b_1 > 0, \quad 0 \le t \le 2\pi. \end{aligned}$$

The exact mapping function is

$$f(z) = \frac{a_0 z}{\sqrt{b_0^2 z^2 + a_0^4 - b_0^4}}, \qquad \mu_1 = \frac{a_0 b_1}{a_1 b_0}.$$

Figure 5.4 shows the region and image based on our method. Tables 5.7, 5.8 and 5.9 show our results together with the results of Amano (1994) and Symm (1969).

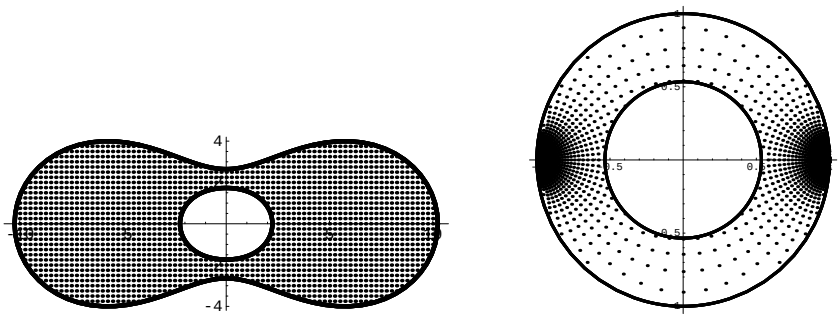

Figure 5.4: Frame of Cassini's Oval : a rectangular grid in Ω with grid size 0.25 and its image with $a_0 = 2\sqrt{14}, a_1 = 2, b_0 = 7$, and $b_1 = 1$.

Table 5.7: Error Norm (Frame of Cassini's oval) using our method

N	minimal $S(\mathbf{x})$	$\|\theta_0(t) - \theta_{0n}(t)\|_\infty$	$\|\theta_1(t) - \theta_{1n}(t)\|_\infty$
16	3.2(−28)	6.3(−03)	1.9(−03)
32	3.1(−28)	6.0(−05)	1.6(−05)
64	7.2(−30)	3.2(−08)	1.2(−08)
128	2.3(−28)	1.9(−08)	7.1(−09)

N	$\|\mu_1 - \mu_{1n}\|_\infty$	$\|\mu_1 - \mu^*_{1n}\|_\infty$
16	1.5(−03)	3.7(−03)
32	1.3(−05)	2.0(−03)
64	1.8(−09)	5.4(−04)
128	0	1.3(−04)

Table 5.8: Error Norm (Interior of Frame of Cassini's oval) using our method

N	$\|f_k(\zeta) - f(\zeta)\|_\infty$
32	9.3(−05)
64	3.8(−08)
128	1.1(−08)

Table 5.9: Error Norm (Frame of Cassini's oval) using Amano's method and Symm's method

Amano's Method			Symm's Method	
N	E_M	E_A	N	E_M
16	9.1(−03)	9.7(−03)	64	1.94(−02)
32	3.4(−04)	3.8(−04)	128	3.00(−03)
64	6.9(−07)	5.0(−08)	256	7.00(−04)
128	7.7(−11)	7.7(−11)		

Example 5.5. *Elliptic Frame:*

$$\begin{aligned}\Gamma_0 : z(t) &= a_0 \cos t + \mathrm{i}\, b_0 \sin t, \quad a_0 > 0,\ b_0 > 0,\\ \Gamma_1 : z(t) &= a_1 \cos t + \mathrm{i}\, b_1 \sin t, \quad a_1 > 0,\ b_1 > 0, \quad 0 \le t \le 2\pi.\end{aligned}$$

The exact mapping function is

$$f(z) = \frac{z + \sqrt{z^2 - (a_0^2 - b_0^2)}}{a_0 + b_0}, \qquad \mu_1 = \frac{a_1 + b_1}{a_0 + b_0}.$$

Figure 5.5 shows the region and image based on our method. Tables 5.10, 5.11 and 5.12 show our results together with the results of Amano (1994) and Symm (1969).

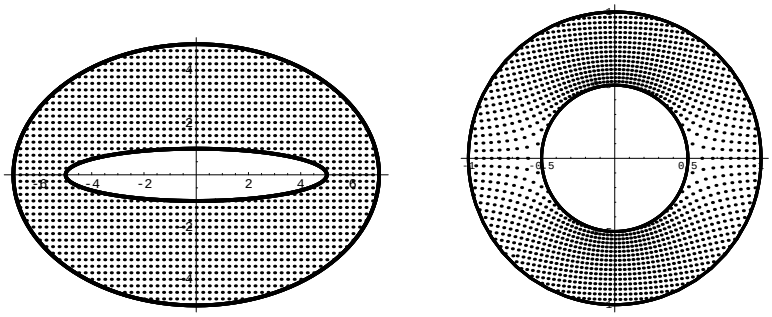

Figure 5.5: Elliptic Frame : a rectangular grid in Ω with grid size 0.25 and its image with $a_0 = 7, a_1 = 5, b_0 = 5$ and $b_1 = 1$.

Table 5.10: Error Norm (Elliptic Frame) using our method

N	minimal $S(\mathbf{x})$	$\|\theta_0(t) - \theta_{0n}(t)\|_\infty$	$\|\theta_1(t) - \theta_{1n}(t)\|_\infty$
16	5.6(−31)	2.3(−03)	6.6(−03)
32	2.8(−19)	3.5(−06)	9.9(−06)
64	3.2(−29)	1.9(−08)	1.7(−08)
128	4.9(−30)	7.6(−09)	6.7(−09)

N	$\|\mu_1 - \mu_{1n}\|_\infty$	$\|\mu_1 - \mu^*_{1n}\|_\infty$
16	2.0(−03)	9.4(−03)
32	3.0(−06)	1.1(−03)
64	7.0(−12)	1.9(−04)
128	5.6(−17)	4.7(−05)

Table 5.11: Error Norm (Interior of Elliptic Frame) using our method

N	$\|f_k(\zeta) - f(\zeta)\|_\infty$
32	1.2(−04)
64	3.1(−08)
128	3.3(−09)

Table 5.12: Error norm (Elliptic frame) using Amano's method and Symm's method

Amano's Method			Symm's Method	
N	E_M	E_A	N	E_M
16	2.8(−02)	3.8(−03)	64	2.52(−02)
32	3.2(−03)	7.0(−04)	128	3.90(−03)
64	8.4(−05)	2.7(−05)	256	6.00(−04)
128	1.2(−07)	1.8(−07)		

Example 5.6. *Frame of Limacon:*

$$\begin{aligned}\Gamma_0 : z(t) &= a_0 \cos t + b_0 \cos 2t + \mathrm{i}(a_0 \sin t + b_0 \sin 2t), \quad a_0 > 0,\ b_0 > 0,\\ \Gamma_1 : z(t) &= a_1 \cos t + b_1 \cos 2t + \mathrm{i}(a_1 \sin t + b_1 \sin 2t), \quad a_1 > 0,\ b_1 > 0.\end{aligned}$$

The exact mapping function is

$$f(z) = \frac{\sqrt{a_0^2 + 4b_0 z} - a_0}{2b_0}, \quad \mu_1 = \frac{a_1}{a_0}.$$

Figure 5.6 shows the region and image based on our method. Table 5.13, 5.14, and 5.15 show our results together with the result of Symm (1969).

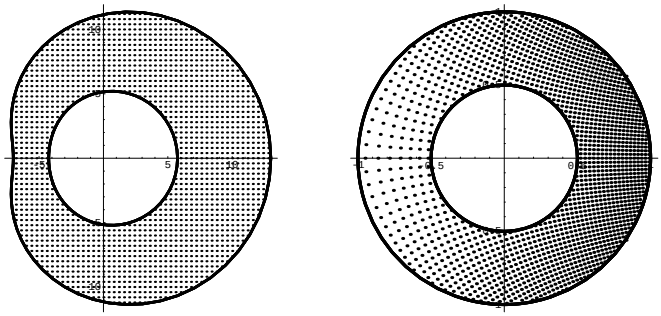

Figure 5.6: Frame of Limacons : a rectangular grid in Ω with grid size 0.4 and its image with $a_0 = 10, a_1 = 5, b_0 = 3$ and $b_1 = b_0/4$.

Table 5.13: Error Norm (Frame of Limacon) using our method

N	minimal $S(\mathbf{x})$	$\|\theta_0(t) - \theta_{0n}(t)\|_\infty$	$\|\theta_1(t) - \theta_{1n}(t)\|_\infty$
8	1.1(−12)	7.4(−04)	4.8(−04)
16	1.3(−24)	4.2(−06)	1.5(−06)
32	7.5(−30)	7.3(−11)	2.5(−11)
64	6.8(−29)	8.9(−16)	8.9(−16)

N	$\|\mu_1 - \mu_{1n}\|_\infty$	$\|\mu_1 - \mu_{1n}^*\|_\infty$
8	4.1(−03)	1.7(−03)
16	1.5(−05)	4.1(−04)
32	2.4(−10)	1.0(−04)
64	0	2.6(−05)

Table 5.14: Error Norm (Interior of Frame of Limacon) using our method

N	$\|f_k(\zeta) - f(\zeta)\|_\infty$
32	1.5(−10)
64	3.4(−14)

Table 5.15: Error Norm (Frame of Limacon) using Symm's method

N	64	128	256
E_M	6.3(−03)	1.0(−03)	2.0(−04)

Example 5.7. *Circular Frame:*

$$\begin{aligned} \Gamma_0 : z(t) &= e^{\mathrm{i}t}, \\ \Gamma_1 : z(t) &= c + \rho e^{\mathrm{i}t}, \qquad 0 \le t \le 2\pi. \end{aligned}$$

The exact mapping function is

$$f(z) = \frac{z-\lambda}{\lambda z - 1}, \quad \lambda = \frac{2c}{1+(c^2-\rho^2)+\sqrt{(1-(c-\rho)^2)(1-(c+\rho)^2)}},$$
$$\mu_1 = \frac{2\rho}{1-(c^2-\rho^2)+\sqrt{(1-(c-\rho)^2)(1-(c+\rho)^2)}}.$$

Figure 5.7 shows the region and image based on our method. Tables 5.16 and 5.17 show the results.

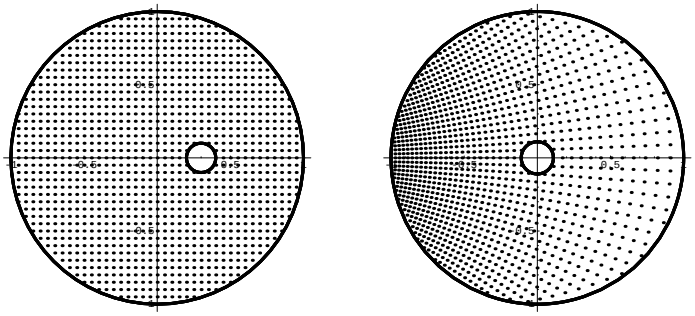

Figure 5.7: Circular Frame : a rectangular grid in Ω with grid size 0.05 and its image with $c = 0.3$ and $\rho = 0.1$.

Table 5.16: Error Norm (Circular Frame) using our method

N	minimal $S(\mathbf{x})$	$\|\theta_0(t) - \theta_{0n}(t)\|_\infty$	$\|\theta_1(t) - \theta_{1n}(t)\|_\infty$
4	1.6(−07)	5.1(−02)	1.1(−01)
8	2.4(−14)	8.7(−04)	1.7(−04)
16	8.7(−29)	1.3(−07)	2.5(−08)
32	1.6(−30)	1.3(−15)	8.9(−16)

N	$\|\mu_1 - \mu_{1n}\|_\infty$	$\|\mu_1 - \mu_{1n}^*\|_\infty$
4	2.6(−03)	1.6(−02)
8	3.7(−05)	3.7(−03)
16	4.7(−09)	8.8(−04)
32	4.2(−17)	2.2(−04)

Table 5.17: Error Norm (Interior of Circular Frame) using our method

N	$\|f_k(\zeta) - f(\zeta)\|_\infty$
16	$4.6(-08)$
32	$2.7(-12)$
64	$1.6(-15)$

Example 5.8. *Ellipse/Ellipse:*

$$\begin{aligned} \Gamma_0 : z(t) &= 2\cos t + \mathrm{i}\sin t, \\ \Gamma_1 : z(t) &= \cos t + \mathrm{i}\,0.5\sin t, \quad 0 \le t \le 2\pi. \end{aligned}$$

We have adopted this example problem from Ellacott (1979) with $\mu_E = 0.5650$ for comparison. See Table 5.18 for radius comparisons. Figure 5.8 shows the region and its image based on our method.

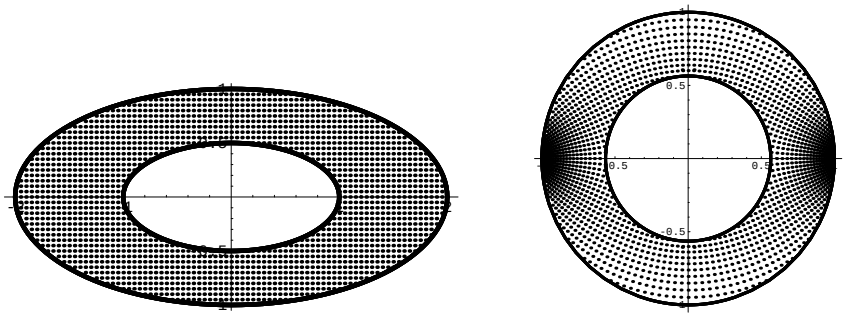

Figure 5.8: Ellipse/Ellipse : a rectangular grid in Ω with grid size 0.25 and its image.

Table 5.18: The radius comparison for ellipse/ellipse

N	minimal $S(\mathbf{x})$	Value of μ	Radius Comparison $\mu - \mu_E$
8	2.6(−25)	0.598436	3.3(−02)
16	5.1(−31)	0.5648148	1.9(−04)
32	3.0(−30)	0.5645690618	4.3(−04)
64	9.3(−30)	0.564569038602491	4.3(−04)

Example 5.9. *Ellipse/Circle:*

$$\begin{aligned} \Gamma_0 : z(t) &= 2\cos t + \mathrm{i}\sin t, \\ \Gamma_1 : z(t) &= 0.5\,(\cos t + \mathrm{i}\sin t), \quad 0 \le t \le 2\pi. \end{aligned}$$

We have adopted this example problem from Ellacott (1979) with $\mu_E = 0.4141$ for comparison. See Table 5.19 for radius comparisons. Figure 5.9 shows the region and its image based on our method.

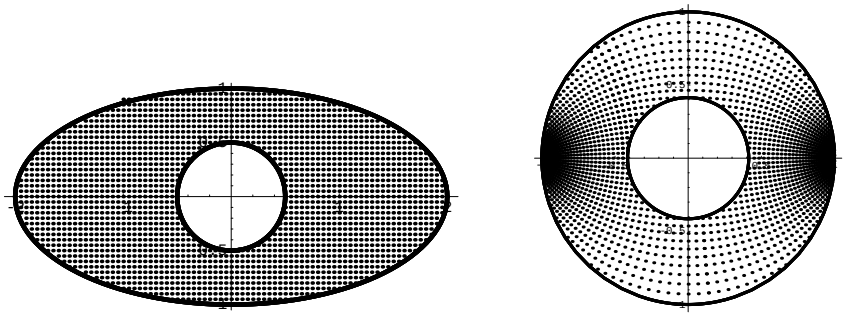

Figure 5.9: Ellipse/circle : a rectangular grid in Ω with grid size 0.25 and its image.

Table 5.19: The radius comparison for ellipse/circle

N	minimal $S(\mathbf{x})$	Value of μ	Radius Comparison $\mu - \mu_E$
8	5.3(−31)	0.469081	5.5(−02)
16	8.6(−31)	0.4156028	1.5(−03)
32	2.1(−30)	0.4141208357	2.1(−05)
64	6.4(−30)	0.414119807861178	2.0(−05)

Example 5.10. *Elliptical Region with Circular Hole:*

$$\Gamma_0 = \{(x,y) : (x + \frac{1}{2}a_0)^2/a_0^2 + y^2 = 1\},$$
$$\Gamma_1 = \{(x,y) : x^2 + y^2 = \frac{1}{9}a_0^2\}, \quad 1 < a_0 \leq 2.$$

We have adopted this example problem from Papamichael and Warby (1984) for comparison of μ_1. Since the conditions of the problem are somewhat different, $A = w : \mu_1 < |w| < 1$ in ours and $A_P = w : 1 < |w| < M$ in Papamichael and Warby (1984), our radius μ_1 should be multiplied by M for comparison (See Table 5.21). In Table 5.20, we list the computed approximations of μ_1 based on our method and the computed approximations to the modulus M based on Papamichael and Warby method. The notation E_N that is used by Papamichael and Warby is defined as (5.16). Figure 5.10 shows the region and its image based on our method.

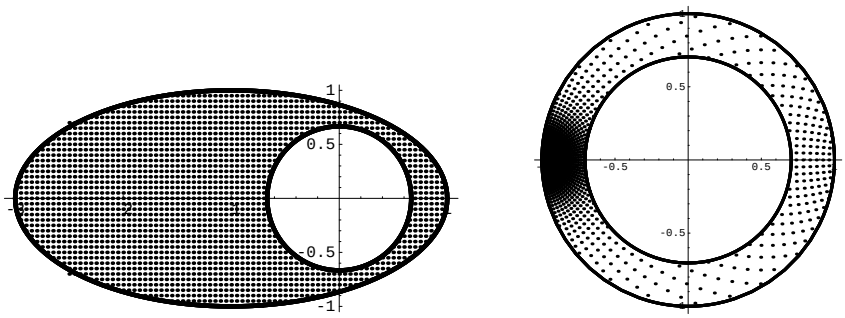

Figure 5.10: Elliptical region with circular hole : a rectangular grid in Ω with grid size 0.05 and its image with $a_0 = 2.0$.

Table 5.20: The computed approximations of μ and M for elliptical region with circular hole

	Our Method	Papamichael and Warby Method	
a_0	μ	M	$1/M$
1.04	0.4803797010444083	2.081686628	0.4803797010315426
1.08	0.4869154853494394	2.053744500	0.4869154853488348
1.20	0.5080480086200779	1.968317921	0.5080480085716803
1.40	0.5480734581257743	1.824572938	0.5480734582724585
1.60	0.5938360511745342	1.683966719	0.5938359640467455
1.80	0.6455396040618699	1.549091634	0.6455396040180280
2.00	0.7043817963288784	1.419684616	0.7043817963017217

5.4 Conformal Mapping of Triply Connected Regions onto an Annulus with a Circular Slit Via the Neumann Kernel

5.4.1 A System of Integral Equations

Suppose Ω is a triply connected region bounded by Γ_0, Γ_1 and Γ_2 (see Figure 4.3 with $M = 2$). For the special case where Ω is a triply connected regions being mapped onto an annulus with a concentric circular slit, the single

Table 5.21: The radius comparison for elliptical region with circular hole

a_0	N	minimal $S(\mathbf{x})$	$\|\mu_1 \times M - 1\|_\infty$	N	E_N
1.04	32	5.1(−12)	3.3(−06)	31	2.1(−05)
1.08	32	3.2(−12)	2.2(−06)	31	8.7(−06)
1.20	32	1.3(−13)	4.1(−07)	29	7.5(−08)
1.40	32	6.1(−17)	2.3(−08)	29	2.0(−06)
1.60	32	1.8(−13)	3.0(−06)	25	3.2(−05)
1.80	32	4.3(−10)	3.9(−05)	23	3.9(−04)
2.00	32	6.4(−06)	2.5(−04)	27	2.0(−03)

integral equation in (4.39) can be separated into a system of equations

$$g(z_0) + \int_{\Gamma_0} N(z_0, w)g(w)|dw| - \int_{-\Gamma_1} P_0(z_0, w)g(w)|dw| - \int_{-\Gamma_2} Q_0(z_0, w)g(w)|dw| = 0, \quad z_0 \in \Gamma_0, \tag{5.63}$$

$$g(z_1) + \int_{\Gamma_0} P_1(z_1, w)g(w)|dw| - \int_{-\Gamma_1} N(z_1, w)g(w)|dw| - \int_{-\Gamma_2} Q_1(z_1, w)g(w)|dw| = 0, \quad z_1 \in \Gamma_1, \tag{5.64}$$

$$g(z_2) + \int_{\Gamma_0} P_2(z_2, w)g(w)|dw| - \int_{-\Gamma_1} Q_2(z_2, w)g(w)|dw| - \int_{-\Gamma_2} N(z_2, w)g(w)|dw| = 0, \quad z_2 \in \Gamma_2, \tag{5.65}$$

where N is the Neumann kernel (2.22) and

$$\begin{aligned} g(z) &= T(z)f'(z), \\ P_0(z,w) &= \frac{1}{2\pi \mathrm{i}}\left[\frac{T(z)}{(z-w)} - \frac{\overline{T(z)}}{\mu_1^2(\overline{z}-\overline{w})}\right], \\ Q_0(z,w) &= \frac{1}{2\pi \mathrm{i}}\left[\frac{T(z)}{(z-w)} - \frac{\overline{T(z)}}{\mu_2^2(\overline{z}-\overline{w})}\right], \\ P_1(z,w) &= \frac{1}{2\pi \mathrm{i}}\left[\frac{T(z)}{(z-w)} - \frac{\mu_1^2\overline{T(z)}}{(\overline{z}-\overline{w})}\right], \end{aligned}$$

$$
\begin{aligned}
Q_1(z,w) &= \frac{1}{2\pi \mathrm{i}}\left[\frac{T(z)}{(z-w)} - \frac{\mu_1^2}{\mu_2^2}\frac{\overline{T(z)}}{(\overline{z}-\overline{w})}\right], \\
P_2(z,w) &= \frac{1}{2\pi \mathrm{i}}\left[\frac{T(z)}{(z-w)} - \frac{\mu_2^2\overline{T(z)}}{(\overline{z}-\overline{w})}\right], \\
Q_2(z,w) &= \frac{1}{2\pi \mathrm{i}}\left[\frac{T(z)}{(z-w)} - \frac{\mu_2^2}{\mu_1^2}\frac{\overline{T(z)}}{(\overline{z}-\overline{w})}\right].
\end{aligned}
$$

As in the doubly connected case, several additional conditions are required to help achieve uniqueness. The single-valuedness requirement on the mapping function $f(z)$ implies

$$\int_{-\Gamma_1} g(w)|dw| = 0, \tag{5.66}$$

$$\int_{-\Gamma_2} g(w)|dw| = 0. \tag{5.67}$$

The set of equations (5.63) to (5.67) does not guarantee a unique solution. The conditions (5.21), (5.22), (5.25) and (5.26) are also valid for the triply connected case under consideration. If the triply connected region is symmetric with respect to the axes, we can also impose the conditions

$$\mathrm{Re}\left[g(z_1(0))\right] = 0, \tag{5.68}$$

$$\mathrm{Re}\left[g(z_2(0))\right] = 0. \tag{5.69}$$

Thus the system of integral equations comprising of (5.63), (5.64), (5.65), (5.66), (5.67) with the conditions (5.21), (5.22), (5.25), (5.26), (5.68) and (5.69) has a unique solution.

5.4.2 Numerical Implementation

In this section we describe a numerical method for computing the mapping function $f(z)$, μ_1 and μ_2 for the case of a triply connected regions. Suppose Γ_0,

Γ_1 and Γ_2 be given in parametric representations as follows:

$$\begin{aligned}
\Gamma_0 : &\qquad z = z_0(t), \quad 0 \le t \le \beta_0, \\
\Gamma_1 : &\qquad z = z_1(t), \quad 0 \le t \le \beta_1, \\
\Gamma_2 : &\qquad z = z_2(t), \quad 0 \le t \le \beta_2.
\end{aligned}$$

Then the system of integral equations (5.63), (5.64), (5.65), (5.66), (5.67), (5.25) and (5.26) become

$$\begin{aligned}
&g(z_0(t)) + \int_0^{\beta_0} N(z_0(t), z_0(s)) g(z_0(s)) |z_0'(s)| ds \\
&\qquad - \int_0^{\beta_1} P_0(z_0(t), z_1(s)) g(z_1(s)) |z_1'(s)| ds \\
&\qquad - \int_0^{\beta_2} Q_0(z_0(t), z_2(s)) g(z_2(s)) |z_2'(s)| ds = 0, \quad z_0(t) \in \Gamma_0, \qquad (5.70) \\
&g(z_1(t)) + \int_0^{\beta_0} P_1(z_1(t), z_0(s)) g(z_0(s)) |z_0'(s)| ds \\
&\qquad - \int_0^{\beta_1} N(z_1(t), z_1(s)) g(z_1(s)) |z_1'(s)| ds \\
&\qquad - \int_0^{\beta_2} Q_1(z_1(t), z_2(s)) g(z_2(s)) |z_2'(s)| ds = 0, \quad z_1(t) \in \Gamma_1, \qquad (5.71) \\
&g(z_2(t)) + \int_0^{\beta_0} P_2(z_2(t), z_0(s)) g(z_0(s)) |z_0'(s)| ds \\
&\qquad - \int_0^{\beta_1} Q_2(z_2(t)), z_1(s)) g(z_1(s)) |z_1'(s)| ds \\
&\qquad - \int_0^{\beta_2} N(z_2(t), z_2(s)) g(z_2(s)) |z_2'(s)| ds = 0, \quad z_2(t) \in \Gamma_2, \qquad (5.72) \\
&\int_0^{\beta_1} g(z_1(s)) |z_1'(s)| ds = 0, \qquad (5.73) \\
&\int_0^{\beta_2} g(z_2(s)) |z_2'(s)| ds = 0, \qquad (5.74) \\
&\int_0^{\beta_0} |g(z_0(s)) z_0'(s)| ds = 2\pi, \qquad (5.75) \\
&\int_0^{\beta_1} |g(z_1(s)) z_1'(s)| ds = 2\pi\mu_1. \qquad (5.76)
\end{aligned}$$

Multiply (5.70), (5.71) and (5.72) by $|z_0'(t)|$, $|z_1'(t)|$ and $|z_2'(t)|$ respectively gives

$$
\begin{aligned}
&|z_0'(t)|g(z_0(t)) + \int_0^{\beta_0} |z_0'(t)|N(z_0(t), z_0(s))g(z_0(s))|z_0'(s)|ds \\
&\quad - \int_0^{\beta_1} |z_0'(t)|P_0(z_0(t), z_1(s))g(z_1(s))|z_1'(s)|ds \\
&\quad - \int_0^{\beta_2} |z_0'(t)|Q_0(z_0(t), z_2(s))g(z_2(s))|z_2'(s)|ds = 0, \quad z_0(t) \in \Gamma_0, \qquad (5.77) \\
&|z_1'(t)|g(z_1(t)) + \int_0^{\beta_0} |z_1'(t)|P_1(z_1(t), z_0(s))g(z_0(s))|z_0'(s)|ds \\
&\quad - \int_0^{\beta_1} |z_1'(t)|N(z_1(t), z_1(s))g(z_1(s))|z_1'(s)|ds \\
&\quad - \int_0^{\beta_2} |z_1'(t)|Q_1(z_1(t), z_2(s))g(z_2(s))|z_2'(s)|ds = 0, \quad z_1(t) \in \Gamma_1. \qquad (5.78) \\
&|z_2'(t)|g(z_2(t)) + \int_0^{\beta_0} |z_2'(t)|P_2(z_2(t), z_0(s))g(z_0(s))|z_0'(s)|ds \\
&\quad - \int_0^{\beta_1} |z_2'(t)|Q_2(z_2(t)), z_1(s))g(z_1(s))|z_1'(s)|ds \\
&\quad - \int_0^{\beta_2} |z_2'(t)|N(z_2(t), z_2(s))g(z_2(s))|z_2'(s)|ds = 0, \quad z_2(t) \in \Gamma_2. \qquad (5.79)
\end{aligned}
$$

We next define

$$
\begin{aligned}
\phi_0(t) &= |z_0'(t)|g(z_0(t)), \\
\phi_1(t) &= |z_1'(t)|g(z_1(t)), \\
\phi_2(t) &= |z_2'(t)|g(z_2(t)), \\
K_{00}(t_0, s_0) &= |z_0'(t)|N(z_0(t), z_0(s)), \\
K_{01}(t_0, s_1) &= |z_0'(t)|P_0(z_0(t), z_1(s)), \\
K_{02}(t_0, s_2) &= |z_0'(t)|Q_0(z_0(t), z_2(s)), \\
K_{10}(t_1, s_0) &= |z_1'(t)|P_1(z_1(t), z_0(s)), \\
K_{11}(t_1, s_1) &= |z_1'(t)|N(z_1(t), z_1(s)), \\
K_{12}(t_1, s_2) &= |z_1'(t)|Q_1(z_1(t), z_2(s)), \\
K_{20}(t_2, s_0) &= |z_2'(t)|P_2(z_2(t), z_0(s)), \\
K_{21}(t_2, s_1) &= |z_2'(t)|Q_2(z_2(t), z_1(s)), \\
K_{22}(t_2, s_2) &= |z_2'(t)|N(z_2(t), z_2(s)).
\end{aligned}
$$

Thus equations (5.77), (5.78), (5.79), (5.73), (5.74), (5.75) and (5.76) can be briefly written as

$$\phi_0(t) + \int_0^{\beta_0} K_{00}(t_0, s_0)\phi_0(s)ds - \int_0^{\beta_1} K_{01}(t_0, s_1)\phi_1(s)ds - \int_0^{\beta_2} K_{02}(t_0, s_2)\phi_2(s)ds = 0, \quad z_0(t) \in \Gamma_0, \tag{5.80}$$

$$\phi_1(t) + \int_0^{\beta_0} K_{10}(t_1, s_0)\phi_0(s)ds - \int_0^{\beta_1} K_{11}(t_1, s_1)\phi_1(s)ds - \int_0^{\beta_2} K_{12}(t_1, s_2)\phi_2(s)ds = 0, \quad z_1(t) \in \Gamma_1, \tag{5.81}$$

$$\phi_2(t) + \int_0^{\beta_0} K_{20}(t_2, s_0)\phi_0(s)ds - \int_0^{\beta_1} K_{21}(t_2, s_1)\phi_1(s)ds - \int_0^{\beta_2} K_{22}(t_2, s_2)\phi_2(s)ds = 0, \quad z_2(t) \in \Gamma_2, \tag{5.82}$$

$$\int_0^{\beta_1} \phi_1(s)ds = 0, \tag{5.83}$$

$$\int_0^{\beta_2} \phi_2(s)ds = 0, \tag{5.84}$$

$$\int_0^{\beta_0} |\phi_0(s)|ds = 2\pi, \tag{5.85}$$

$$\int_0^{\beta_1} |\phi_1(s)|ds = 2\pi\mu_1. \tag{5.86}$$

We choose $\beta_0 = \beta_1 = \beta_2 = 2\pi$ and n equidistant collocation points $t_i = (i-1)\beta_0/n$, $1 \le i \le n$ on Γ_0, m equidistant collocation points $t_{\tilde{i}} = (\tilde{i}-1)\beta_1/m$, $1 \le \tilde{i} \le m$, on Γ_1 and l equidistant collocation points $t_{\hat{i}} = (\hat{i}-1)\beta_2/l$, $1 \le \hat{i} \le l$, on Γ_2. Applying the Nyström's method with trapezoidal rule to discretize (5.80) to (5.86), we obtain

$$\phi_0(t_i) + \frac{\beta_0}{n}\sum_{j=1}^{n} K_{00}(t_i, t_j)\phi_0(t_j) - \frac{\beta_1}{m}\sum_{\tilde{j}=1}^{m} K_{01}(t_i, t_{\tilde{j}})\phi_1(t_{\tilde{j}}) - \frac{\beta_2}{l}\sum_{\hat{j}=1}^{l} K_{02}(t_i, t_{\hat{j}})\phi_2(t_{\hat{j}}) = 0, \tag{5.87}$$

$$\phi_1(t_{\tilde{i}}) + \frac{\beta_0}{n}\sum_{j=1}^{n} K_{10}(t_{\tilde{i}}, t_j)\phi_0(t_j) - \frac{\beta_1}{m}\sum_{\tilde{j}=1}^{m} K_{11}(t_{\tilde{i}}, t_{\tilde{j}})\phi_1(t_{\tilde{j}}) - \frac{\beta_2}{l}\sum_{\hat{j}=1}^{l} K_{12}(t_{\tilde{i}}, t_{\hat{j}})\phi_2(t_{\hat{j}}) = 0, \tag{5.88}$$

$$\phi_2(t_{\hat{i}}) + \frac{\beta_0}{n}\sum_{j=1}^{n} K_{20}(t_{\hat{i}}, t_j)\phi_0(t_j) - \frac{\beta_1}{m}\sum_{\tilde{j}=1}^{m} K_{21}(t_{\hat{i}}, t_{\tilde{j}})\phi_1(t_{\tilde{j}}) - \frac{\beta_2}{l}\sum_{\hat{j}=1}^{l} K_{22}(t_{\hat{i}}, t_{\hat{j}})\phi_2(t_{\hat{j}}) = 0, \tag{5.89}$$

$$\sum_{\tilde{j}=1}^{m} \phi_1(t_{\tilde{j}}) = 0, \tag{5.90}$$

$$\sum_{\hat{j}=1}^{l} \phi_2(t_{\hat{j}}) = 0, \tag{5.91}$$

$$\sum_{j=1}^{n} |\phi_0(t_j)| = n, \tag{5.92}$$

$$\sum_{\tilde{j}=1}^{m} |\phi_1(t_{\tilde{j}})| = m\mu_1. \tag{5.93}$$

Equations (5.87) to (5.93) lead to a system of $(n + m + l + 4)$ non-linear complex equations in n unknowns $\phi_0(t_i)$, m unknowns $\phi_1(t_{\tilde{i}})$, l unknowns $\phi_2(t_{\hat{i}})$, μ_1 and μ_2, as well as the unknown parameters μ_1 and μ_2. By defining the matrix

$$\begin{aligned}
&\mathbf{x}_{0i} = \phi_0(t_i), && \mathbf{x}_{1\tilde{i}} = \phi_1(t_{\tilde{i}}), && \mathbf{x}_{2\hat{i}} = \phi_2(t_{\hat{i}}),\\
&B_{ij} = \frac{\beta_0}{n}K_{00}(t_i, t_j), && C_{i\tilde{j}} = \frac{\beta_1}{m}K_{01}(t_i, t_{\tilde{j}}), && D_{i\hat{j}} = \frac{\beta_2}{l}K_{02}(t_i, t_{\hat{j}}),\\
&E_{\tilde{i}j} = \frac{\beta_0}{n}K_{10}(t_{\tilde{i}}, t_j), && F_{\tilde{i}\tilde{j}} = \frac{\beta_1}{m}K_{11}(t_{\tilde{i}}, t_{\tilde{j}}), && G_{\tilde{i}\hat{j}} = \frac{\beta_2}{l}K_{12}(t_{\tilde{i}}, t_{\hat{j}}),\\
&H_{\hat{i}j} = \frac{\beta_0}{n}K_{20}(t_{\hat{i}}, t_j), && J_{\hat{i}\tilde{j}} = \frac{\beta_1}{m}K_{21}(t_{\hat{i}}, t_{\tilde{j}}), && L_{\hat{i}\hat{j}} = \frac{\beta_2}{l}K_{22}(t_{\hat{i}}, t_{\hat{j}}),
\end{aligned}$$

the system of equations (5.87), (5.88) and (5.89) can be written as $n + m + l$ by $n + m + l$ system of non-linear equations

$$[I_{nn} + B_{nn}]x_{0n} - C_{nm}x_{1m} - D_{nl}x_{2l} = 0, \tag{5.94}$$

$$E_{mn}x_{0n} + [I_{mm} - F_{mm}]x_{1m} - G_{ml}x_{2l} = 0, \tag{5.95}$$

$$H_{ln}x_{0n} - J_{lm}x_{1m} + [I_{ll} - L_{ll}]x_{2l} = 0. \tag{5.96}$$

The result in matrix form for the system of equations (5.94), (5.95) and (5.96) is

$$\begin{pmatrix} I_{nn}+B_{nn} & \cdots & -C_{nm} & \cdots & -D_{nl} \\ \vdots & \ddots & \vdots & \ddots & \vdots \\ E_{mn} & \cdots & I_{mm}-F_{mm} & \cdots & G_{ml} \\ \vdots & \ddots & \vdots & \ddots & \vdots \\ H_{ln} & \cdots & -J_{lm} & \cdots & I_{ll}-L_{ll} \end{pmatrix} \begin{pmatrix} \mathbf{x}_{0n} \\ \vdots \\ \mathbf{x}_{1m} \\ \vdots \\ \mathbf{x}_{2l} \end{pmatrix} = \begin{pmatrix} 0_{0n} \\ \vdots \\ 0_{1m} \\ \vdots \\ 0_{2l} \end{pmatrix}. \quad (5.97)$$

Defining

$$\mathbf{A} = \begin{pmatrix} I_{nn}+B_{nn} & \cdots & -C_{nm} & \cdots & -D_{nm} \\ \vdots & \ddots & \vdots & \ddots & \vdots \\ E_{mn} & \cdots & I_{mm}-F_{mm} & \cdots & -G_{mm} \\ \vdots & \ddots & \vdots & \ddots & \vdots \\ H_{ln} & \cdots & -J_{lm} & \cdots & I_{ll}-L_{ll} \end{pmatrix},$$

$$\mathbf{x}= \begin{pmatrix} \mathbf{x}_{0n} \\ \vdots \\ \mathbf{x}_{1m} \\ \vdots \\ \mathbf{x}_{2l} \end{pmatrix}, \quad \text{and} \quad \mathbf{0} = \begin{pmatrix} 0_{0n} \\ \vdots \\ 0_{1m} \\ \vdots \\ 0_{2l} \end{pmatrix},$$

the $(n+m+l)\times(n+m+l)$ system can be written briefly as $\mathbf{Ax}=\mathbf{0}$. Separating $\mathbf{A}$ and $\mathbf{x}$ in terms of the real and imaginary parts, the system can be written as

$$\mathrm{Re}\,\mathbf{A}\,\mathrm{Re}\,\mathbf{x} - \mathrm{Im}\,\mathbf{A}\,\mathrm{Im}\,\mathbf{x} + \mathrm{i}(\,\mathrm{Im}\mathbf{A}\,\mathrm{Re}\,\mathbf{x} + \mathrm{Re}\,\mathbf{A}\,\mathrm{Im}\,\mathbf{x}) = \mathbf{0} + \mathbf{0}\mathrm{i}. \quad (5.98)$$

The single $(n+m+l)\times(n+m+l)$ complex system (5.98) can also be written as $2(n+m+l)\times 2(n+m+l)$ system matrix

$$\begin{pmatrix} \mathrm{Re}\,\mathbf{A} & \cdots & \mathrm{Im}\,\mathbf{A} \\ \vdots & \ddots & \vdots \\ \mathrm{Im}\,\mathbf{A} & \cdots & \mathrm{Re}\,\mathbf{A} \end{pmatrix} \begin{pmatrix} \mathrm{Re}\,\mathbf{x} \\ \vdots \\ \mathrm{Im}\,\mathbf{x} \end{pmatrix} = \begin{pmatrix} \mathbf{0} \\ \vdots \\ \mathbf{0} \end{pmatrix}. \quad (5.99)$$

Note however that the $2(n+m+l)\times 2(n+m+l)$ matrix in (5.99) contains the unknown parameters μ_1 and μ_2. Since $\phi = \operatorname{Re}\phi + \mathrm{i}\operatorname{Im}\phi$, equations (5.90), (5.91), (5.92), (5.93), (5.21), (5.22), (5.68) and (5.69) become

$$\sum_{\tilde{j}=1}^{m}(\operatorname{Re} x_{1\tilde{j}} + \mathrm{i}\operatorname{Im} x_{1\tilde{j}}) = 0, \tag{5.100}$$

$$\sum_{\hat{j}=1}^{l}(\operatorname{Re} x_{2\hat{j}} + \mathrm{i}\operatorname{Im} x_{2\hat{j}}) = 0, \tag{5.101}$$

$$\sum_{j=1}^{n}\sqrt{(\operatorname{Re} x_{0j})^2 + (\operatorname{Im} x_{0j})^2} = n, \tag{5.102}$$

$$\sum_{\tilde{j}=1}^{m}\sqrt{(\operatorname{Re} x_{1\tilde{j}})^2 + (\operatorname{Im} x_{1\tilde{j}})^2} = m\mu_1, \tag{5.103}$$

$$\operatorname{Re} x_{01} = 0, \tag{5.104}$$

$$\operatorname{Im}\left[x_{01}/\sqrt{(\operatorname{Re} x_{01})^2 + (\operatorname{Im} x_{01})^2}\right] = 1, \tag{5.105}$$

$$\operatorname{Re} x_{11} = 0, \tag{5.106}$$

$$\operatorname{Re} x_{21} = 0, \tag{5.107}$$

Thus a unique solution can be obtained from the system of equations (5.99) to (5.107). This system is an over-determined system of nonlinear equations involving $2(n+m+l)+8$ equations in $2(n+m+l)+2$ unknowns. We use a modification of the Gauss-Newton called the Lavenberg-Marquardt algorithm to solve this nonlinear least square problem. The Lavenberg-Marquardt algorithm which is stated in (5.56), i.e.

$$\mathbf{x}_{k+1} = \mathbf{x}_k - H(\mathbf{x}_k)\mathbf{f}(\mathbf{x}_k), \qquad \lambda_k \geq 0,$$

where $H(\mathbf{x}_k) = ((J_{\mathbf{f}}(\mathbf{x}_k))^T J_{\mathbf{f}}(\mathbf{x}_k) + \lambda_k I)^{-1}(J_{\mathbf{f}}(\mathbf{x}_k))^T$ and $J_{\mathbf{f}}(\mathbf{x})$. Here, $\mathbf{x}$ stands for the $2(n+m+l)+2$ vector $(\operatorname{Re} x_{01}, \operatorname{Re} x_{02}, ..., \operatorname{Re} x_{0n}, \operatorname{Re} x_{11}, \operatorname{Re} x_{12}, ..., \operatorname{Re} x_{1m}, \operatorname{Re} x_{21}, \operatorname{Re} x_{22}, ..., \operatorname{Re} x_{2l}, \operatorname{Im} x_{01}, \operatorname{Im} x_{02}, ..., \operatorname{Im} x_{0n}, \operatorname{Im} x_{11}, \operatorname{Im} x_{12}, ..., \operatorname{Im} x_{1m}, \operatorname{Im} x_{21}, \operatorname{Im} x_{22}, ..., \operatorname{Im} x_{2l}, \mu_1, \mu_2)$, and $\mathbf{f} = (f_1, f_2, ..., f_{2(n+m+l)+8})$.

Our strategy for getting the initial estimation $\mathbf{x}_0$ is based on (4.27) and

(4.28) where upon differentiating, we obtain

$$\begin{aligned}
\phi_0(t) &= f'(z_0(t))z_0'(t) = \mathrm{i}\theta_0'(t)e^{\mathrm{i}\theta_0(t)}, \\
\phi_1(t) &= f'(z_1(t))z_1'(t) = \mu_1\mathrm{i}\theta_1'(t)e^{\mathrm{i}\theta_1(t)}, \\
\phi_2(t) &= f'(z_2(t))z_2'(t) = \mu_2\mathrm{i}\theta_2'(t)e^{\mathrm{i}\theta_2(t)}.
\end{aligned}$$

For initial estimation, we assume $\theta_0(t) = \theta_1(t) = \theta_2(t) = t$ which implies $\theta_0'(t) = \theta_1'(t) = \theta_2'(t) = 1$ and choose $\mu_1 = \mu_2 = 0.5$ as our initial guess of the inner radii. In our experiments, we have chosen the number of collocation points on Γ_0, Γ_1 and Γ_2 being equal, N, i.e., $n = m = l$. After solving this system of equation for the unknown functions $\phi_0(t) = |z_0'(t)|T(z_0(t))f'(z_0(t))$, $\phi_1(t) = |z_1'(t)|T(z_1(t))f'(z_1(t))$, $\phi_2(t) = |z_2'(t)|T(z_2(t))f'(z_2(t))$, μ_1 and μ_2, the boundary correspondence functions $\theta_0(t)$, $\theta_1(t)$ and $\theta_2(t)$ are then computed approximately by the formulas

$$\begin{aligned}
\theta_0(t) &= \mathrm{Arg}\, f(z_0(t)) \approx \mathrm{Arg}\,(-\mathrm{i}\phi_0(t)), \\
\theta_1(t) &= \mathrm{Arg}\, f(z_1(t)) \approx \mathrm{Arg}\,(-\mathrm{i}\phi_1(t)), \\
\theta_2(t) &= \mathrm{Arg}\, f(z_2(t)) \approx \mathrm{Arg}\,(\pm\mathrm{i}\phi_2(t)).
\end{aligned}$$

5.4.3 Interior of Triply Connected Region

Section 5.4.2 deal with conformal mapping on the boundary of triply connected regions. In this section, we describe a numerical procedure for computing the mapping of interior points. Once the boundary values of the mapping function f are known, the values of the mapping function for triply connected regions may be calculated by quadrature at any interior points of its domain of definition through Cauchy's integral formula (see Theorem 5.1).

Let f be analytic on the boundaries $\Gamma = \Gamma_0 \cup \Gamma_1 \cup \Gamma_2$ and the region Ω bounded by Γ_0, Γ_1 and Γ_2. If ζ is any point on Ω, then

$$\begin{aligned} f(\zeta) &= \frac{1}{2\pi \mathrm{i}} \int_{\Gamma} \frac{f(z)}{z-\zeta} dz \\ &= \frac{1}{2\pi \mathrm{i}} \int_{\Gamma_0} \frac{f(z)}{z-\zeta} dz - \frac{1}{2\pi \mathrm{i}} \int_{-\Gamma_1} \frac{f(z)}{z-\zeta} dz - \frac{1}{2\pi \mathrm{i}} \int_{-\Gamma_2} \frac{f(z)}{z-\zeta} dz. \end{aligned} \quad (5.108)$$

The Cauchy's integral formula (5.108) can be also written in the parametrized form, i.e.

$$\begin{aligned} f(\zeta) = \frac{1}{2\pi \mathrm{i}} \int_0^{\beta_0} \frac{f(z_0(t)) z_0'(t)}{z_0(t)-\zeta} dt - \frac{1}{2\pi \mathrm{i}} \int_0^{\beta_1} \frac{f(z_1(t)) z_1'(t)}{z_1(t)-\zeta} dt \\ - \frac{1}{2\pi \mathrm{i}} \int_0^{\beta_2} \frac{f(z_2(t)) z_2'(t)}{z_2(t)-\zeta} dt. \end{aligned} \quad (5.109)$$

By means of (4.27) and (4.28), the Cauchy's integral formula (5.108) can then be written in the form

$$\begin{aligned} f(\zeta) = \frac{1}{2\pi \mathrm{i}} \int_0^{\beta_0} \frac{e^{\mathrm{i}\theta_0(t)} z_0'(t)}{z_0(t)-\zeta} dt - \frac{1}{2\pi \mathrm{i}} \int_0^{\beta_1} \frac{\mu_1 e^{\mathrm{i}\theta_1(t)} z_1'(t)}{z_1(t)-\zeta} dt \\ - \frac{1}{2\pi \mathrm{i}} \int_0^{\beta_2} \frac{\mu_2 e^{\mathrm{i}\theta_2(t)} z_2'(t)}{z_2(t)-\zeta} dt. \end{aligned} \quad (5.110)$$

For the points which are not close to the boundary, the integrands are well behaved. However for points near the boundary, the numerical integration is inaccurate due to the influence of the singularity. This difficulty is overcome through the introduction of an iterative technique as given in (5.60) (see Swarztrauber (1972)).

5.4.4 Numerical Results

For numerical experiment, we have used two test regions. We have not found any exact mapping function documented in the literature. These test region are chosen base on the example in the Reichel (1986), Okano *et al.* (2003),

Kokkinos *et al.* (1990) and Ellacott (1979). We have adopted the example problem from the above literature for comparison. All the computations were done using MATHEMATICA package (Wolfram, 1991) in single precision (16 digit machine precision).

Example 5.11. *Ellipse/two circles:*

Let

$$\begin{aligned}
\Gamma_0 : z_0(t) &= 2\cos t + \mathrm{i}\sin t, \\
\Gamma_1 : z_1(t) &= 0.5\,(\cos t + \mathrm{i}\sin t), \\
\Gamma_2 : z_2(t) &= 1.2 + 0.3\,(\cos t + \mathrm{i}\sin t), \quad t : 0 \le t \le 2\pi.
\end{aligned}$$

We have adopted the example problems from Reichel (1986) and Kokkinos *et al.* (1990) for comparison of μ_1 and μ_2 (see Tables 5.22 and 5.23). We obtain the results $\mu_1 = 0.42588654195460685$ and $\mu_2 = 0.810970795718853$. Since the conditions of the problems are somewhat different, $\mu_0 = 1$ in ours, $\mu_0 = 1.5$ in Reichel's and $\mu_0 = 2$ in Kokkinos *et al.*, our radii μ_1 and μ_2 should be multiplied by 1.5 and 2 respectively. Values of μ_1 and μ_2 in Reichel are denoted here by $\mu_{1,R}$ and $\mu_{2,R}$ respectively. While the values of μ_1 and μ_2 in Kokkinos *et al.* are denoted here by $\mu_{1,K}$ and $\mu_{2,K}$ respectively. Figure 5.11 shows the region and its image based on our method.

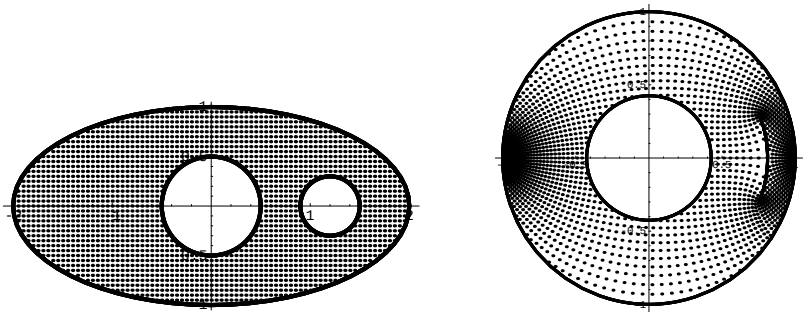

Figure 5.11: Ellipse/two circles : a rectangular grid in Ω with grid size 0.05 and its image.

Table 5.22: Radii comparison with Reichel (1986) for Ellipse/two circles.

	minimal	Radii Comparison	
N	$S(\mathbf{x})$	$\|\mu_1 \times 1.5 - \mu_{1,R}\|_\infty$	$\|\mu_2 \times 1.5 - \mu_{2,R}\|_\infty$
16	3.3(−11)	1.4(−03)	1.3(−02)
32	6.8(−22)	9.8(−07)	6.6(−06)
64	1.1(−23)	8.6(−09)	4.3(−09)

Table 5.23: Radii comparison with Kokkinos *et al.* (1990) for Ellipse/two circles

	Radii Comparison	
N	$\|\mu_1 \times 2 - \mu_{1,K}\|_\infty$	$\|\mu_2 \times 2 - \mu_{2,K}\|_\infty$
16	1.4(−03)	1.3(−02)
32	9.7(−07)	6.6(−06)
64	2.0(−09)	7.2(−10)

Example 5.12. *Ellipse/Circle/Ellipse:*

Let

$$\begin{aligned}
\Gamma_0 : z_0(t) &= 2\cos t + \mathrm{i}\sin t, \\
\Gamma_1 : z_1(t) &= 0.25\,(\cos t + \mathrm{i}\sin t), \\
\Gamma_2 : z_2(t) &= 1 + 0.5\cos t + 0.25\,\mathrm{i}\sin t, \quad t : 0 \le t \le 2\pi.
\end{aligned}$$

We have adopted the example problems from Ellacott (1979) for comparison of μ_1 and μ_2 (see Table 5.24). We have chosen $n = m = l = 64$ number of collocation points. Figure 5.12 and 5.13 shows the region and its image based on our method and Ellacott method respectively.

Table 5.24: Radii comparison for Ellipse/two circles

Our Method	Ellacott (1979)	
Radius	Radius	$\|\mu_p - \mu_{p,E}\|_\infty$
$\mu_1 = 0.24061238546734354$	$\mu_{1,E} = 0.25$	$9.4(-03)$
$\mu_2 = 0.6859816257842841$	$\mu_{2,E} = 0.68$	$6.0(-03)$

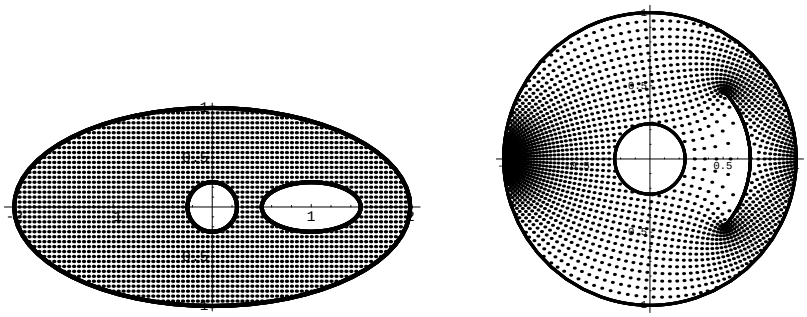

Figure 5.12: Ellipse/Circle/Ellipse : a rectangular grid in Ω with grid size 0.05 and its image.

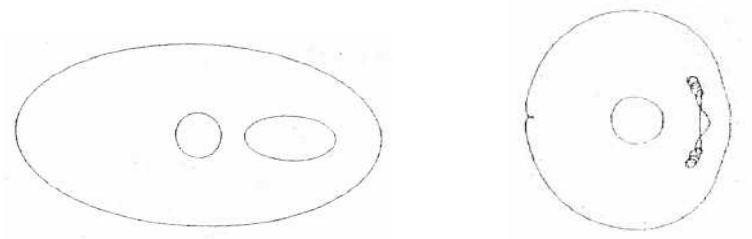

Figure 5.13: Conformal mapping of Ellipse/circles/ellipse onto an annulus with a concentric circular slit base on Ellacott method.

CHAPTER 6

NUMERICAL CONFORMAL MAPPING OF MULTIPLY CONNECTED REGIONS ONTO A DISK WITH CIRCULAR SLITS

6.1 Introduction

We have shown in Chapter 5 that the proposed method for the numerical conformal mapping of multiply connected regions onto an annulus with circular slits via the Kerzman-Stein and the Neumann kernels can produced approximations of high accuracy. In this chapter, we shall discuss numerical aspects of conformal mapping of multiply connected regions onto a disk with circular slits based on the integral equation developed in Chapter 4.

6.2 Conformal Mapping of Doubly Connected Regions onto a Disk with a Circular Slit Via the Neumann Kernel

6.2.1 A System of Integral Equations

Suppose Ω is a doubly connected region bounded by Γ_0 and Γ_1 (see Figure 4.4 with $M = 1$). For the special case where Ω is a doubly connected region being

mapped onto a disk with a circular slit, the single integral equation in (4.58) can be separated into a system of equations

$$\begin{aligned} g(z_0,a) &+ \int_{\Gamma_0} N(z_0,w)g(w,a)|dw| - \int_{-\Gamma_1} P_0(z_0,w)g(w,a)|dw| \\ &= r^2 h(a,z_0), \quad z_0 \in \Gamma_0, \end{aligned} \tag{6.1}$$

$$\begin{aligned} g(z_1,a) &+ \int_{\Gamma_0} P_1(z_1,w)g(w,a)|dw| - \int_{-\Gamma_1} N(z_1,w)g(w,a)|dw| \\ &= \mu_1^2 r^2 h(a,z_1), \quad z_1 \in \Gamma_1, \end{aligned} \tag{6.2}$$

where

$$\begin{aligned} g(z,a) &= f'(a)T(z)f'(z), \\ h(a,z) &= -\frac{\overline{T(z)}}{(\overline{a}-\overline{z})^2}, \\ P_0(z,w) &= \frac{1}{2\pi \mathrm{i}}\left[\frac{T(z)}{(z-w)} - \frac{\overline{T(z)}}{\mu_1^2(\overline{z}-\overline{w})}\right], \\ P_1(z,w) &= \frac{1}{2\pi \mathrm{i}}\left[\frac{T(z)}{(z-w)} - \frac{\mu_1^2\overline{T(z)}}{(\overline{z}-\overline{w})}\right], \\ N(z,w) &= \begin{cases} \dfrac{1}{2\pi \mathrm{i}}\left[\dfrac{T(z)}{z-w} - \dfrac{\overline{T(z)}}{\overline{z}-\overline{w}}\right], & \text{if } w,z \in \Gamma, w \neq z, \\ \dfrac{1}{2\pi}\dfrac{\mathrm{Im}[z''(t)\overline{z'(t)}]}{|z'(t)|^3}, & \text{if } w = z \in \Gamma. \end{cases} \end{aligned}$$

The kernel N is also known as Neumann kernel.

Note that there are four unknown quantities in the integral equations (6.1) and (6.2), namely, $g(z_0,a)$, $g(z_1,a)$, r and μ_1. Naturally it is also required that the unknown mapping function $f(z)$ be single-valued in the problem domain (Henrici, 1986), i.e.

$$\int_{-\Gamma_1} f'(w)dw = 0, \tag{6.3}$$

which implies

$$\int_{-\Gamma_1} g(w,a)|dw| = 0. \tag{6.4}$$

Several conditions can be obtained to help achieve uniqueness. We first consider equation (4.47). Upon differentiation and taking modulus to both sides

of equation (4.47), gives

$$\begin{aligned} |f'(a)T(z_0(t))f'(z_0(t))z_0'(t)| &= |f'(a)T(z_0(t))re^{\mathrm{i}\theta_0(t)}\mathrm{i}\theta_0'(t)| \\ &= f'(a)r|\theta_0'(t)|. \end{aligned} \tag{6.5}$$

Since the boundary correspondence function $\theta_0(t)$ is an increasing monotone function and it's derivative is positive, this implies $|\theta_0'(t)| = \theta_0'(t)$. Upon integrating (6.5) with respect to t form 0 to 2π gives

$$\int_0^{2\pi} |g(z_0(t), a)z_0'(t)|dt = f'(a)\, r \int_0^{2\pi} \theta_0'(t)dt = f'(a)\, r\, 2\pi. \tag{6.6}$$

Next we consider the Cauchy integral formula

$$f'(a) = \frac{1}{2\pi\mathrm{i}} \int_\Gamma \frac{f'(z)}{z-a}dz = \frac{1}{2\pi\mathrm{i}} \int_{\Gamma_0} \frac{f'(z)}{z-a}dz - \frac{1}{2\pi\mathrm{i}} \int_{-\Gamma_1} \frac{f'(z)}{z-a}dz, \tag{6.7}$$

which implies

$$f'(a)^2 = \frac{1}{2\pi\mathrm{i}} \int_0^{2\pi} \frac{f'(a)f'(z_0(t))z_0'(t)}{z_0(t)-a}dt - \frac{1}{2\pi\mathrm{i}} \int_0^{2\pi} \frac{f'(a)f'(z_1(t))z_1'(t)}{z_1(t)-a}dt. \tag{6.8}$$

We have two possibilities: set a value for $f'(a)$ and treat r as unknown, or set a value of r and treat $f'(a)$ as unknown. Thus the system of integral equations comprising of (6.1), (6.2), (6.4) with the conditions (6.6) and (6.7) will lead to a unique solution. In the following section, we show the numerical implementation and numerical results with the value of $f'(a)$ predetermined.

6.2.2 Numerical Implementation

Suppose Γ_0 and Γ_1 be given in parametric representations as follows:

$$\begin{aligned} \Gamma_0 : &\qquad z = z_0(t), \quad 0 \le t \le \beta_0, \\ \Gamma_1 : &\qquad z = z_1(t), \quad 0 \le t \le \beta_1. \end{aligned}$$

Then the system of integral equations (6.1), (6.2) and (6.4) become

$$g(z_0(t),a)+\int_0^{\beta_0} N(z_0(t),z_0(s))g(z_0(s),a)|z_0'(s)|ds$$
$$-\int_0^{\beta_1} P_0(z_0(t),z_1(s))g(z_1(s),a)|z_1'(s)|ds = r^2h(a,z_0(t)),$$
$$z_0(t)\in\Gamma_0, \tag{6.9}$$
$$g(z_1(t),a)+\int_0^{\beta_0} P_1(z_1(t),z_0(s))g(z_0(s),a)|z_0'(s)|ds$$
$$-\int_0^{\beta_1} N(z_1(t),z_1(s))g(z_1(s),a)|z_1'(s)|ds = r^2\mu_1^2h(a,z_1(t)),$$
$$z_1(t)\in\Gamma_1, \tag{6.10}$$
$$\int_0^{\beta_1} g(z_1(s),a)|z_1'(s)|ds = 0. \tag{6.11}$$

Multiply (6.9) and (6.10) by $|z_0'(t)|$ and $|z_1'(t)|$ respectively gives

$$|z_0'(t)|g(z_0(t),a)+\int_0^{\beta_0}|z_0'(t)|N(z_0(t),z_0(s))g(z_0(s),a)|z_0'(s)|ds$$
$$-\int_0^{\beta_1}|z_0'(t)|P_0(z_0(t),z_1(s))g(z_1(s),a)|z_1'(s)|ds$$
$$= r^2|z_0'(t)|h(a,z_0(t)),\qquad z_0(t)\in\Gamma_0, \tag{6.12}$$
$$|z_1'(t)|g(z_1(t),a)+\int_0^{\beta_0}|z_1'(t)|P_1(z_1(t),z_0(s))g(z_0(s),a)|z_0'(s)|ds$$
$$-\int_0^{\beta_1}|z_1'(t)|N(z_1(t),z_1(s))g(z_1(s),a)|z_1'(s)|ds$$
$$= r^2\mu_1^2|z_1'(t)|h(a,z_1(t)),\qquad z_1(t)\in\Gamma_1. \tag{6.13}$$

Defining

$$\begin{aligned}
\phi_0(t) &= |z_0'(t)|g(z_0(t),a),\\
\phi_1(t) &= |z_1'(t)|g(z_1(t),a),\\
\gamma_0(t) &= r^2|z_0'(t)|h(a,z_0(t)),\\
\gamma_1(t) &= r^2\mu_1^2|z_1'(t)|h(a,z_1(t)),\\
K_{00}(t_0,s_0) &= |z_0'(t)|N(z_0(t),z_0(s)),\\
K_{01}(t_0,s_1) &= |z_0'(t)|P_0(z_0(t),z_1(s)),\\
K_{10}(t_1,s_0) &= |z_1'(t)|P_1(z_1(t),z_0(s)),\\
K_{11}(t_1,s_1) &= |z_1'(t)|N(z_1(t),z_1(s)),
\end{aligned}$$

the system of equations (6.12), (6.13), (6.11), (6.6) and (6.8) can be briefly written as

$$\phi_0(t) + \int_0^{\beta_0} K_{00}(t_0, s_0)\phi_0(s)ds - \int_0^{\beta_1} K_{01}(t_0, s_1)\phi_1(s)ds = \gamma_0(t), \quad (6.14)$$

$$\phi_1(t) + \int_0^{\beta_0} K_{10}(t_1, s_0)\phi_0(s)ds - \int_0^{\beta_1} K_{11}(t_1, s_1)\phi_1(s)ds = \gamma_1(t), \quad (6.15)$$

$$\int_0^{\beta_1} \phi_1(s)ds = 0, \quad (6.16)$$

$$\int_0^{\beta_0} |\phi_0(s)|ds = f'(a)r2\pi, \quad (6.17)$$

$$\frac{1}{2\pi\mathrm{i}} \int_0^{\beta_0} \frac{\phi_0(s)}{z_0(s) - a}ds - \frac{1}{2\pi\mathrm{i}} \int_0^{\beta_1} \frac{\phi_1(s)}{z_1(s) - a}ds = f'(a)^2. \quad (6.18)$$

Since the functions ϕ, γ, and K in the above systems are β-periodic, a reliable procedure for solving (6.14) to (6.18) numerically is using the Nyström's method with trapezoidal rule (Atkinson, 1976). We choose $\beta_0 = \beta_1 = 2\pi$ and n equidistant collocation points $t_i = (i-1)\beta_0/n$, $1 \le i \le n$ on Γ_0 and m equidistant collocation points $t_\imath = (\imath - 1)\beta_1/m$, $1 \le \imath \le m$, on Γ_1. Applying the Nyström's method with trapezoidal rule to discretize (6.14) to (6.18), we obtain

$$\phi_0(t_i) + \frac{\beta_0}{n} \sum_{j=1}^{n} K_{00}(t_i, t_j)\phi_0(t_j) - \frac{\beta_1}{m} \sum_{\jmath=1}^{m} K_{01}(t_i, t_\jmath)\phi_1(t_\jmath) = \gamma_0(t_i), \quad (6.19)$$

$$\phi_1(t_\imath) + \frac{\beta_0}{n} \sum_{j=1}^{n} K_{10}(t_\imath, t_j)\phi_0(t_j) - \frac{\beta_1}{m} \sum_{\jmath=1}^{m} K_{11}(t_\imath, t_\jmath)\phi_1(t_\jmath) = \gamma_1(t_\imath), \quad (6.20)$$

$$\sum_{\jmath=1}^{m} \phi_1(t_\jmath) = 0, \quad (6.21)$$

$$\sum_{j=1}^{n} |\phi_0(t_j)| = f'(a)rn, \quad (6.22)$$

$$\frac{1}{n\mathrm{i}} \sum_{j=1}^{n} \frac{1}{z_0(t_j) - a}\phi_0(t_j) - \frac{1}{m\mathrm{i}} \sum_{\jmath=1}^{m} \frac{1}{z_1(t_\jmath) - a}\phi_1(t_\jmath) = f'(a)^2. \quad (6.23)$$

Equations (6.19) to (6.23) lead to a system of $(n + m + 3)$ non-linear complex equations in n unknowns $\phi_0(t_i)$, m unknowns $\phi_1(t_\imath)$, $f'(a)$, r and μ_1. By

defining the matrices

$$\begin{aligned}
x_{0i} &= \phi_0(t_i), \\
x_{1\imath} &= \phi_1(t_\imath), \\
\gamma_{0i} &= \gamma_0(t_i), \\
\gamma_{1\imath} &= \gamma_1(t_\imath), \\
B_{ij} &= \frac{\beta_0}{n} K_{00}(t_i, t_j), \\
C_{i\jmath} &= \frac{\beta_1}{m} K_{01}(t_i, t_\jmath), \\
E_{\imath j} &= \frac{\beta_0}{n} K_{10}(t_\imath, t_j), \\
D_{\imath\jmath} &= \frac{\beta_1}{m} K_{11}(t_\imath, t_\jmath), \\
F_n &= \frac{1}{\mathrm{i}n} \sum_{j=1}^{n} \frac{1}{z_0(t_j) - a}, \\
G_m &= \frac{1}{\mathrm{i}m} \sum_{\jmath=1}^{m} \frac{1}{z_1(t_\jmath) - a},
\end{aligned}$$

the system of equations (6.19), (6.20) and (6.23) can be written as $n + m + 1$ by $n + m$ system of equations

$$[I_{nn} + B_{nn}]\mathbf{x}_{0n} - C_{nm}\mathbf{x}_{1m} = \gamma_{0n}, \tag{6.24}$$

$$E_{mn}\mathbf{x}_{0n} + [I_{mm} - D_{mm}]\mathbf{x}_{1m} = \gamma_{1m}, \tag{6.25}$$

$$F_n\mathbf{x}_{0n} + G_m\mathbf{x}_{1m} = f'(a)^2. \tag{6.26}$$

Since $\phi = \operatorname{Re}\phi + \mathrm{i}\operatorname{Im}\phi$, equations (6.21) and (6.22) becomes

$$\sum_{\jmath=1}^{m} (\operatorname{Re} x_{1\jmath} + \mathrm{i}\operatorname{Im} x_{1\jmath}) = 0, \tag{6.27}$$

$$\sum_{j=1}^{n} \sqrt{(\operatorname{Re} x_{0j})^2 + (\operatorname{Im} x_{0j})^2} = f'(a) r n. \tag{6.28}$$

The result in matrix form for the system of equations (6.24), (6.25) and (6.26) is

$$\begin{pmatrix} I_{nn}+B_{nn} & \cdots & -C_{nm} \\ \vdots & \ddots & \vdots \\ E_{mn} & \cdots & I_{mm}-D_{mm} \\ \vdots & \ddots & \vdots \\ F_n & \cdots & G_m \end{pmatrix} \begin{pmatrix} \mathbf{x}_{0n} \\ \vdots \\ \mathbf{x}_{1m} \end{pmatrix} = \begin{pmatrix} \gamma_{0n} \\ \vdots \\ \gamma_{1m} \\ \vdots \\ f'(a)^2 \end{pmatrix}. \tag{6.29}$$

Defining

$$\mathbf{A} = \begin{pmatrix} I_{nn}+B_{nn} & \cdots & -C_{nm} \\ \vdots & \ddots & \vdots \\ E_{mn} & \cdots & I_{mm}-D_{mm} \\ \vdots & \ddots & \vdots \\ F_n & \cdots & G_m \end{pmatrix}, \mathbf{x}= \begin{pmatrix} \mathbf{x}_{0n} \\ \vdots \\ \mathbf{x}_{1m} \end{pmatrix} \text{ and } \mathbf{y} = \begin{pmatrix} \gamma_{0n} \\ \vdots \\ \gamma_{1m} \\ \vdots \\ f'(a)^2 \end{pmatrix},$$

the $(n+m+1)\times(n+m)$ system can be written briefly as $\mathbf{Ax}=\mathbf{y}$. Separating $\mathbf{A}$, $\mathbf{x}$ and $\mathbf{y}$ in terms of the real and imaginary parts, the system can be written as

$$\operatorname{Re}\mathbf{A}\operatorname{Re}\mathbf{x} - \operatorname{Im}\mathbf{A}\operatorname{Im}\mathbf{x} + \mathrm{i}(\operatorname{Im}\mathbf{A}\operatorname{Re}\mathbf{x} + \operatorname{Re}\mathbf{A}\operatorname{Im}\mathbf{x}) = \operatorname{Re}\mathbf{y} + \mathrm{i}\operatorname{Im}\mathbf{y}. \tag{6.30}$$

The single $(n+m+1)\times(n+m)$ complex system (6.30) above is equivalent to the $2(n+m+1)\times 2(n+m)$ system matrix involving the real (Re) and imaginary (Im) of the unknown functions, i.e.,

$$\begin{pmatrix} \text{Re A} & \cdots & \text{Im A} \\ \vdots & \ddots & \vdots \\ \text{Im A} & \cdots & \text{Re A} \end{pmatrix} \begin{pmatrix} \text{Re } \mathbf{x} \\ \vdots \\ \text{Im } \mathbf{x} \end{pmatrix} = \begin{pmatrix} \text{Re } \mathbf{y} \\ \vdots \\ \text{Im } \mathbf{y} \end{pmatrix}. \tag{6.31}$$

Note that the matrix in (6.31) contains the unknown parameters r and μ_1. The value of $f'(a)$ is predetermined. The system of equations (6.31), (6.27) and (6.28) is an over-determined system of non-linear equations involving $2(n+m+1)+2$ equations in $2(n+m)+2$ unknowns.

We use a modification of the Gauss-Newton called the Lavenberg-Marquardt with the Fletcher's algorithm to solve this nonlinear least square problem. Our nonlinear least square problem consists in finding the vector $\mathbf{x}$ for which the function $S : R^{2(n+m)+4} \rightarrow R^1$ defined by the sum of squares

$$S(\mathbf{x}) = \mathbf{f}^{\mathrm{T}}\mathbf{f} = \sum_{i=1}^{2(n+m)+4} (f_i(\mathbf{x}))^2$$

is minimal. Here, $\mathbf{x}$ stands for the $2(n+m)+2$ vector ($\mathrm{Re}\, x_{01}$, $\mathrm{Re}\, x_{02}$, ..., $\mathrm{Re}\, x_{0n}$, $\mathrm{Re}\, x_{11}$, $\mathrm{Re}\, x_{12}$, ..., $\mathrm{Re}\, x_{1m}$, $\mathrm{Im}\, x_{01}$, $\mathrm{Im}\, x_{02}$, ..., $\mathrm{Im}\, x_{0n}$, $\mathrm{Im}\, x_{11}$, $\mathrm{Im}\, x_{12}$, ..., $\mathrm{Im}\, x_{1m}$, μ_1, r), and $\mathbf{f} = (f_1, f_2, ..., f_{2(n+m+1)+2})$. The Lavenberg-Marquardt algorithm is an iterative procedure with starting value denoted as $\mathbf{x}_0$. This initial approximation, which, if at all possible, should be well-informed guess and generate a sequence of approximations $\mathbf{x}_1$, $\mathbf{x}_2$, $\mathbf{x}_3$, ... base on the formula (5.56) i.e.

$$\mathbf{x}_{k+1} = \mathbf{x}_k - H(\mathbf{x}_k)\mathbf{f}(\mathbf{x}_k), \qquad \lambda_k \geq 0,$$

where $H(\mathbf{x}_k) = ((J_{\mathbf{f}}(\mathbf{x}_k))^{\mathrm{T}} J_{\mathbf{f}}(\mathbf{x}_k) + \lambda_k I)^{-1} (J_{\mathbf{f}}(\mathbf{x}_k))^{\mathrm{T}}$.

The strategy for getting the initial estimation is to provide rough estimates of the slit radius, $\mu \approx 0.5$, $r = 1$ and set $f'(a) = 1$ for the test region. Then the non-linear system of equations (6.29) and (6.27) reduces to over-determined linear system. Writing the over-determined system as $\mathbf{Bx} = \mathbf{y}$, we use the least-squares solutions of $\mathbf{Bx} = \mathbf{y}$ which are precisely the solutions of $\mathbf{B}^{\mathrm{T}}\mathbf{Bx} = \mathbf{B}^{\mathrm{T}}\mathbf{y}$ (Johnson *et al.*, 1998). The solutions are then taken as initial estimation. These initial guesses are applied for the lowest number of n and m of our experiments. In all our experiments, we have chosen the number of collocation points on Γ_0 and Γ_1 being equal, i.e., $n = m$. The information from the solution of μ_1 and r of lower n is then exploited as an estimate of μ_1 and r for the next $2n$ number of collocations points.

The system of equations (6.31) with (6.27) and (6.28) are then solved for the unknown functions

$$\phi_0(t) = |z_0'(t)| f'(a) T(z_0(t)) f'(z_0(t)),$$

$$\phi_1(t) = |z_1'(t)|f'(a)T(z_1(t))f'(z_1(t)),$$

μ and r. Finally the boundary correspondence functions $\theta_0(t)$ and $\theta_1(t)$ are computed approximately by the formulas

$$\theta_0(t) = \operatorname{Arg} f(z_0(t)) \approx \operatorname{Arg}(-\mathrm{i}\phi_0(t)),$$
$$\theta_1(t) = \operatorname{Arg} f(z_1(t)) \approx \operatorname{Arg}(\pm\mathrm{i}\phi_1(t)).$$

6.2.3 The Interior Mapping

Once the boundary values of the mapping function f are known, the values of the mapping function may be calculated by quadrature at any interior points of its domain of definition through Cauchy's integral formula (see Theorem 5.1).

By using (4.47) and (4.48), the Cauchy's integral formula (5.57) can then be written in the form

$$f(\zeta) = \frac{1}{2\pi\mathrm{i}} \int_0^{\beta_0} \frac{re^{\mathrm{i}\theta_0(t)} z_0'(t)}{z_0(t) - \zeta} dt - \frac{1}{2\pi\mathrm{i}} \int_0^{\beta_1} \frac{\mu_1 re^{\mathrm{i}\theta_1(t)} z_1'(t)}{z_1(t) - \zeta} dt, \tag{6.32}$$

where ζ is any point on Ω.

For the points which are close to the boundary, we use the iterative technique as given in equation (5.60). In practice the iteration converges rapidly. Using this technique, we are able to maintain the same accuracy throughout the region Ω.

6.2.4 Numerical Results

For numerical results, we have used five test regions whose exact boundary correspondence functions are known as given in Section 2.5. The test regions are annulus, frame of Limacon, elliptic frame, circular frame and frame of Cassini's oval. We set $f'(a) = 1$ for all test regions. Note that, $f(z)$ maps Ω conformally onto a disk $|w| < r$ with a circular slit of radius $\mu_1 r$, where $0 < \mu_1 < 1$. Thus $g(z) = f(z)/r$ maps Ω onto a disk $|w| < 1$ with a circular slit of radius μ_1. This implies that f and g have the same values of $\theta_0(t)$, $\theta_1(t)$ and μ_1. The results for the sub-norm error between the exact values of $\theta_0(t)$, $\theta_1(t)$, μ_1, $f(\zeta)$ and their corresponding approximations $\theta_{0n}(t)$, $\theta_{1n}(t)$, μ_{1n}, $f_k(\zeta)$ are shown in Tables 6.1 to 6.10. Figures 5.1 to 5.5 shows the regions and corresponding images based on our method. All the computations are done using MATHEMATICA package (Wolfram, 1991) in single precision (16 digit machine precision).

Example 6.1. *Annulus:*

$$\begin{aligned} \Gamma_0 : z(t) &= \cos t + \mathrm{i} \sin t, \\ \Gamma_1 : z(t) &= \tilde{r}(\cos t + \mathrm{i} \sin t), \quad 0 \le t \le 2\pi. \end{aligned}$$

The exact mapping function is

$$g(z) = -e^{2\sigma} \frac{\theta_4\left(\dfrac{1}{2\mathrm{i}} \log z + \dfrac{\mathrm{i}\pi\tau}{2} - \mathrm{i}\sigma;\, q\right)}{\theta_4\left(\dfrac{1}{2\mathrm{i}} \log z + \dfrac{\mathrm{i}\pi\tau}{2} + \mathrm{i}\sigma;\, q\right)}, \quad 0 < \sigma < \frac{\pi\tau}{2}, \quad \mu_1 = e^{-2\sigma}.$$

For the purpose of numerical comparison, we set $\tilde{r} = q = e^{-\pi\tau}$ (see Section 2.5.1) and since $\theta_4(\pi\tau\mathrm{i}/2; q) = 0$ (Whittaker and Watson, 1927), this implies $a = e^{-2\sigma}$. We have chosen $\tau = 0.50$, and $\sigma = 0.20$. Figure 6.1 shows the region and image based on our method. See Tables 6.1 and 6.2 for results.

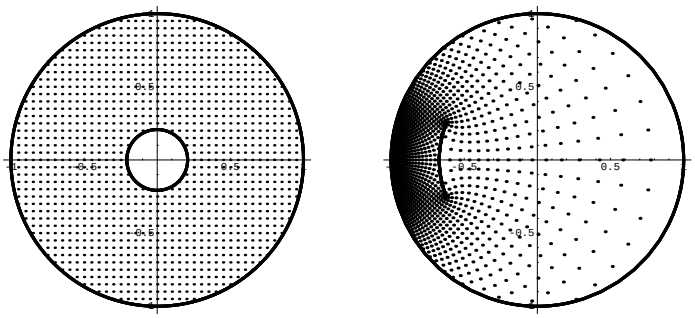

Figure 6.1: Annulus : a rectangular grid in Ω with grid size 0.05 and its image with radius $\mu_1 = e^{-2\sigma}$.

Table 6.1: Error Norm (Annulus)

$n = m$	minimal $S(\mathbf{x})$	$\|\theta_0(t) - \theta_{0n}(t)\|_\infty$	$\|\theta_1(t) - \theta_{1n}(t)\|_\infty$	$\|\mu_1 - \mu_{1n}\|_\infty$
16	8.4(−15)	1.9(−02)	6.3(−01)	1.7(−02)
32	2.7(−24)	5.0(−05)	8.9(−04)	2.8(−05)
64	3.5(−30)	2.4(−10)	2.3(−09)	8.2(−11)
128	2.4(−30)	8.9(−16)	7.0(−14)	2.2(−16)

Table 6.2: Error Norm (Interior of Annulus)

$n = m$	$\|f_k(\zeta) - f(\zeta)\|_\infty$
32	1.8(−04)
64	3.0(−10)
128	1.3(−15)

Example 6.2. *Circular Frame:*

$$\begin{aligned} \Gamma_0 : z(t) &= e^{\mathrm{i}t}, \\ \Gamma_1 : z(t) &= c + \rho e^{\mathrm{i}t}, \qquad 0 \le t \le 2\pi. \end{aligned}$$

The exact mapping function is

$$g(z) = e^{2\sigma}\frac{\theta_4\left(\dfrac{1}{2\mathrm{i}}\log f(z) + \dfrac{\mathrm{i}\pi\tau}{2} - \mathrm{i}\sigma;\, q\right)}{\theta_4\left(\dfrac{1}{2\mathrm{i}}\log f(z) + \dfrac{\mathrm{i}\pi\tau}{2} + \mathrm{i}\sigma;\, q\right)}, \quad 0 < \sigma < \frac{\pi\tau}{2}, \quad \mu_1 = e^{-2\sigma},$$

with

$$\begin{aligned} f(z) &= \frac{z-\lambda}{\lambda z - 1}, \quad \lambda = \frac{2c}{1 + (c^2-\rho^2) + \sqrt{(1-(c-\rho)^2)(1-(c+\rho)^2)}}, \\ \tilde{r} &= \frac{2\rho}{1 - (c^2-\rho^2) + \sqrt{(1-(c-\rho)^2)(1-(c+\rho)^2)}}. \end{aligned}$$

For the purpose of numerical comparison, we set $\tilde{r} = q = e^{-\pi\tau}$ and since $\theta_4(\pi\tau\mathrm{i}/2; q) = 0$, this implies $\tau = \dfrac{\ln(\tilde{r})}{-\pi}$ and $a = \dfrac{\lambda - e^{-2\sigma}}{1 - \lambda e^{-2\sigma}}$. We have chosen $c = 0.3$, $\rho = 0.1$, and $\sigma = 0.50$. Figure 6.2 shows the region and image based on our method. See Tables 6.3 and 6.4 for results.

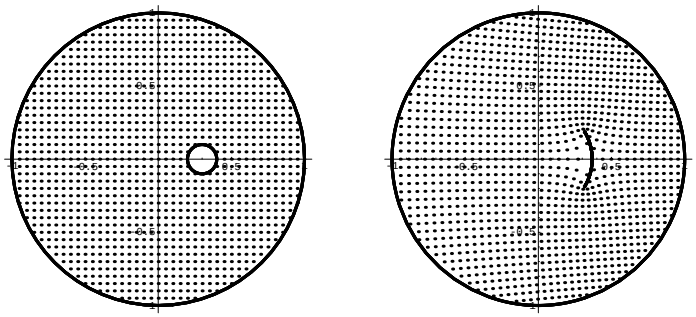

Figure 6.2: Circular frame : a rectangular grid in Ω with grid size 0.05 and its image with radius $\mu_1 = e^{-2\sigma}$.

Table 6.3: Error Norm (Circular Frame)

$n = m$	minimal $S(\mathbf{x})$	$\|\theta_0(t) - \theta_{0n}(t)\|_\infty$	$\|\theta_1(t) - \theta_{1n}(t)\|_\infty$	$\|\mu_1 - \mu_{1n}\|_\infty$
4	1.0(−04)	1.0(−01)	5.9(−01)	4.9(−01)
8	3.6(−08)	2.3(−04)	2.0(−03)	1.6(−04)
16	2.1(−16)	1.0(−08)	4.2(−07)	2.0(−08)
32	4.6(−29)	8.9(−16)	5.1(−14)	1.8(−15)

Table 6.4: Error Norm (Interior of Circular Frame)

$n = m$	$\|f_k(\zeta) - f(\zeta)\|_\infty$
16	4.5(−06)
32	2.7(−12)
64	2.9(−15)

Example 6.3. *Frame of Limacon:*

$$\begin{aligned}\Gamma_0 : z(t) &= a_0\cos t + b_0\cos 2t + \mathrm{i}(a_0\sin t + b_0\sin 2t), \quad a_0 > 0,\ b_0 > 0,\\ \Gamma_1 : z(t) &= a_1\cos t + b_1\cos 2t + \mathrm{i}(a_1\sin t + b_1\sin 2t), \quad a_1 > 0,\ b_1 > 0.\end{aligned}$$

The exact mapping function is

$$g(z) = -e^{2\sigma}\frac{\theta_4\left(\dfrac{1}{2\mathrm{i}}\log f(z) + \dfrac{\mathrm{i}\pi\tau}{2} - \mathrm{i}\sigma;\, q\right)}{\theta_4\left(\dfrac{1}{2\mathrm{i}}\log f(z) + \dfrac{\mathrm{i}\pi\tau}{2} + \mathrm{i}\sigma;\, q\right)}, \quad 0 < \sigma < \frac{\pi\tau}{2}, \quad \mu_1 = e^{-2\sigma},$$

with

$$f(z) = \frac{\sqrt{a_0^2 + 4b_0 z} - a_0}{2b_0}, \quad \tilde{r} = \frac{a_1}{a_0}.$$

For the purpose of numerical comparison, we set $\tilde{r} = q = e^{-\pi\tau}$ and since $\theta_4(\pi\tau\mathrm{i}/2; q) = 0$, this implies $\tau = \dfrac{\ln(\tilde{r})}{-\pi}$ and $a = \dfrac{(2b_0e^{-2\sigma} + a_0)^2 - a_0^2}{4b_0}$. We have chosen $a_0 = 10$, $a_1 = 5$, $b_0 = 3$, $b_1 = b_0/4$, and $\sigma = 0.10$. Figure 6.3 shows the region and image based on our method. See Tables 6.5 and 6.6 for results.

Table 6.5: Error Norm (Frame of Limacon)

$n = m$	minimal $S(\mathbf{x})$	$\|\theta_0(t) - \theta_{0n}(t)\|_\infty$	$\|\theta_1(t) - \theta_{1n}(t)\|_\infty$	$\|\mu_1 - \mu_{1n}\|_\infty$
32	7.8(−10)	2.5(−02)	4.0(−02)	6.9(−03)
64	1.4(−22)	6.3(−05)	2.4(−04)	1.5(−05)
128	4.8(−28)	2.9(−10)	3.8(−09)	5.8(−11)

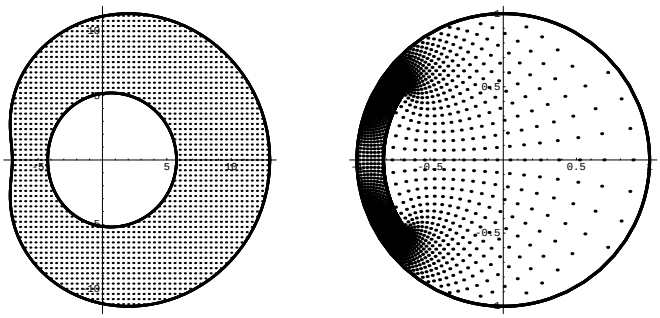

Figure 6.3: Frame of Limacons : a rectangular grid in Ω with grid size 0.4 and its image with radius $\mu_1 = e^{-2\sigma}$.

Table 6.6: Error Norm (Interior of Frame of Limacon)

$n = m$	$\|f_k(\zeta) - f(\zeta)\|_\infty$
32	9.2(−03)
64	5.2(−05)
128	1.1(−09)

Example 6.4. *Elliptic Frame:*

$$\begin{aligned}\Gamma_0 : z(t) &= a_0 \cos t + \mathrm{i}\, b_0 \sin t, \quad a_0 > 0,\ b_0 > 0,\\ \Gamma_1 : z(t) &= a_1 \cos t + \mathrm{i}\, b_1 \sin t, \quad a_1 > 0,\ b_1 > 0, \quad 0 \le t \le 2\pi.\end{aligned}$$

The exact mapping function is

$$g(z) = -e^{2\sigma} \frac{\theta_4\left(\dfrac{1}{2\mathrm{i}} \log f(z) + \dfrac{\mathrm{i}\pi\tau}{2} - \mathrm{i}\sigma;\, q\right)}{\theta_4\left(\dfrac{1}{2\mathrm{i}} \log f(z) + \dfrac{\mathrm{i}\pi\tau}{2} + \mathrm{i}\sigma;\, q\right)}, \quad 0 < \sigma < \frac{\pi\tau}{2}, \quad \mu_1 = e^{-2\sigma},$$

with

$$f(z) = \frac{z + \sqrt{z^2 - (a_0^2 - b_0^2)}}{a_0 + b_0}, \quad \tilde{r} = \frac{a_1 + b_1}{a_0 + b_0}.$$

For the purpose of numerical comparison, we set $\tilde{r} = q = e^{-\pi\tau}$ and since $\theta_4(\pi\tau\mathrm{i}/2; q) = 0$, this implies $\tau = \dfrac{\ln(\tilde{r})}{-\pi}$ and $a = \dfrac{e^{-4\sigma}(a_0 + b_0)^2 + (a_0 - b_0)^2}{2e^{-2\sigma}(a_0 + b_0)}$. We have chosen $a_0 = 7$, $a_1 = 5$, $b_0 = 5$, $b_1 = 1$, and $\sigma = 0.15$. Figure 6.4 shows the region and image based on our method. See Tables 6.7 and 6.8 for results.

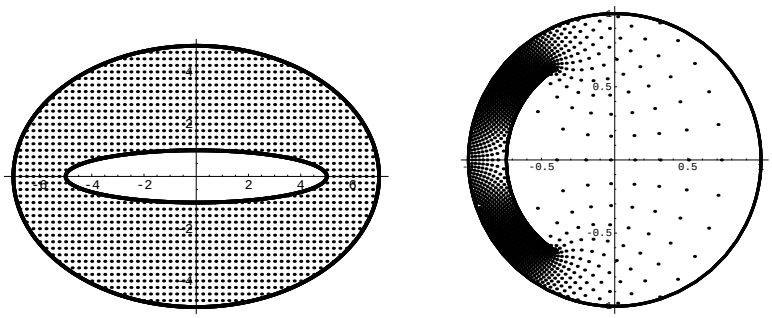

Figure 6.4: Elliptic frame : a rectangular grid in Ω with grid size 0.25 and its image with radius $\mu_1 = e^{-2\sigma}$.

Table 6.7: Error Norm (Elliptic Frame)

$n = m$	minimal $S(\mathbf{x})$	$\|\theta_0(t) - \theta_{0n}(t)\|_\infty$	$\|\theta_1(t) - \theta_{1n}(t)\|_\infty$	$\|\mu_1 - \mu_{1n}\|_\infty$
16	2.0(−03)	1.6(−01)	6.4(−01)	1.7(−02)
32	6.5(−08)	8.9(−04)	2.3(−03)	3.2(−04)
64	6.2(−18)	1.0(−07)	8.7(−07)	2.8(−08)
128	1.2(−25)	1.2(−14)	3.2(−13)	1.2(−14)

Table 6.8: Error Norm (Interior of Elliptic Frame)

$n = m$	$\|f_k(\zeta) - f(\zeta)\|_\infty$
32	9.4(−04)
64	2.8(−07)
128	1.2(−13)

Example 6.5. *Frame of Cassini's Oval:*

$$\Gamma_0 : z(t) = \sqrt{b_0^2 \cos 2t + \sqrt{a_0^4 - b_0^4 \sin^2 2t}}\, e^{it}, \quad a_0 > 0,\ b_0 > 0,$$

$$\Gamma_1 : z(t) = \sqrt{b_1^2 \cos 2t + \sqrt{a_1^4 - b_1^4 \sin^2 2t}}\, e^{it}, \quad a_1 > 0,\ b_1 > 0, \quad 0 \le t \le 2\pi.$$

The exact mapping function is

$$g(z) = -e^{2\sigma}\frac{\theta_4\left(\dfrac{1}{2\mathrm{i}}\log f(z) + \dfrac{\mathrm{i}\pi\tau}{2} - \mathrm{i}\sigma;\, q\right)}{\theta_4\left(\dfrac{1}{2\mathrm{i}}\log f(z) + \dfrac{\mathrm{i}\pi\tau}{2} + \mathrm{i}\sigma;\, q\right)}, \quad 0 < \sigma < \frac{\pi\tau}{2}, \quad \mu_1 = e^{-2\sigma},$$

with

$$f(z) = \frac{a_0 z}{\sqrt{b_0^2 z^2 + a_0^4 - b_0^4}}, \quad \tilde{r} = \frac{a_0 b_1}{a_1 b_0}.$$

For the purpose of numerical comparison, we set $\tilde{r} = q = e^{-\pi\tau}$ and since $\theta_4(\pi\tau\mathrm{i}/2; q) = 0$, this implies $\tau = \dfrac{\ln(\tilde{r})}{-\pi}$ and $a = \sqrt{\dfrac{e^{-4\sigma}(a_0^4 - b_0^4)}{a_0^2 - b_0^2 e^{-4\sigma}}}$. We have chosen $a_0 = 2\sqrt{14}$, $a_1 = 2$, $b_0 = 7$, $b_1 = 1$, and $\sigma = 0.15$. Figure 6.5 shows the region and image based on our method. See Tables 6.9 and 6.10 for results.

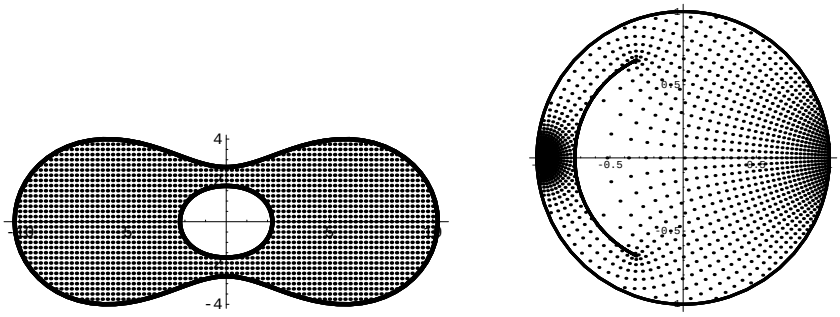

Figure 6.5: Frame of Cassini's oval : a rectangular grid in Ω with grid size 0.25 and its image with $\mu_1 = e^{-2\sigma}$.

Table 6.9: Error Norm (Frame of Cassini's oval)

$n = m$	minimal $S(\mathbf{x})$	$\|\theta_0(t) - \theta_{0n}(t)\|_\infty$	$\|\theta_1(t) - \theta_{1n}(t)\|_\infty$	$\|\mu_1 - \mu_{1n}\|_\infty$
32	1.2(−08)	4.0(−03)	5.0(−03)	6.0(−04)
64	2.1(−20)	1.0(−06)	1.1(−06)	1.2(−07)
128	1.1(−22)	4.9(−14)	7.5(−12)	8.4(−14)

Table 6.10: Error Norm (Interior of Frame of Cassini's oval)

$n = m$	$\|f_k(\zeta) - f(\zeta)\|_\infty$
32	3.1(−03)
64	6.9(−07)
128	2.9(−13)

6.3 Conformal Mapping of Triply Connected Regions onto a Disk with Circular Slits Via the Neumann Kernel

6.3.1 A System of Integral Equations

Suppose Ω is a triply connected region bounded by Γ_0, Γ_1 and Γ_2 (see Figure 4.4 with $M = 2$). For the special case where Ω is a triply connected regions being mapped onto a disk with concentric circular slits, the single integral equation in (4.58) can be separated into a system of equations

$$\begin{aligned} g(z_0,a) + \int_{\Gamma_0} N(z_0,w)g(w,a)|dw| - \int_{-\Gamma_1} P_0(z_0,w)g(w,a)|dw| \\ - \int_{-\Gamma_2} Q_0(z_0,w)g(w,a)|dw| = r^2 h(a,z_0), \quad z_0 \in \Gamma_0, \end{aligned} \tag{6.33}$$

$$\begin{aligned} g(z_1,a) + \int_{\Gamma_0} P_1(z_1,w)g(w,a)|dw| - \int_{-\Gamma_1} N(z_1,w)g(w,a)|dw| \\ - \int_{-\Gamma_2} Q_1(z_1,w)g(w,a)|dw| = \mu_1^2 r^2 h(a,z_1), \quad z_1 \in \Gamma_1, \end{aligned} \tag{6.34}$$

$$\begin{aligned} g(z_2,a) + \int_{\Gamma_0} P_2(z_2,w)g(w,a)|dw| - \int_{-\Gamma_1} Q_2(z_2,w)g(w,a)|dw| \\ - \int_{-\Gamma_2} N(z_2,w)g(w,a)|dw| = \mu_2^2 r^2 h(a,z_2), \quad z_2 \in \Gamma_2, \end{aligned} \tag{6.35}$$

where N is as Neumann kernel (2.22) and

$$\begin{aligned} g(z,a) &= f'(a)T(z)f'(a), \\ h(a,z) &= -\frac{\overline{T(z)}}{(\overline{a}-\overline{z})^2}, \\ P_0(z,w) &= \frac{1}{2\pi \mathrm{i}}\left[\frac{T(z)}{(z-w)} - \frac{\overline{T(z)}}{\mu_1^2(\overline{z}-\overline{w})}\right], \end{aligned}$$

$$
\begin{aligned}
Q_0(z,w) &= \frac{1}{2\pi \mathrm{i}}\left[\frac{T(z)}{(z-w)} - \frac{\overline{T(z)}}{\mu_2^2(\overline{z}-\overline{w})}\right], \\
P_1(z,w) &= \frac{1}{2\pi \mathrm{i}}\left[\frac{T(z)}{(z-w)} - \frac{\mu_1^2\overline{T(z)}}{(\overline{z}-\overline{w})}\right], \\
Q_1(z,w) &= \frac{1}{2\pi \mathrm{i}}\left[\frac{T(z)}{(z-w)} - \frac{\mu_1^2}{\mu_2^2}\frac{\overline{T(z)}}{(\overline{z}-\overline{w})}\right], \\
P_2(z,w) &= \frac{1}{2\pi \mathrm{i}}\left[\frac{T(z)}{(z-w)} - \frac{\mu_2^2\overline{T(z)}}{(\overline{z}-\overline{w})}\right], \\
Q_2(z,w) &= \frac{1}{2\pi \mathrm{i}}\left[\frac{T(z)}{(z-w)} - \frac{\mu_2^2}{\mu_1^2}\frac{\overline{T(z)}}{(\overline{z}-\overline{w})}\right].
\end{aligned}
$$

There are five unknown quantities in the integral equations (6.33), (6.34) and (6.35), namely $g(z_0,a)$, $g(z_1,a)$, $g(z_2,a)$, μ_1, μ_2 and r. The single-valuedness requirement on the mapping function $f(z)$ implies

$$\int_{-\Gamma_1} g(w,a)|dw| = 0, \tag{6.36}$$

$$\int_{-\Gamma_2} g(w,a)|dw| = 0. \tag{6.37}$$

The set of equation (6.33) to (6.37) does not guarantee a unique solution. Several conditions can be obtained to help achieve uniqueness. Suppose f maps Ω conformally onto a unit disk with circular slits. Thus the value of $r = 1$. Next we consider applying the condition $f(z_0(0)) = 1$. From (4.49), this implies $g(z_0(0),a)/|g(z_0(0),a)| = \mathrm{i}$, which means

$$\mathrm{Re}\,[g(z_0(0),a)] = 0, \tag{6.38}$$

$$\mathrm{Im}\,[g(z_0(0),a)/|g(z_0(0),a)|] = 1. \tag{6.39}$$

If the region is symmetric with respect to the axes, we can also impose the conditions

$$\mathrm{Re}\,[g(z_1(0),a)] = 0, \tag{6.40}$$

$$\mathrm{Re}\,[g(z_2(0),a)] = 0. \tag{6.41}$$

Thus the system of integral equations comprising of (6.33), (6.34), (6.35), (6.36), (6.37) with the conditions (6.38), (6.39), (6.40) and (6.41) will lead to a unique solution.

6.3.2 Numerical Implementation

Suppose Γ_0, Γ_1 and Γ_2 be given in parametric representations as follows:

$$\begin{aligned}
\Gamma_0 : &\qquad z = z_0(t), \quad 0 \le t \le \beta_0, \\
\Gamma_1 : &\qquad z = z_1(t), \quad 0 \le t \le \beta_1, \\
\Gamma_2 : &\qquad z = z_2(t), \quad 0 \le t \le \beta_2.
\end{aligned}$$

Then the system of integral equations (6.33), (6.34), (6.35), 6.36) and 6.37) become

$$\begin{aligned}
&g(z_0(t),a) + \int_0^{\beta_0} N(z_0(t),z_0(s))g(z_0(s),a)|z_0'(s)|ds \\
&\quad - \int_0^{\beta_1} P_0(z_0(t),z_1(s))g(z_1(s),a)|z_1'(s)|ds \\
&\quad - \int_0^{\beta_2} Q_0(z_0(t),z_2(s))g(z_2(s),a)|z_2'(s)|ds = h(a,z_0(t)), \\
&\qquad\qquad\qquad\qquad\qquad\qquad z_0(t) \in \Gamma_0, \qquad (6.42) \\
&g(z_1(t),a) + \int_0^{\beta_0} P_1(z_1(t),z_0(s))g(z_0(s),a)|z_0'(s)|ds \\
&\quad - \int_0^{\beta_1} N(z_1(t),z_1(s))g(z_1(s),a)|z_1'(s)|ds \\
&\quad - \int_0^{\beta_2} Q_1(z_1(t),z_2(s))g(z_2(s),a)|z_2'(s)|ds = \mu_1^2 h(a,z_1(t)), \\
&\qquad\qquad\qquad\qquad\qquad\qquad z_1(t) \in \Gamma_1, \qquad (6.43) \\
&g(z_2(t),a) + \int_0^{\beta_0} P_2(z_2(t),z_0(s))g(z_0(s),a)|z_0'(s)|ds \\
&\quad - \int_0^{\beta_1} Q_2(z_2(t),z_1(s))g(z_1(s),a)|z_1'(s)|ds \\
&\quad - \int_0^{\beta_2} N(z_2(t),z_2(s))g(z_2(s),a)|z_2'(s)|ds = \mu_2^2 h(a,z_2(t)), \\
&\qquad\qquad\qquad\qquad\qquad\qquad z_2(t) \in \Gamma_2, \qquad (6.44)
\end{aligned}$$

$$\int_0^{\beta_1} g(z_1(s),a)|z_1'(s)|ds = 0, \tag{6.45}$$

$$\int_0^{\beta_2} g(z_2(s),a)|z_2'(s)|ds = 0. \tag{6.46}$$

Multiply (6.42), (6.43) and (6.44) respectively by $|z_0'(t)|$, $|z_1'(t)|$ and $|z_2'(t)|$ gives

$$\begin{aligned}
&|z_0'(t)|g(z_0(t),a) + \int_0^{\beta_0} |z_0'(t)|N(z_0(t),z_0(s))g(z_0(s),a)|z_0'(s)|ds \\
&\quad - \int_0^{\beta_1} |z_0'(t)|P_0(z_0(t),z_1(s))g(z_1(s),a)|z_1'(s)|ds \\
&\quad - \int_0^{\beta_2} |z_0'(t)|Q_0(z_0(t),z_2(s))g(z_2(s),a)|z_2'(s)|ds \\
&\qquad = |z_0'(t)|h(a,z_0(t)), \qquad z_0(t) \in \Gamma_0,
\end{aligned} \tag{6.47}$$

$$\begin{aligned}
&|z_1'(t)|g(z_1(t),a) + \int_0^{\beta_0} |z_1'(t)|P_1(z_1(t),z_0(s))g(z_0(s),a)|z_0'(s)|ds \\
&\quad - \int_0^{\beta_1} |z_1'(t)|N(z_1(t),z_1(s))g(z_1(s),a)|z_1'(s)|ds \\
&\quad - \int_0^{\beta_2} |z_1'(t)|Q_1(z_1(t),z_2(s))g(z_2(s),a)|z_2'(s)|ds \\
&\qquad = \mu_1^2|z_1'(t)|h(a,z_1(t)), \qquad z_1(t) \in \Gamma_1,
\end{aligned} \tag{6.48}$$

$$\begin{aligned}
&|z_2'(t)|g(z_2(t),a) + \int_0^{\beta_0} |z_2'(t)|P_2(z_2(t),z_0(s))g(z_0(s),a)|z_0'(s)|ds \\
&\quad - \int_0^{\beta_1} |z_2'(t)|Q_2(z_2(t),z_1(s))g(z_1(s),a)|z_1'(s)|ds \\
&\quad - \int_0^{\beta_2} |z_2'(t)|N(z_2(t),z_2(s))g(z_2(s),a)|z_2'(s)|ds \\
&\qquad = \mu_2^2|z_1'(t)|h(a,z_1(t)), \qquad z_2(t) \in \Gamma_2.
\end{aligned} \tag{6.49}$$

We next define

$$\begin{aligned}
\phi_0(t) &= |z_0'(t)|g(z_0(t),a), \\
\phi_1(t) &= |z_1'(t)|g(z_1(t),a), \\
\phi_2(t) &= |z_2'(t)|g(z_2(t),a), \\
\varphi_0(t) &= |z_0'(t)|h(a,z_0(t)), \\
\varphi_1(t) &= \mu_1^2|z_1'(t)|h(a,z_1(t)), \\
\varphi_2(t) &= \mu_2^2|z_2'(t)|h(a,z_2(t)),
\end{aligned}$$

$$
\begin{aligned}
K_{00}(t_0, s_0) &= |z_0'(t)| N(z_0(t), z_0(s)), \\
K_{01}(t_0, s_1) &= |z_0'(t)| P_0(z_0(t), z_1(s)), \\
K_{02}(t_0, s_2) &= |z_0'(t)| Q_0(z_0(t), z_2(s)), \\
K_{10}(t_1, s_0) &= |z_1'(t)| P_1(z_1(t), z_0(s)), \\
K_{11}(t_1, s_1) &= |z_1'(t)| N(z_1(t), z_1(s)), \\
K_{12}(t_1, s_2) &= |z_1'(t)| Q_1(z_1(t), z_2(s)), \\
K_{20}(t_2, s_0) &= |z_2'(t)| P_2(z_2(t), z_0(s)), \\
K_{21}(t_2, s_1) &= |z_2'(t)| Q_2(z_2(t), z_1(s)), \\
K_{22}(t_2, s_2) &= |z_2'(t)| N(z_2(t), z_2(s)).
\end{aligned}
$$

Thus equations (6.47), (6.48), (6.49), (6.45) and (6.46) can be briefly written as

$$
\begin{aligned}
&\phi_0(t) + \int_0^{\beta_0} K_{00}(t_0, s_0)\phi_0(s)ds - \int_0^{\beta_1} K_{01}(t_0, s_1)\phi_1(s)ds \\
&\qquad - \int_0^{\beta_2} K_{02}(t_0, s_2)\phi_2(s)ds = \varphi_0(t), \qquad (6.50) \\
&\phi_1(t) + \int_0^{\beta_0} K_{10}(t_1, s_0)\phi_0(s)ds - \int_0^{\beta_1} K_{11}(t_1, s_1)\phi_1(s)ds \\
&\qquad - \int_0^{\beta_2} K_{12}(t_1, s_2)\phi_2(s)ds = \varphi_1(t), \qquad (6.51) \\
&\phi_2(t) + \int_0^{\beta_0} K_{20}(t_2, s_0)\phi_0(s)ds - \int_0^{\beta_1} K_{21}(t_2, s_1)\phi_1(s)ds \\
&\qquad - \int_0^{\beta_2} K_{22}(t_2, s_2)\phi_2(s)ds = \varphi_2(t), \qquad (6.52) \\
&\int_0^{\beta_1} \phi_1(s)ds = 0, \qquad (6.53) \\
&\int_0^{\beta_2} \phi_2(s)ds = 0. \qquad (6.54)
\end{aligned}
$$

We choose $\beta_0 = \beta_1 = \beta_2 = 2\pi$ and n equidistant collocation points $t_i = (i-1)\beta_0/n$, $1 \le i \le n$ on Γ_0, m equidistant collocation points $t_{\tilde{i}} = (\tilde{i}-1)\beta_1/m$, $1 \le \imath \le m$, on Γ_1 and l equidistant collocation points $t_{\hat{i}} = (\hat{i}-1)\beta_2/l$, $1 \le \hat{i} \le l$,

on Γ_2. Applying the Nyström's method with trapezoidal rule to discretize (6.50) to (6.54), we obtain

$$\phi_0(t_i) + \frac{\beta_0}{n}\sum_{j=1}^{n} K_{00}(t_i,t_j)\phi_0(t_j) - \frac{\beta_1}{m}\sum_{\jmath=1}^{m} K_{01}(t_i,t_\jmath)\phi_1(t_\jmath) - \frac{\beta_2}{l}\sum_{\hat{\jmath}=1}^{l} K_{02}(t_i,t_{\hat{\jmath}})\phi_2(t_{\hat{\jmath}}) = \gamma_0(t_i), \tag{6.55}$$

$$\phi_1(t_\imath) + \frac{\beta_0}{n}\sum_{j=1}^{n} K_{10}(t_\imath,t_j)\phi_0(t_j) - \frac{\beta_1}{m}\sum_{\jmath=1}^{m} K_{11}(t_\imath,t_\jmath)\phi_1(t_\jmath) - \frac{\beta_2}{l}\sum_{\hat{\jmath}=1}^{l} K_{12}(t_\imath,t_{\hat{\jmath}})\phi_2(t_{\hat{\jmath}}) = \gamma_1(t_\imath), \tag{6.56}$$

$$\phi_2(t_{\hat{\imath}}) + \frac{\beta_0}{n}\sum_{j=1}^{n} K_{20}(t_{\hat{\imath}},t_j)\phi_0(t_j) - \frac{\beta_1}{m}\sum_{\jmath=1}^{m} K_{21}(t_{\hat{\imath}},t_\jmath)\phi_1(t_\jmath) - \frac{\beta_2}{l}\sum_{\hat{\jmath}=1}^{l} K_{22}(t_{\hat{\imath}},t_{\hat{\jmath}})\phi_2(t_{\hat{\jmath}}) = \gamma_2(t_{\hat{\imath}}), \tag{6.57}$$

$$\sum_{\jmath=1}^{m}\phi_1(t_\jmath) = 0, \tag{6.58}$$

$$\sum_{\hat{\jmath}=1}^{m}\phi_2(t_{\hat{\jmath}}) = 0. \tag{6.59}$$

Equations (6.55) to (6.59) lead to a system of $(n+m+l+2)$ non-linear complex equations in n unknowns $\phi_0(t_i)$, m unknowns $\phi_1(t_\imath)$, l unknowns $\phi_2(t_{\hat{\imath}})$, as well as the unknown parameters μ_1 and μ_2. By defining the matrices

$$x_{0i} = \phi_0(t_i), \qquad x_{1\imath} = \phi_1(t_\imath),$$
$$x_{2\hat{\imath}} = \phi_2(t_{\hat{\imath}}), \qquad \varphi_{0i} = \varphi_0(t_i),$$
$$\varphi_{1\imath} = \varphi_1(t_\imath), \qquad \varphi_{2\hat{\imath}} = \varphi_2(t_{\hat{\imath}}),$$
$$B_{ij} = \frac{\beta_0}{n}K_{00}(t_i,t_j), \qquad C_{i\jmath} = \frac{\beta_1}{m}K_{01}(t_i,t_\jmath),$$
$$D_{i\hat{\jmath}} = \frac{\beta_1}{l}K_{02}(t_i,t_{\hat{\jmath}}), \qquad E_{\imath j} = \frac{\beta_0}{n}K_{10}(t_\imath,t_j),$$
$$F_{\imath\jmath} = \frac{\beta_1}{m}K_{11}(t_\imath,t_\jmath), \qquad G_{\imath\hat{\jmath}} = \frac{\beta_1}{l}K_{12}(t_\imath,t_{\hat{\jmath}}),$$
$$H_{\hat{\imath}j} = \frac{\beta_0}{n}K_{20}(t_{\hat{\imath}},t_j), \qquad J_{\hat{\imath}\jmath} = \frac{\beta_1}{m}K_{21}(t_{\hat{\imath}},t_\jmath),$$
$$L_{\hat{\imath}\hat{\jmath}} = \frac{\beta_1}{l}K_{22}(t_{\hat{\imath}},t_{\hat{\jmath}}),$$

the system of equations (6.55), (6.56) and (6.57) can be written as $n+m+l$ by $n+m+l$ system of equations

$$\begin{aligned} [I_{nn}+B_{nn}]x_{0n} - C_{nm}x_{1m} - D_{nl}x_{2l} &= \varphi_{0n}, && (6.60)\\ E_{mn}x_{0n} + [I_{mm}-F_{mm}]x_{1m} - G_{ml}x_{2l} &= \varphi_{1m}, && (6.61)\\ H_{ln}x_{0n} - J_{lm}x_{1m} + [I_{ll}-L_{ll}]x_{2l} &= \varphi_{2l}. && (6.62) \end{aligned}$$

The result in matrix form for the system of equations (6.60), (6.61) and (6.62) is

$$\begin{pmatrix} I_{nn}+B_{nn} & \cdots & -C_{nm} & \cdots & -D_{nl} \\ \vdots & \ddots & \vdots & \ddots & \vdots \\ E_{mn} & \cdots & I_{mm}-F_{mm} & \cdots & G_{ml} \\ \vdots & \ddots & \vdots & \ddots & \vdots \\ H_{ln} & \cdots & -J_{lm} & \cdots & I_{ll}-L_{ll} \end{pmatrix} \begin{pmatrix} \mathbf{x}_{0n} \\ \vdots \\ \mathbf{x}_{1m} \\ \vdots \\ \mathbf{x}_{2l} \end{pmatrix} = \begin{pmatrix} \varphi_{0n} \\ \vdots \\ \varphi_{1m} \\ \vdots \\ \varphi_{2l} \end{pmatrix}. \tag{6.63}$$

Defining

$$\mathbf{F} = \begin{pmatrix} I_{nn}+B_{nn} & \cdots & -C_{nm} & \cdots & -D_{nm} \\ \vdots & \ddots & \vdots & \ddots & \vdots \\ E_{mn} & \cdots & I_{mm}-F_{mm} & \cdots & -G_{mm} \\ \vdots & \ddots & \vdots & \ddots & \vdots \\ H_{ln} & \cdots & -J_{lm} & \cdots & I_{ll}-L_{ll} \end{pmatrix},$$

$$\mathbf{x} = \begin{pmatrix} \mathbf{x}_{0n} \\ \vdots \\ \mathbf{x}_{1m} \\ \vdots \\ \mathbf{x}_{2l} \end{pmatrix}, \quad \text{and} \quad \mathbf{Y} = \begin{pmatrix} \varphi_{0n} \\ \vdots \\ \varphi_{1m} \\ \vdots \\ \varphi_{2l} \end{pmatrix},$$

the $(n+m+l)\times(n+m+l)$ system can be written briefly as $\mathbf{Fx} = \mathbf{Y}$. Separating

$\mathbf{F}$, $\mathbf{x}$ and $\mathbf{Y}$ in terms of the real and imaginary parts, the system can be written as

$$\operatorname{Re}\mathbf{F}\operatorname{Re}\mathbf{x} - \operatorname{Im}\mathbf{F}\operatorname{Im}\mathbf{x} + \mathrm{i}\,(\operatorname{Im}\mathbf{F}\operatorname{Re}\mathbf{x} + \operatorname{Re}\mathbf{F}\operatorname{Im}\mathbf{x}) = \operatorname{Re}\mathbf{Y} + \mathrm{i}\operatorname{Im}\mathbf{Y}. \quad (6.64)$$

The single $(n+m+l)\times(n+m+l)$ complex system (6.64) above is equivalent to the $2(n+m+l)\times 2(n+m+l)$ system matrix involving the real (Re) and imaginary (Im) of the unknown functions, i.e.,

$$\begin{pmatrix} \operatorname{Re}\mathbf{F} & \cdots & \operatorname{Im}\mathbf{F} \\ \vdots & \ddots & \vdots \\ \operatorname{Im}\mathbf{F} & \cdots & \operatorname{Re}\mathbf{F} \end{pmatrix} \begin{pmatrix} \operatorname{Re}\mathbf{x} \\ \vdots \\ \operatorname{Im}\mathbf{x} \end{pmatrix} = \begin{pmatrix} \operatorname{Re}\mathbf{Y} \\ \vdots \\ \operatorname{Im}\mathbf{Y} \end{pmatrix}. \quad (6.65)$$

Note however that the $2(n+m+l)\times 2(n+m+l)$ matrix in (6.65) contains the unknown parameters μ_1 and μ_2.

Since $\phi = \operatorname{Re}\phi + \mathrm{i}\operatorname{Im}\phi$, equations (6.58), (6.59), (6.38), (6.39), (6.40) and (6.41) become

$$\sum_{\jmath=1}^{m}(\operatorname{Re}x_{1\jmath} + \mathrm{i}\operatorname{Im}x_{1\jmath}) = 0, \quad (6.66)$$

$$\sum_{\hat{\jmath}=1}^{l}(\operatorname{Re}x_{2\hat{\jmath}} + \mathrm{i}\operatorname{Im}x_{2\hat{\jmath}}) = 0, \quad (6.67)$$

$$\operatorname{Re}x_{01} = 0, \quad (6.68)$$

$$\operatorname{Im}[x_{01}/\sqrt{(\operatorname{Re}x_{01})^2 + (\operatorname{Im}x_{01})^2}] = 1, \quad (6.69)$$

$$\operatorname{Re}x_{11} = 0, \quad (6.70)$$

$$\operatorname{Re}x_{21} = 0. \quad (6.71)$$

The system of equations (6.65) to (6.71) is an over-determined system of nonlinear equations involving $2(n+m+l)+6$ equations in $2(n+m+l)+2$ unknowns. We use the Lavenberg-Marquardt algorithm to solve this nonlinear least square problem. The Lavenberg-Marquardt algorithm which is stated in (5.56). Here, $\mathbf{x}$ stands for the $(2n+2m+2l+2)$ vector ($\operatorname{Re}x_{01}$, $\operatorname{Re}x_{02}$, ..., $\operatorname{Re}x_{0n}$, $\operatorname{Re}x_{11}$, $\operatorname{Re}x_{12}$,

..., $\mathrm{Re}\, x_{1m}$, $\mathrm{Re}\, x_{21}$, $\mathrm{Re}\, x_{22}$, ..., $\mathrm{Re}\, x_{2l}$, $\mathrm{Im}\, x_{01}$, $\mathrm{Im}\, x_{02}$, ..., $\mathrm{Im}\, x_{0n}$, $\mathrm{Im}\, x_{11}$, $\mathrm{Im}\, x_{12}$, ..., $\mathrm{Im}\, x_{1m}$, $\mathrm{Im}\, x_{21}$, $\mathrm{Im}\, x_{22}$, ..., $\mathrm{Im}\, x_{2l}$, μ_1, μ_2), and $\mathbf{f} = (f_1, f_2, ..., f_{2(n+m+l)+6})$.

The strategy for getting the initial estimation is to provide rough estimates of the slit radius, $\mu_1 \approx 0.8$ and $\mu_2 \approx 0.7$ for the test region. Then the non-linear system of equations (6.63), (6.58) and (6.59) reduces to over-determined linear system. Writing the over-determined system as $\mathbf{Cx} = \dot{\mathbf{y}}$, we use the least-squares solutions of $\mathbf{Cx} = \dot{\mathbf{y}}$ which are precisely the solutions of $\mathbf{C}^{\mathrm{T}}\mathbf{Cx} = \mathbf{C}^{\mathrm{T}}\dot{\mathbf{y}}$ (Johnson *et al.*, 1998). The solutions are then taken as initial estimation. In our experiment, we have chosen the number of collocation points on Γ_0, Γ_1 and Γ_2 being equal, i.e., $N = n = m = l$.

The system of equations (6.65) together with (6.66) to (6.71) are then solved for the unknown function

$$\phi_0(t) = |z_0'(t)|f'(a)T(z_0(t))f'(z_0(t)),$$

$$\phi_1(t) = |z_1'(t)|f'(a)T(z_1(t))f'(z_1(t)),$$

$$\phi_2(t) = |z_2'(t)|f'(a)T(z_2(t))f'(z_2(t)),$$

μ_1 and μ_2. Finally the boundary correspondence functions $\theta_0(t)$, $\theta_1(t)$ and $\theta_2(t)$ are then computed approximately by the formulas

$$\theta_0(t) = \mathrm{Arg}\, f(z_0(t)) \approx \mathrm{Arg}(-\mathrm{i}\phi_0(t)),$$
$$\theta_1(t) = \mathrm{Arg}\, f(z_1(t)) \approx \mathrm{Arg}(\pm\mathrm{i}\phi_1(t)).$$
$$\theta_2(t) = \mathrm{Arg}\, f(z_2(t)) \approx \mathrm{Arg}(\pm\mathrm{i}\phi_2(t)).$$

6.3.3 Numerical Results

For numerical results, we have used an ellipse and two circle as a test regions (see Figure 6.6). Let

$$\begin{aligned}
\Gamma_0 : z_0(t) &= 4\cos t + \mathrm{i}\sin t, \\
\Gamma_1 : z_1(t) &= -1 + 0.6\,(\cos t + \mathrm{i}\sin t), \\
\Gamma_2 : z_2(t) &= 1.2 + 0.3\,(\cos t + \mathrm{i}\sin t), \quad t : 0 \le t \le 2\pi.
\end{aligned}$$

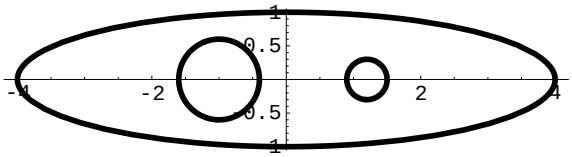

Figure 6.6: Ellipse/two circle

We have adopted the example from Reichel (1986) and Kokkinos *et al.* (1990) for comparison of μ_1 and μ_2 (see Tables 6.11 and 6.12). Figure 6.7 shows the image of the mapping based on our method. Since the conditions of the problems are somewhat different, $\mu_0 = 1$ in ours and $\mu_0 = 2.5$ in Reichel's and Kokkinos *et al.*, our radius should be multiplied by 2.5. Values of μ_1 and μ_2 in Reichel are denoted here by $\mu_{1,R}$ and $\mu_{2,R}$ respectively. While the values of μ_1 and μ_2 in Kokkinos *et al.* are denoted here by $\mu_{1,K}$ and $\mu_{2,K}$ respectively. All the computations are done using MATHEMATICA package (Wolfram, 1991) in single precision (16 digit machine precision).

Table 6.11: Radii comparison with Reichel (1986)

N	minimal $S(\mathbf{x})$	$\|\mu_1 \times 2.5 - \mu_{1,R}\|_\infty$	$\|\mu_2 \times 2.5 - \mu_{2,R}\|_\infty$
64	2.4(−24)	1.8(−02)	6.0(−04)

Table 6.12: Radii comparison with Kokkinos *et al.* (1990)

N	$\|\mu_1 \times 2.5 - \mu_{1,K}\|_\infty$	$\|\mu_2 \times 2.5 - \mu_{2,K}\|_\infty$
64	1.8(−02)	5.9(−04)

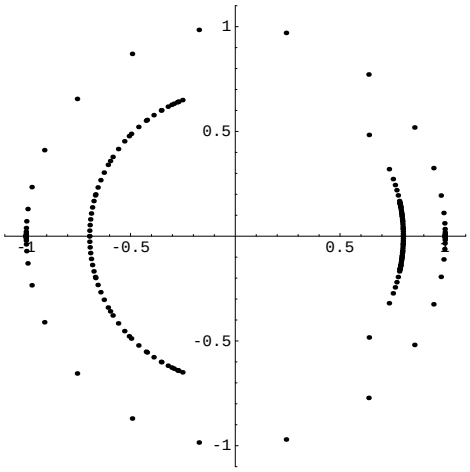

Figure 6.7: The image of the mapping.

We think that the accuracy can be further improved by using $N = 128$. However, for triply connected regions, this leads to very large nonlinear system involving $128 \times 6 + 6 = 774$ equations which require more powerful computer to handle it.

CHAPTER 7

SUMMARY AND CONCLUSIONS

7.1 Summary of the Research

The main contribution of this project is the construction of some new boundary integral equations involving the Kerzman-Stein and the Neumann kernels for conformal mapping of multiply connected regions. The boundary integral equations involve the unknown parameter radii. The integral equations are used to solve numerically the problem of conformal mapping of multiply connected regions onto an annulus with circular slits and a disk with circular slits.

Chapter 1 contains a general introduction and overview of the research including the research background, the scope and objectives and the project outline of. The literature review on the ideas of conformal mapping, some theories of the Riemann mapping function and conformal mapping of multiply connected regions are given in Chapter 2. We also presented some well-known exact conformal mappings of doubly connected regions for certain special regions like annulus, circular frame, frame of limacon, frame of Cassini's oval and elliptic frame. These regions are used as a part of the test regions in our numerical

implementations that had been carried out in Chapters 3, 5 and 6. Several methods that have been proposed in the literature for the numerical conformal mapping of doubly and multiply connected regions were discussed in the last section of Chapter 2.

In Chapter 3, we showed how the integral equation for conformal mapping of doubly connected regions via the Kerzman-Stein can be modified to a new numerically tractable integral equation which also involves the unknown inner radius, μ. However, the integral equation has no unique solution. By imposing the uniqueness condition and discretizing the integral equation led to an over-determined system of non-linear equations. The system obtained was the solved simultaneously using Gauss-Newton algorithm and Lavenberg-Marquardt with Fletcher's algorithm for solving the non-linear least squares problems.

The main contribution of this project begin with Chapter 4 where the boundary relationship satisfied by a function analytic in a doubly connected region by Murid and Razali (1999) was extended to construction of the bounded multiply connected regions. Some new boundary integral equations for conformal mapping of multiply connected regions were constructed. Special cases of this boundary integral equation are the conformal mapping of multiply connected regions onto an annulus with concentric circular slits and onto a disk with concentric circular slits. Furthermore this integral equation leads to a much simpler derivation of a system of an integral equations developed in Chapter 3 for the case of doubly connected region onto an annulus with the Kerzman-Stein kernel.

In Chapter 5, we used the integral equations derived in Chapter 4 to solve numerically the problem of conformal mapping for doubly and triply connected regions onto an annulus and an annulus with a circular slit with the Kerzman-Stein and the Neumann kernels respectively. However, the integral equation has no unique solution. By imposing some normalizing conditions and discretizing the

integral equations led to an over-determined system of non-linear equations. The system obtained was then solved simultaneously using Gauss-Newton algorithm and Lavenberg-Marquardt algorithm. The Lavenberg-Marquardt algorithm is more robust than the Gauss-Newton algorithm. As a general rule, if one faced with a convergence problem with the Gauss-Newton algorithm, then it is recommended to use the Lavenberg-Marquardt algorithm instead.

After the boundary values of the mapping function are calculated, we use the Cauchy's integral formula to determine the mapping function in the interior of the regions. Numerical examples on some test regions are also presented. From comparison for some test regions, it can be deduced that our method produce approximation of higer accuracy than the result obtained by Amano (1994), Ellacott (1979), Papamicheal and Warby (1984), Reichel (1986), Okano *et al.* (2003), Kokkinos *et al.* (1990) and Symm (1969). This results have improved the theoretical and numerical technique used in Chapter 3.

In Chapter 6, we used the integral equations constructed in Chapter 4 to solve numerically another problem of conformal mapping of multiply connected regions onto a disk with circular slits with Neumann kernel. The system of integral equations obtained also involved the unknown parameter radii. For the doubly connected regions case, the new system of integral equations is based on a boundary integral equation satisfied by $f'(z)$, $f'(a)$, r and μ, where a is a fixed interior point with $f'(a)$ predetermined. The boundary values of $f(z)$ is completely determined from the boundary values of $f'(z)$ through a boundary relationship. Discretization of the integral equation has led to a system of non-linear equations. Together with condition of single-valuedness, uniqueness and the Cauchy integral formula, a unique solution to the system is then computed by means of an optimization method called the Lavenberg-Marquadt algorithm. The Cauchy integral formula also used to compute the interior of the regions. Typical examples for some doubly connected regions show that numerical results of high accuracy can be obtained for the conformal mapping problem when the boundaries are sufficiently smooth.

The same approach in doubly connected regions is further extended to the case of triply connected region with different normalizing conditions to avoid the difficulty of computing unknown parameter $f'(a)$. The result obtained however does not produce a good accuracy compared to the doubly connected regions.

The advantage of our method is that it calculates the boundary correspondence functions and the unknown parameter radii simultaneously with same degree of accuracy. The numerical examples show the effectiveness of the proposed method.

7.2 Suggestions for Future Research

The numerical results shown for the case of triply connected regions onto a disk with circular slits does not produce reasonable accuracy compared to the case of doubly connected region. Further work on improving the numerical technique or normalizing conditions used in this project need to be carried out. We have also tried out other methods likes the Broyden–Fletcher–Goldfarb–Shanno (BFGS) method, homotopy method and Gauss-Newton method to solved our over-determined systems of non-linear equations but these methods lead to convergence problem. The nonlinear systems are in fact expressible as multivariate polynomial system. We think that finding suitable technique for solving these multivariate polynomial systems that arise for conformal mapping constitutes a good problem for future research.

The derivation of integral equations in Chapter 4 was only for two important cannonical regions for conformal mapping of bounded multiply connected regions i.e. a disk with concentric circular slits and an annulus with concentric circular slits. The integral equations (4.35) and (4.56) are the same for both canonical regions with only the right-hand side depending on the type of

the canonical regions. Probably some extensions or modifications of the theories are required to obtain the integral equations related to the other three important cannonical unbounded regions, namely the circular slit regions, the radial slit region and the the parallel slit region.

All the numerical implementation in Chapters 5 and 6 were based on solving the system of integral equations of conformal mapping problem when the boundaries are sufficiently smooth. More research is required to modify the integral equations presented in this project to multiply connected region involving corners.

With the above summary and recommendations for further research, we conclude this project.

REFERENCES

Abramowitz, M. and Stegun, I. A. (1970). *Handbook of Mathematical Functions.* New York: Dover Pubs.

Ahlfors, L. V. (1979). *Complex Analysis.* Singapore: International Student Edition, McGraw-Hill,

Amano, K. (1994). A Charge Simulation Method for the Numerical Conformal Mapping of Interior, Exterior and Doubly Connected Domains. *Journal of Computational and Applied Mathematics.* 53: 353–370.

Andersen, C., Christiansen, S. E., Moller, O. and Tornehave, H. (1962). Conformal mapping. In: Gram, C. (Ed.) *Selected numerical methods.* Coppenhagen: Regnecentralen. 114–261.

Antia, H. M. (1991). *Numerical Methods for Scientists and Engineers,* New Delhi: Tata McGraw-Hill Publishing Company Limited.

Atkinson, K. E. (1976). *A Survey of Numerical Methods for the Solution of Fredholm Integral Equations.* Philadelphia: Society for Industrial and Applied Mathematics.

Bergman, S. (1970). *The Kernel Function and Conformal Mapping.* Providence, RI : American Mathematical Society.

Churchill, R. V. and Brown, J. W. (1984). *Complex Variables and Applications.* New York: McGraw-Hill.

Cohn, H. (1967). *Conformal Mapping On Riemann Surfaces.* New York: McGraw-Hill.

Crowdy D. G. and Marshall, J. S. (2006). Conformal Mapping Between Canonical Multiply Connected Domains. *Comput. Methods Funct. Theory.* 6: 59–76.

Davis, P. J and Rabinowitz, P. (1984). *Methods of Numerical Integration.* 2nd Edition. Orlando: Academic Press.

Ellacott, S. W. (1979). On the Approximate Conformal Mapping of Multiply Connected Domains. *Numerische Mathematik.* 33: 437–446.

Fletcher, R. (1986). *Practical Methods of Optimization, Vol. 1.* New York: John Wiley.

Goluzin, G. M. (1969). *Geometric Theory of Functions of a Complex Variable.* Trans. Math. monographs, vol. 26, Providence: American Mathematical Society.

Gonzalez, M. O. (1992). *Classical Complex Analysis.* New York: Marcel Decker.

Henrici, P. (1974). *Applied and Computational Complex Analysis, Volume 1.* New York: John Wiley.

Henrici, P. (1986). *Applied and Computational Complex Analysis, Volume 3.* New York: John Wiley.

Hille, E. (1962). *Analytic Function Theory. Volume 2.* Boston: Ginn.

Hille, E. (1973). *Analytic Function Theory. Volume 1.* New York : Chelsea Publishing Company.

Hough, D. M. and Papamichael, N. (1983). An Integral equation Method for the Numerical Conformal Mapping of Interior, Exterior and Doubly-Connected Domains. *Numerische Mathematik.* 14: 287–307.

Johnson, L. W., Riess, R. D. and Arnold, J. T. (1998). *Linear Algebra,* 4^{th} *Edition.* New York: Addison-Wesley Longman.

Kerzman, N. and Trummer, M. (1986). Numerical Conformal Mapping via the Szegö Kernel. *Journal of Computational and Applied Mathematics.* 14: 111-123.

Kokkinos, C. A., Papamichael, N. and Sideridis, A. B. (1990). An Orthonoermalization Method for the Approximate Conformal Mapping of Multiply-Connected Domains. *IMA Journal of Numerical Analysis.* 9: 343–359.

Kythe, P. K. (1998). *Computational Conformal Mapping.* New Orleans: Birkhäuser Boston.

Marsden, J. E. (1973). *Basic Complex Analysis.* Washington: W. H. Freeman.

Mayo, A. (1986). Rapid Method for the Conformal Mapping of Multiply Connected Regions. *Journal of Computational and Applied Mathematics.* 14: 143–153.

Murid, A. H. M. (1997). *Boundary Integral Equation Approach for Numerical Conformal Mapping.* Ph.D. Thesis. Universiti Teknologi Malaysia, Skudai.

Murid, A. H. M., Nashed, M. Z. and Razali, M. R. M. (1999). Some Integral Equations Related to the Riemann Map, in *Proceedings of the Third CMFT Conference: Computational Methods and Function Theory 1997.* Papamichael, N., Ruscheweyh, St. and Saff, E. B. (Eds). Singapore:World Scientific. 405–419.

Murid, A. H. M. and Razali, M. R. M. (1999). An Integral Equation Method for Conformal Mapping of Doubly Connected Regions. *Matematika.* 15(2): 79–93.

Murray, W. (1972). *Numerical Methods for Unconstrained Optimization.* London and New York: Academic Press.

Nasser, M. M. S. (2009). A Boundary Integral Equation for Conformal Mapping of Bounded Multiply Connected Regions. *CMFT.* 9(1): 127–143.

Nehari, Z. (1975). *Conformal Mapping, Originally published by the McGraw-Hill in 1952* New York: Dover.

Okano, D., Ogata, H., Amano, K. and Sugihara, M. (2003). Numerical Conformal Mapping of Bounded Multiply Connected Domains by the Charge Simulation Method. *Journal of Computational and Applied Mathematics.* 159: 109–117.

Papamicheal, N. and Warby, M. K. (1984). Pole-type Singularities and the Numerical Conformal Mapping of Doubly Connected Domains. *Journal of Computational and Applied Mathematics.* 10: 93–106.

Papamichael, N. and Kokkinos, C. A. (1984). The Use of Singular Function for the Approximate Conformal Mapping of Doubly-Connected Domains. *SIAM J. Sci. Stst. Comput.* 5(3): 684–700.

Razali, M. R. M., Nashed, M. Z. and Murid, A. H. M. (1997). Numerical Conformal Mapping via the Bergman Kernel. *Journal of Computational and Applied Mathematics.* 82(1,2): 333–350.

Reichel, L. (1986). A Fast Method for Solving Certain Integral Equation of The First Kind with Application to Conformal Mapping. *Journal of Computational and Applied Mathematics.* 14: 125–142.

Saff. E. B and Snider. A. D (2003). *Fundamentals of Complex Analysis.* New Jersey: Pearson Education. Inc.

Schinzinger, R. and Laura, P. A. A. (1991). *Conformal Mapping: Methods and Applications.* Amsterdam: Elsevier.

Swarztrauber, P. N. (1972). On The Numerical Solution of The Dirichlet Problem for a Region of General Shape. *SIAM J. Numer. Anal.* 9(2): 300–306.

Symm, G. T. (1969). Conformal Mapping of Doubly Connected Domain. *Numerische Mathematik.* 13: 448–457.

Trefethen, L. N. (1986). *Numerical Conformal Mapping.* Amsterdam: North-Holland.

Von Koppenfels, W. and Stallmann, F. (1959). *Praxis der konformen Abbildung.* Berlin, Gttingen: Heidelberg.

Wegmann, R. (2005). *Methods for Numerical Conformal Mapping, in: R. Kühnau (Ed.), Handbook of Complex Analysis: Geometric Function Theory, Vol. 2.* Elsevier: Amsterdam. 351–477.

Wen, G. C. (1992). *Conformal Mappings and Boundary Value Problems.* English translation of Chinese edition 1984. Providence: American Mathematical Society.

Whittaker, E. T. and Watson, G. N. (1927). *A Course of Modern Analysis.* Cambridge: University Press.

Wolfe, M. A. (1978). *Numerical Methods for Unconstrained Optimization.* New York: Van Nostrand Reinhold Company.

Wolfram, S. (1991). *Mathematica: A system of Doing Mathematics by Computer.* Redwood City: Addison-Wesley.

Woodford, C. (1992). *Solving Linear and Non-Linear Equations.* New York: McGraw-Hill.

APPENDIX A

PAPERS PUBLISHED

.

The results of this research project have been published as follows:

PhD Thesis

P1. Laey-Nee Hu, *Boundary Integral Equations Approach for Numerical Conformal Mapping of Multiply Connected Regions.* Ph.D. Thesis, Universiti Teknologi Malaysia; 2009.

Papers Published in International Journals

P2. Ali H. M. Murid and Laey-Nee Hu, Numerical Experiment On Conformal Mapping of Doubly Connected Regions Onto A Disk With A Slit, Accepted in *International Journal of Pure and Applied Mathematics*, Academic Publication, Bulgaria, December 2008.

P3. Ali H. M. Murid and Laey-Nee Hu, Numerical Conformal Mapping of Bounded Multiply Connected Regions by An Integral Equation Method, Accepted in *International Journal of Contemporary Mathematical Sciences*, Academic Publication, Bulgaria, December 2008.

P4. Ali H. M. Murid and Nurul Akmal Mohamed. (2007). Numerical Conformal Mapping of Doubly Connected Regions via the Kerzman Stein kernel. Accepted for Publication in *International Journal of Pure and Applied Mathematics*.

Papers Published in National Journals

P5. Ali H. M. Murid, Laey-Nee Hu and Mohd Nor Mohamad An Integral Equation Method For Conformal Mapping of Doubly Connected Regions Involving The Neumann Kernel, *Matematika*, Vol. 24, No. 2, (2008), 99-111.

P6. Ali H. M. Murid, Laey-Nee Hu and Mohamad Nor Mohamad, Numerical Conformal Mapping of Doubly Connected Regions Onto a Disc With a Circular Slit, Accepted in *Journal of Quality Measurement and Analysis*, Academic Publication, UKM, September 2008.

Papers Published in International Proceedings

P7. Laey-Nee Hu and Ali H. M. Murid, Conformal Mapping of Doubly Connected Regions onto an Annulus via an Integral Equation with the Kerzman-Stein Kernel, *Proceedings of International Symposium on Geometric Function Theory and its Applications 2008*, Universiti Kebangsaan Malaysia, Kuala Lumpur, 10-13 November 2008, 359-369.

P8. Ali H. M. Murid, Laey-Nee Hu and Mohd Nor Mohamad, Numerical Conformal Mapping of Triply Connected Regions onto an Annulus with slit via an Integral Equation with the Neumann Kernel, *Proceedings of International Symposium on Geometric Function Theory and its Applications*

2008, Universiti Kebangsaan Malaysia, Kuala Lumpur, 10-13 November 2008, 431-440.

P9. Laey-Nee Hu and Ali H. M. Murid, An Integral Equation for Conformal Mapping of Triply Connected Regions Onto A Disk with Circular Slits, *Proceedings of International Graduate Conference on Engineering and Science 2008*, Universiti Teknologi Malaysia, Skudai, Johor, 23-24 December 2008.

P10. Ali H. M. Murid, Laey-Nee Hu and Mohd Nor Mohamad, An Integral Equation Method Involving The Neumann Kernel For Conformal Mapping of Doubly Connected Regions Onto A Disc With A Circular Slit, *Proceedings of International Conference Mathematical Sciences 2007*, Universiti Kebangsaan Malaysia, Kuala Lumpur, 28-29 November 2007, 178-186. CD Proceedings.

Papers Published in National Proceedings

P11. Ali H. M. Murid, Laey-Nee Hu, Mohd Nor Mohamad and Nor Izzati Jaini, Numerical Conformal Mapping of Doubly Connected Regions onto an Annulus via an Integral Equation with the Neumann Kernel, *Proceedings of the Seminar on Science and Technology 2008* Uinversiti Malaysia Sabah, Kota Kinabalu, Sabah, 29-30 October 2008, 60-67.

P12. Ali H. M. Murid and Laey-Nee Hu, Numerical Conformal Mapping For Boundary And Interior Of Doubly Connected Regions, *Prosiding Seminar Kebangsaan Aplikasi Sains dan Matematik 2008*, Universiti Tun Hussein Onn Malaysia, Batu Pahat, Johor, 24-25 November 2008.

P13. Ali H. M. Murid, Laey-Nee Hu, Mohd Nor Mohamad, Conformal Mapping Of Doubly Connected Regions Onto A Disc With A Circular Slit By Using An Integral Equation Method Via The Neumann Kernel, *Prosiding Seminar Kebangsaan Aplikasi Sains dan Matematik 2007*, Universiti Tun Hussein Onn Malaysia, Batu Pahat, Johor, 5 December 2007.

P14. Nurul Akmal Mohamed and Ali H. M. Murid (2007). Numerical Conformal Mapping of Doubly Connected Regions Using The Integral Equation via the Kerzman-Stein Kernel and Cauchy's Integral Formula. *Prosiding Simposium Kebangsaan Sains Matematik Ke-XV*. Selangor: UiTM, 83-93.

Papers Presented at International Conferences

P15. Ali H. M. Murid, Laey-Nee Hu and Mohd Nor Mohamad, An Integral Equation Method For Conformal Mapping of Doubly Connected Regions Involving The Neumann Kernel, *2nd International Conference on Mathematical Sciences (ICoMS 2007)*, 28-29 May 2007, Universiti Teknologi Malaysia, Johor.

Paper Presented at National Conferences

P16. Ali H. M. Murid and Laey-Nee Hu, An Integral Equation Related To A boundary Relationship with Application To Conformal Mapping of Multiply Connected Regions, *Regional Annual Fundamental Science Seminar (RAFF 2008)*, 27-28 May 2008, IIS, UTM.

P17. Ali H. M. Murid and Laey-Nee Hu, An Integral Equation Method for Conformal Mapping of Multiply Connected Regions onto an Annulus with Circular Slits Via The Neumann Kernel, *Simposium Kebangsaan Sains Matematik ke-16 (SKSM 2008)*, 2-5 June 2008, UMT, Kota Bahru.

Submitted Presentation at National Conferences

P18. Ali H. M. Murid and Laey-Nee Hu, A Boundary Integral Equation for Conformal Mapping of Multiply Connected Regions onto the Circular Slit Regions Via The Neumann Kernel, *5th Asian Mathematical Conference* 22-26 June 2009, Kuala Lumpur, Malaysia

Submitted Book Chapter

P19. Ali H. M. Murid, Laey-Nee Hu and Mohd Nor Mohamad. A book chapter was submitted to UTM, with the title, *Conformal Mapping of Multiply Connected Regions via the Kerzman-Stein and Neumann Kernels*, on 31 December 2008.